



Influence of ocean acidification on elemental mass balances and particulate organic matter stoichiometry in natural plankton communities

Dissertation

zur Erlangung des Doktorgrades
der Mathematisch-Naturwissenschaftlichen Fakultät der
Christian-Albrechts-Universität zu Kiel

vorgelegt von
Tim Boxhammer

Kiel, Januar 2018

Titelbild

Tim Boxhammer

1. Gutachter: Prof. Dr. Ulf Riebesell
2. Gutachter: Prof. Dr. Leif Anderson
Tag der Disputation: 24. Januar 2018
Zum Druck genehmigt: 24. Januar 2018

Für meine Großmutter Irene

Zusammenfassung

Die Stoffkreisläufe im Ozean beginnen mit der Umwandlung anorganischer Nährstoffe und Kohlenstoffdioxid (CO_2) in Biomasse durch Primärproduzenten. Diese Organismen bestimmen somit das Verhältnis der Elemente im partikulären, organischen Material und die Menge an Kohlenstoff (C), die pro Stickstoff- (N) und Phosphor- (P) Einheit organisch gebunden werden kann. Die Phytoplanktonbiomasse bildet die Grundlage des pelagischen Nahrungsnetzes, in welchem die Elemente zwischen Organismen und trophischen Ebenen sowie zwischen gelösten und partikulären Formen zirkulieren.

Anthropogene Einflüsse, insbesondere die Verbrennung fossiler Brennstoffe, erhöhen gegenwärtig die CO_2 -Konzentration in der Erdatmosphäre in einer noch nie dagewesenen Geschwindigkeit. Der Ozean ist die zweitgrößte Senke für anthropogenes CO_2 und absorbiert etwa ein Viertel der jährlichen Emissionen. Die Reaktion von CO_2 mit Meerwasser führt jedoch zu einer tiefgreifenden Veränderung des marinen Karbonatsystems, die als Ozeanversauerung bezeichnet wird. Es ist bereits bekannt, dass die daraus resultierende Erhöhung der CO_2 -Konzentration und die Abnahme des pH-Wertes im Meerwasser das marine Plankton sowohl auf der Organismen- (Physiologie) als auch auf der Gemeinschaftsebene (Artenzusammensetzung und Wechselwirkungen im Nahrungsnetz) beeinflussen. Die potentiellen Auswirkungen auf die Stoffkreisläufe im Ozean sind jedoch weitgehend unbekannt. Die Serviceleistungen des Ozeans, anthropogenen Kohlenstoff aufzunehmen und Nahrung für die Menschheit zu produzieren, hängen jedoch von diesen marinen Stoffkreisläufen ab. Daher ist es essentiell zu untersuchen, wie und in welchem Ausmaß die Stoffkreisläufe durch die zunehmende Versauerung der Meere beeinflusst werden. Die ersten Studien zum Einfluss von Ozeanversauerung auf natürliche Planktongemeinschaften mit mehreren trophischen Ebenen wurden in pelagischen Mesokosmen durchgeführt. Diese Studien waren jedoch begrenzt in ihrer Laufzeit (Tage bis Wochen) und oft fehlten ausreichende Messungen der biogeochemischen Reservoirs und Stoffflüsse, insbesondere des vertikalen Partikelflusses.

Ziel dieser Doktorarbeit war es daher, den Einfluss von Ozeanversauerung auf die biogeochemischen Kreisläufe von C, N und P in natürlichen pelagischen Nahrungsnetzen mit mehreren trophischen Ebenen (bis hin zu Fischlarven) über Zeiträume von mehreren Wochen bis Monaten zu untersuchen. Neben methodischen Verbesserungen zur Quantifizierung des vertikalen Partikel- und Stoffflusses innerhalb von Mesokosmen, werden Ergebnisse von zwei unabhängigen pelagischen *in situ* Mesokosmenstudien vorgestellt und mit weiteren Ozeanversauerungsstudien aus verschiedenen Meeresgebieten verglichen. Darüber hinaus werden methodische Probleme bei biogeochemischen Messungen in pelagischen Mesokosmen diskutiert, die für die Massenbilanzierung von Elementen verbessert werden müssen.

Für die effiziente und quantitative Probenahme und Verarbeitung von absinkendem Material innerhalb von Mesokosmen wurde ein neues Protokoll entwickelt. Die Sedimentfallen können ohne Einfluss auf die darüber liegende Wassersäule und mit minimaler Auswirkung auf das gesammelte Material geleert werden. Durch Ausfällung mittels Eisen(III)chlorid und durch Zentrifugieren des gesamten Probevolumens wurde eine hocheffiziente Konzentration von partikulärem Material erreicht

(>98% des partikulären Kohlenstoffgehaltes). Der Feinheitsgrad des gefriergetrockneten und gemahlten Probenmaterials erreichte den von feinem bis grobem Schluff, wodurch die Homogenität des Materials und eine vernachlässigbare Messvariabilität von biogeochemischen Parametern garantiert wird. Dies wiederum ermöglicht eine hochgenaue quantitative biogeochemische Analyse des absinkenden partikulären Materials, was als Grundlage für die vertikalen Flussmessungen von Elementen während der Mesokosmenstudien dieser Arbeit diente.

Für die erste Studie wurden zehn pelagische Mesokosmen im Gullmar Fjord (Schweden) verankert, um den Einfluss von Ozeanversauerung auf eine küstennahe Planktongemeinschaft während der natürlichen Planktonsukzession zwischen Winter und Sommer zu untersuchen. Die Entwicklung der gelösten und partikulären Reservoirs von C, N, P und Silikat (Si) wurde über einen Zeitraum von mehr als 100 Tagen bei natürlich vorherrschenden und für das Jahr 2100 prognostizierten CO_2 -Konzentrationen ($\sim 760 \mu\text{atm } p\text{CO}_2$) beobachtet. Um durch Ozeanversauerung induzierte Veränderungen in der Partitionierung und dem Kreislauf dieser Elemente aufzudecken wurden Massenbilanzen berechnet. Die wichtigste Beobachtung unter erhöhter CO_2 -Konzentration war ein signifikant verstärkter Transfer von C, N und P vom Phyto- zum Zooplankton. Dies hatte sowohl eine verlängerte Retentionszeit der drei Elemente im pelagischen Nahrungsnetz als auch eine um ca. ein Zehntel reduzierte Sedimentation von N und P zur Folge. Darüber hinaus wurde eine Tendenz zur verstärkten Kohlenstofffixierung im Verhältnis zur Stickstoffaufnahme in der dominierenden Diatomee *Coscinodiscus concinnus* unter Ozeanversauerung beobachtet. Dies wirkte sich ebenfalls auf das C:N-Verhältnis im suspendierten partikulären Material sowie im absinkenden Partikelfluss aus.

Die zweite pelagische Mesokosmenstudie wurde im Raunefjord (Norwegen) durchgeführt. Ziel war die Evaluierung des partikulären C:N-Verhältnisses natürlicher Planktongemeinschaften unter erhöhten CO_2 -Konzentrationen und *in situ* Bedingungen. Ein CO_2 -Gradient von 300 bis 1615 μatm (durchschnittlicher $f\text{CO}_2$ während der Studie) wurde in acht Mesokosmen generiert. Zur Mitte des 35 Tage andauernden Experimentes wurden anorganische Nährstoffe hinzugegeben, um eine Phytoplanktonblüte zu erzeugen. Das C:N-Verhältnis im partikulären, organischen Material und absinkenden Partikeln korrelierte linear mit dem CO_2 -Gradienten, doch die Wirkungsrichtung des CO_2 -Effektes veränderte sich im Verlauf der Studie. Dies geschah in Abhängigkeit von der Struktur und der Wachstumsphase der Phytoplanktongemeinschaft. Diese Ergebnisse zeigen, dass die Veränderung der C:N-Verhältnisse im partikulären, organischen Material eng mit der durch CO_2 verursachten Veränderungen in der Struktur der Planktongemeinschaften und den C:N Signaturen einzelner Planktonarten verbunden sein wird.

Beide Studien weisen darauf hin, dass Ozeanversauerung die C:N-Verhältnisse in Planktonbiomasse und absinkenden Partikeln mit variabler Wirkungsrichtung und -stärke beeinflussen kann. Dies ist wiederum abhängig, von der untersuchten Planktonzusammensetzung, Jahreszeit und Wachstumsphase des Planktons. Zusammen mit der Möglichkeit, die Partitionierung von C, N und P in der Oberflächenschicht der Meere zu verändern, hat Ozeanversauerung das Potenzial, den Kreislauf von Elementen auf globaler Ebene im Ozean zu beeinflussen.

Summary

The cycling of elements in the ocean begins with the transformation of inorganic nutrients and carbon dioxide (CO₂) into biomass by primary producers. These organisms determine the proportion of the elements that are incorporated into particulate organic matter and the amount of carbon (C) that can be organically bound per unit of nitrogen (N) and phosphorus (P). Phytoplankton biomass is the basis of the pelagic food web in which the elements circulate between organisms and trophic levels as well as dissolved and particulate forms.

Anthropogenic activities, primarily the burning of fossil fuels, currently increase the atmospheric CO₂ concentration at a rate that is unprecedented in recent Earth's history. The ocean is the second largest sink of anthropogenic CO₂, absorbing about one quarter of global annual CO₂ emissions. The reaction of CO₂ with seawater leads to profound shifts in seawater carbonate chemistry, commonly termed as 'ocean acidification' (OA). The resulting increase in CO₂ concentration and decrease in seawater pH has already shown to impact marine plankton from the organism (physiology) to the community level (species composition and food web effects), but with largely unknown consequences for the cycling of elements in the ocean. However, the ocean services of absorbing anthropogenic C and providing food for humankind depend on these oceanic material cycles. Therefore, it is essential to assess how and to what extent the element cycles will be affected by OA. The first OA studies that investigated entire plankton communities with several trophic levels were conducted inside pelagic mesocosms, but were limited in their runtime (days to weeks) and often lacked sufficient measurement of the biogeochemical pools and fluxes, especially the downward flux of particulate organic matter.

Thus, the aim of this doctoral dissertation was to investigate the influence of OA on biogeochemical cycles of C, N, and P in natural pelagic food webs of several trophic levels (up to fish larvae) over extended time scales of weeks to months. Methodological improvements for quantification of the downward flux of particulate matter inside mesocosms as well as results from two independent *in situ* pelagic mesocosm experiments (up to 75 m³ per mesocosm unit) are presented and compared with similar OA studies from different ocean regions. Furthermore, methodological issues in biogeochemical measurements inside pelagic mesocosms that need to be improved for mass balance calculation of elements are elucidated.

A new protocol was developed for efficient sample recovery and processing of quantitatively collected sinking particulate matter inside mesocosms. The sediment traps can be sampled without any disturbance of the overlying water column and with minimized impact on the collected material. Highly efficient concentration of particulate matter (>98% of the particulate C content) was achieved in large volume sediment trap samples by both ferric chloride flocculation and entire sample centrifugation. Grain size of the freeze-dried and ground sample material ranged from fine to coarse silt, which guarantees sample homogeneity and negligible measurement variability of biogeochemical parameters. This allows for highly accurate quantitative biogeochemical analysis

of the sinking particulate matter that was the basis for vertical flux measurements of elements during the mesocosm studies of this thesis.

In the first study, ten pelagic mesocosms were deployed in Gullmar Fjord (Sweden) to investigate the impact of OA on a coastal plankton community during the natural winter-to-summer plankton succession. The development of particulate and dissolved element pools was monitored at ambient and realistic end-of-the-century CO_2 concentrations ($\sim 760 \mu\text{atm } p\text{CO}_2$) over a time span of more than 100 days. Mass balances were calculated to uncover OA induced changes in the partitioning and cycling of C, N, P, and silica (Si). The key observation under high CO_2 was a significantly amplified transfer of C, N, and P from phytoplankton to mesozooplankton, resulting in (1) a prolonged retention of all three elements in the pelagic food web and (2) a significantly reduced N and P sedimentation by about one tenth. These observations provide some of the first evidence that OA effects on primary producers can propagate through the food web and modify partitioning of element pools and thus impact biogeochemical cycling in a future acidified ocean. Furthermore a tendency towards enhanced C fixation relative to N utilisation in the dominant diatom *Coscinodiscus concinnus* was observed, which created a signal of elevated C:N ratios in the suspended particulate matter pool, as well as in the downward particle flux under OA.

The second pelagic mesocosm study considered in this thesis was conducted in Raunefjord (Norway). The goal was the assessment of the C:N response of natural plankton communities to increased CO_2 concentrations at *in situ* conditions. A CO_2 gradient from 300 to 1615 μatm (average $f\text{CO}_2$ during study period) was established in eight mesocosm units and inorganic nutrients were added to induce a phytoplankton bloom half way through the 35 days long study. The C:N stoichiometry in particulate organic matter and sinking particles correlated linearly with CO_2 concentrations, but the direction of this CO_2 response shifted over the course of the study depending on plankton community structure and phytoplankton growth phase. These findings illustrate that the CO_2 response of C:N ratios in particulate organic matter will be closely linked to corresponding future changes in plankton community structure and the C:N signatures of individual plankton species.

Both studies indicate that OA can influence the C:N stoichiometry of plankton biomass and sinking particulate matter with variable effect direction and strength, depending on the investigated plankton community composition, season, and plankton growth phase. Thus, together with the potential to alter partitioning of C, N, and P in the surface ocean, OA has the potential to effect oceanic cycling of elements on a global scale.

Contents

Zusammenfassung	VII
Summary	XI
1. General introduction	1
1.1 Marine biogeochemical cycles	3
1.1.1 Primary production and organic matter stoichiometry	3
1.1.2 Cycling of carbon and nutrients in the ocean	4
1.2 Ocean acidification	8
1.2.1 Origin and impact on ocean chemistry	8
1.2.2 Plankton responses to ocean acidification	10
1.3 Pelagic mesocosms	13
1.3.1 The plankton's 'world' in a test tube	13
1.3.2 Pelagic mesocosm and sediment trap design and their application for biogeochemical flux measurements	14
1.4 Thesis outline	16
1.4.1 Overview	16
1.4.2 Thesis manuscripts and declaration of contribution	17
References	19
2. Manuscript I: Technical note: Sampling and processing of mesocosm sediment trap material for quantitative biogeochemical analysis	31
3. Manuscript II: Enhanced transfer of organic matter to higher trophic levels caused by ocean acidification and its implications for export production: A mass balance approach	45
4. Manuscript III: Plankton community structure controls the response of particulate organic matter stoichiometry to ocean acidification	83

5. Synthesis	105
5.1 Pitfalls of elemental mass balance calculations in mesocosm enclosures and methodological improvements	107
5.1.1 Mesocosm sediment trap design and sampling	107
5.1.2 Wall growth	108
5.1.3 Correction of dissolved inorganic carbon for the air-sea gas exchange of CO ₂	109
5.1.4 Dissolved organic matter	110
5.1.5 Relevance of the mesozooplankton pool for particulate organic matter	111
5.2 Ocean acidification effects on carbon and nutrient cycling	113
5.2.1 Impact of ocean acidification on the carbon to nitrogen ratio of particulate organic matter	113
5.2.2 Impact of ocean acidification on transfer of photoautotrophic biomass to higher trophic levels	116
5.3 Future perspectives	118
5.3.1 Future methodological improvements for biogeochemical research with pelagic mesocosms	118
5.3.2 Future perspectives of ocean acidification research on biogeochemical cycling of elements	119
Epilogue	120
References	121
Curriculum Vitae	127
Publication record	131
a. Published manuscripts (peer reviewed)	133
b. Manuscripts under review	135
c. Manuscripts in preparation	135
d. Video publications (non-peer reviewed)	136
Danksagung	139
Eidesstattliche Erklärung	143

1. General introduction

1.1 Marine biogeochemical cycles

1.1.1 Primary production and organic matter stoichiometry

The vast majority of primary production in the ocean is mediated by free drifting, photosynthetic microorganisms - the phytoplankton (Strickland, 1965). These pelagic photoautotrophs inhabit the sunlit surface layer (i.e. the euphotic zone) of all marine ecosystems and represent the basis of the marine food web. Through the process of photosynthesis, phytoplankton transforms inorganic nutrients and carbon dioxide (CO₂) into organic compounds and oxygen (O₂) using sunlight energy and water (H₂O) as electron donor (Fig. 1.1). Estimations based on satellite (Chlorophyll *a*) data indicate that phytoplankton net primary production, defined as the amount of photosynthetically fixed carbon (C) available to the next trophic level, almost equals that of the terrestrial vegetation (Field et al., 1998).

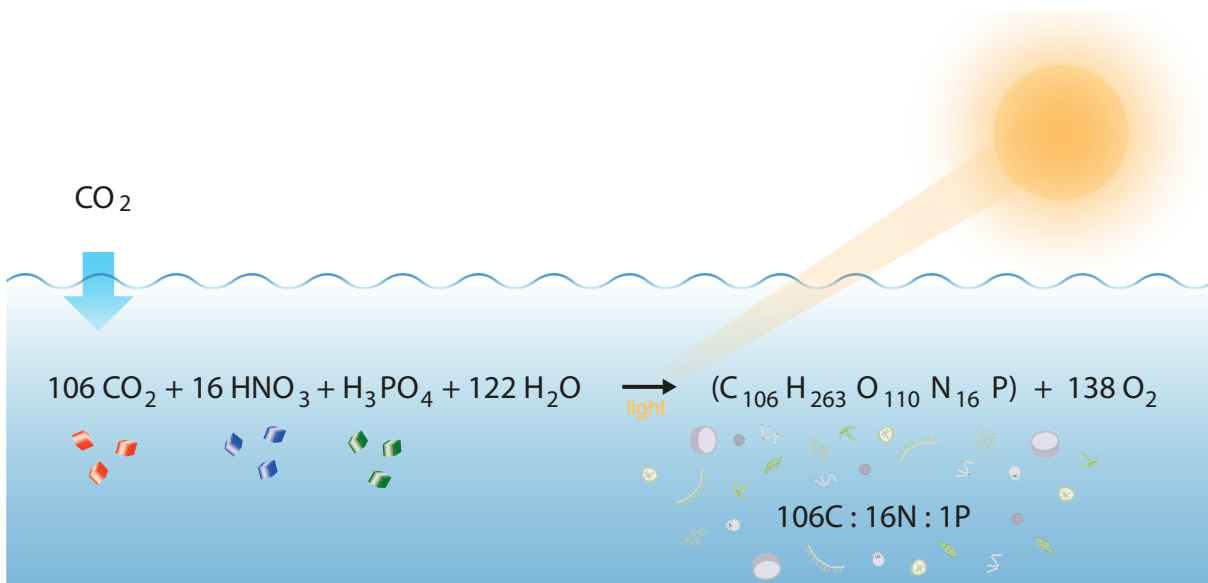


Figure 1.1. Chemical equation for photosynthetic production of marine particulate organic matter following the stoichiometric composition of the 'Redfield ratio' (106C:16N:1P) (Redfield et al., 1963). Phytoplankton organisms modified from Rita Erven (GEOMAR).

The key nutrients required for and thus limiting phytoplankton organic matter production are nitrogen (N), phosphorus (P), and trace metals such as iron or zinc. N is a key element in proteins and nucleic acids, P is a major constituent of the cell membrane and organism's DNA/RNA, while trace metals are essential for diverse enzyme functionality (Geider and La Roche, 2002;

Twining and Baines, 2013). Silica (Si) can furthermore limit growth of silicifying phytoplankton taxa such as diatoms, which often dominate the phytoplankton community. According to Liebig's Law of the minimum (von Liebig, 1855) the nutrient element that is limiting at a particular site and time mainly controls marine primary production (Falkowski et al., 1992).

Already in 1934, Alfred C. Redfield discovered a remarkable consistency in the proportion of the three major elements C, N, and P in both marine phytoplankton biomass and in dissolved inorganic nutrients (N and P) in the deep ocean (Redfield, 1934). The so-called 'Redfield ratio' of 106C:16N:1P (Fig. 1.1) is a tenet in marine biogeochemistry and is still used for calculation of nutrient-based phytoplankton productivity, potential C sequestration through sinking organic matter, as well as for definition of ecological niches for specific phytoplankton groups such as N₂ (nitrogen gas) fixing cyanobacteria. However, the elemental composition of phytoplankton can vary strongly among different ocean regions, phytoplankton taxa, and even growth conditions of the same taxon (Geider and La Roche, 2002; Ho et al., 2003; Klausmeier et al., 2004; Martiny et al., 2013; Rhee, 1978). The observed plasticity of bulk C:N:P ratios is mainly driven by (1) the taxonomic composition of phytoplankton assemblages, (2) the nutrient supply ratio influencing the cellular elemental ratios, (3) the dominating phytoplankton growth strategy, and (4) detritus accumulating in the water column and influencing bulk composition (Martiny et al., 2013). In fact, Quigg et al. (2003) found evidence that the phylogenetic origin of phytoplankton, defined by their accessory photosynthetic pigments, correlates with substantial differences in their elemental composition. Furthermore, the condition of the N-rich light and nutrient acquisition machinery (proteins and chlorophyll) and the N- and P-rich growth machinery (ribosomal RNA) are thought to impact cellular elemental composition (Arrigo, 2005; Falkowski, 2000; Geider and La Roche, 2002).

Despite the wide range of particulate C:N:P ratios found in the ocean (Martiny et al., 2014), the Redfield ratio can be seen as a benchmark of global average particulate organic matter (POM) elemental stoichiometry (Geider and La Roche, 2002).

1.1.2 Cycling of carbon and nutrients in the ocean

C and the key nutrients for phytoplankton growth (N, P, and Si) are cycled between three major pools in the upper ocean: (1) the inorganic C and nutrients pool, (2) the dissolved organic matter pool (DOM, only including C, N, and P), and (3) the particulate matter (PM) pool containing both POM as well as biominerals such as biogenic opal and calcium carbonate (CaCO₃) (Fig. 1.2).

As illustrated in Figure 1.2, the pool of PM can be further subdivided into three separate components: (1) phytoplankton, i.e. primary producers, (2) zooplankton, i.e. primary and to some extent secondary consumers, and (3) detritus, representing dead biomass from the two other pools.

Bacteria are not shown separately as they contribute to both DOM and POM as well as to primary producers and primary consumers.

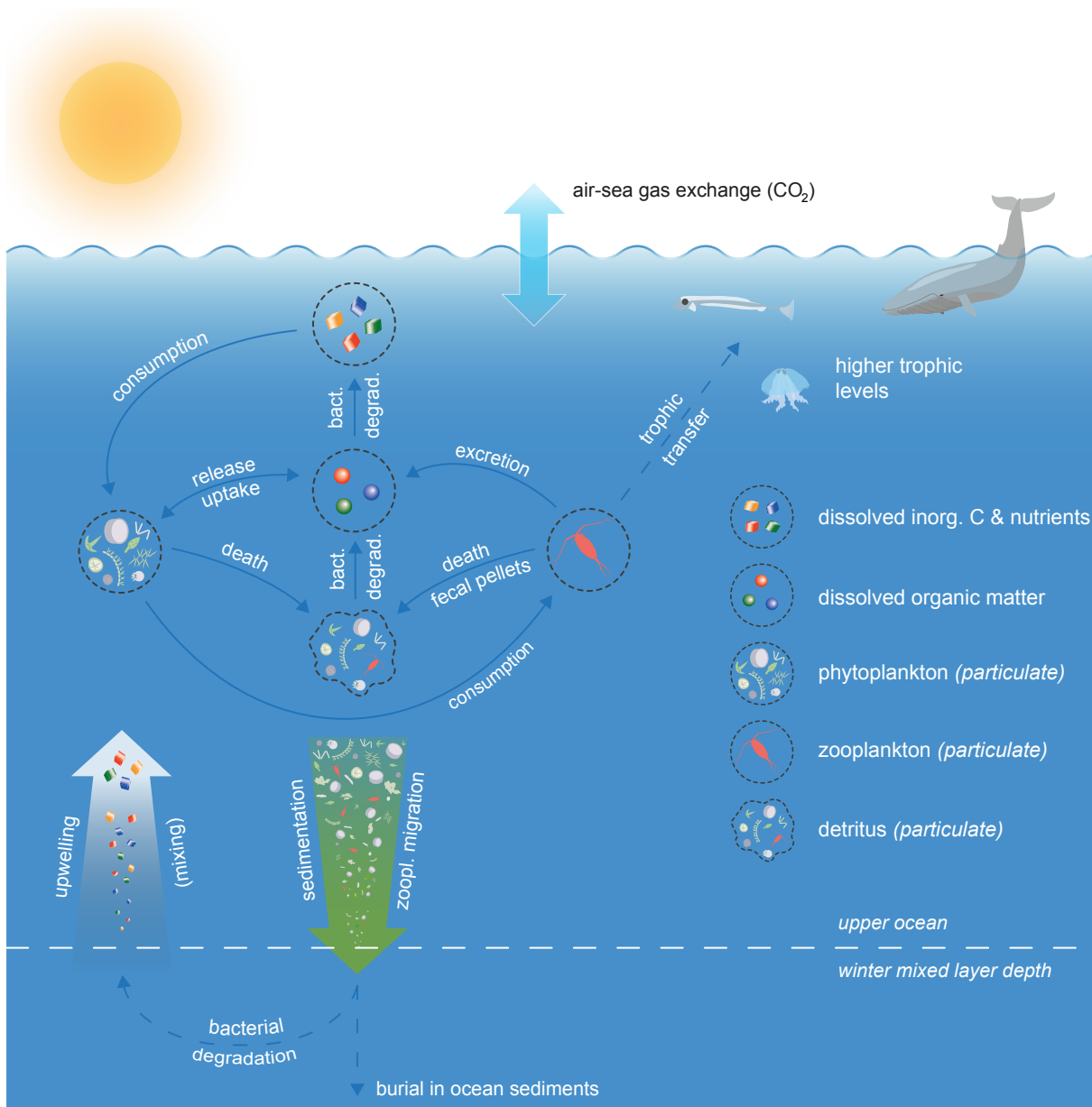


Figure 1.2. Main element pools and fluxes of carbon and nutrients within the upper ocean layer. Blue arrows indicate the direction of exchange between different pools with the underlying mechanism described in white. The blue dashed arrows illustrate the transfer of biomass from zooplankton to higher trophic levels (e.g. fish or jellyfish) and the bacterial degradation or sedimentation of organic matter in the deep ocean. Larger arrows in green, white or blue display fluxes leaving or entering the ocean surface layer. Organisms modified from Rita Erven (GEOMAR).

Cycling of C, N, P, and Si within the surface layer of the ocean begins with the build-up of biomass and silica shells (biogenic opal) by phytoplankton from CO_2 and dissolved inorganic nutrients. Primary producers thus form the basis of the marine food web. A significant proportion of C, N, and P organically bound by primary producers is directly released and contributes to the DOM pool. The percentage of DOM exuded by phytoplankton is usually in the range of 10 to 20% of primary production, but can reach up to 44% depending on the physiological state and phytoplankton community composition (see review by Thornton, 2014). The basic principals behind this are overproduction of carbohydrates at high light but low nutrient conditions and passive diffusion of organic molecules leaking out of phytoplankton cells (Carlson and Hansell, 2015). DOM produced by phytoplankton but also by grazer-mediated release and excretion, viral cell lysis or bacterial degradation processes is a major food source for heterotrophic bacteria. These bacteria degrade the organic compounds and return C and nutrients to the food chain (bacteria biomass) as well as to primary producers (inorganic nutrients), a mechanism called the ‘microbial loop’ (Azam et al., 1983). However, it became more and more clear in the last decades that probably most phytoplankton are also capable of directly using at least some dissolved organic compounds as N and P sources (Bronk et al., 2007; Cotner and Wetzel, 1992; Granéli et al., 1999). Furthermore, a considerable fraction of phytoplankton is known to be capable of mixotrophy, which enables these primary producers to acquire nutrients to some extent from the POM pool (Stoecker et al., 2017).

Generally, a large proportion of autotrophic primary production is consumed by heterotrophic micro- and mesozooplankton with 17-52% and approximately 23%, respectively (Calbet, 2001; Landry and Hassett, 1982). In a classic description of the marine food web the zooplankton biomass is then consumed by higher trophic levels for instance fish larvae or jellyfish although these organisms also contribute significantly to the remineralisation of nutrients in the water column (Fig. 1.2).

Both autotrophic and heterotrophic organisms contribute to the third component of the PM pool: ‘Suspended detritus’ consisting of dead organisms and zooplankton faecal pellets, as well as shells of primary producers such as diatoms (biogenic opal) and coccolithophores (CaCO_3) (Fenchel and Jørgensen, 1977). Detritus is another major food source for bacteria attached to suspended particles, degrading the POM and releasing DOM and ‘recycled’ inorganic nutrients (Ducklow and Carlson, 1992).

Particles that are not remineralised in the upper ocean eventually sink below the winter mixed layer depth where they are physically isolated from the surface ocean. This means that C and nutrients released through degradation processes below this depth accumulate in the deep ocean layer (Fig. 1.2) (Sarmiento and Gruber, 2006). The so-called ‘export’ of photosynthetically fixed C to depth by settling particles, as well as downwelling of dissolved organic carbon (DOC) and zooplankton vertical migration, leads to a surface to depth gradient in dissolved inorganic carbon (DIC). This biologically mediated process, termed as the ‘biological carbon pump’ (Volk and Hoffert, 2013),

increases the ocean's uptake capacity for atmospheric CO₂. Thus, the ocean biology plays an important role in controlling atmospheric CO₂ concentrations, by sequestering C in the deep ocean. The fraction of photosynthetically fixed C reaching the deep ocean below 1000 m water depth (~15%) and the sediments (~0.8%) is relatively small (Sarmiento and Gruber, 2006) and depends on particle remineralisation rates and sinking velocities. Remineralisation rates of settling particles are driven by biology (organic matter) and chemical dissolution (biogenic opal and CaCO₃), while their sinking velocity mainly depends on their dimensions, structure, and density (Kiørboe, 2000; Monroy et al., 2017; Ploug et al., 1999; Tréguer et al., 1995). The 'ballast ratio hypothesis' implies that high-density (i.e. ballast) minerals such as biogenic opal and CaCO₃ mainly drive deep ocean organic C sequestration by increasing the particle's density and sinking velocity (Armstrong et al., 2009). However, recent studies suggest that the most important factor determining export efficiency of organic matter (i.e. the fraction of newly produced biomass reaching the deep ocean) is the tight packaging of settling particles, which has been strongly linked to plankton community composition (phytoplankton cell size and repackaging by grazers) (Bach et al., 2016a; Francois et al., 2002; Henson et al., 2012b; 2012a). While only a very small proportion of exported organic matter is buried in deep-sea sediments for geological timescales (~0.3% with respect to C; Sarmiento and Gruber, 2006), DIC and nutrients in the deep ocean are upwelled back to the surface on timescales of decades to centuries or millennia, supporting new primary production and closing the oceanic C and nutrient cycles.

1.2 Ocean acidification

1.2.1 Origin and impact on ocean chemistry

During the past 420,000 years, atmospheric CO₂ concentration has varied naturally between 180 and 300 ppm (parts per million), correlating with glacial and interglacial periods of the Earth (Joos and Spahni, 2008; Petit et al., 1999). Since the beginning of the industrial era in the 19th century, land-use-changes (i.a. deforestation and agriculture) and the burning of fossil fuels have increased atmospheric CO₂ concentration from approximately 280 ppm to above 400 ppm in 2017 (Joos and Spahni, 2008, The Keeling Curve). The rapid rate of increasing atmospheric CO₂ concentration is unprecedented in at least the last 800,000 years of Earth's history, as documented in Antarctic ice core records (Lüthi et al., 2008; Petit et al., 1999; The Keeling Curve). Since the 1960s, global CO₂ emissions have tripled from on average 3.1 ± 0.2 Gt C yr⁻¹ to more than 10 Gt C yr⁻¹ in 2015 (Fig. 1.3A) (Le Quéré et al., 2016). Future CO₂ emissions, and thus atmospheric CO₂ levels, depend on socio-economic parameters and may reach levels of up to 1000 ppm (RCP8.5; van Vuuren et al., 2011) by the end of the century, an almost four-fold increase compared to pre-industrial levels (Fig. 1.3B) (IPCC, 2014: Synthesis Report).

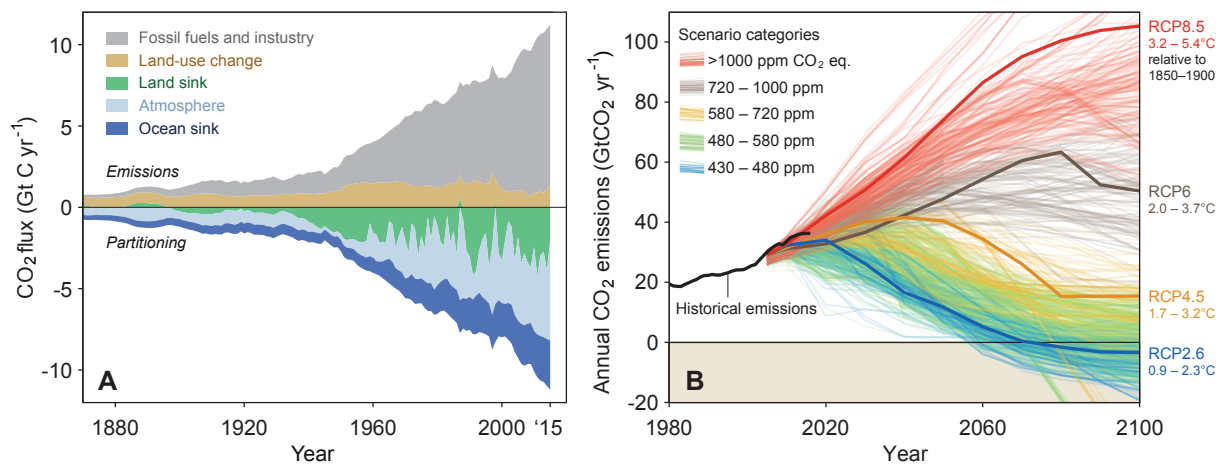
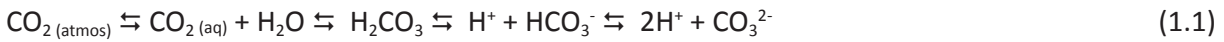


Figure 1.3. Global CO₂ emissions. (A) Emissions from fossil fuels and industry (grey) and land-use change (brown), as well as their partitioning among the atmosphere (light blue), land (green), and the ocean (dark blue). Modified from Le Quéré et al. (2016). (B) Annual emissions of carbon dioxide (CO₂) alone in the Representative Concentration Pathways (RCPs) (lines) and the associated scenario categories of atmospheric CO₂ eq. concentrations. The scenario categories summarize the wide range of emission scenarios published in the scientific literature and are defined on the basis of CO₂ eq. concentrations levels (ppm) in 2100. Modified from the Global Carbon Project.

Besides the terrestrial vegetation, the ocean is the second largest sink of anthropogenic CO_2 , absorbing more than 2 Gt C per year (Fig. 1.3A) (Le Quéré et al., 2016). In total the ocean has already absorbed about one third of human CO_2 emissions, buffering atmospheric concentrations and the greenhouse effect of CO_2 on Earth's climate (Le Quéré et al., 2016). In contrast to other gases that dissolve in seawater, the majority of CO_2 reacts with water (H_2O), forming carbonic acid (H_2CO_3), which then dissociates by losing hydrogen ions (H^+) to form bicarbonate (HCO_3^-) and carbonate (CO_3^{2-}) ions (Doney et al., 2009) (Eq. 1.1).



Thus, with increasing atmospheric CO_2 concentration (ppm), both CO_2 partial pressure ($p\text{CO}_{2(\text{aq})}$) and concentration of H^+ ions in the surface ocean are increasing, which is expressed by a corresponding decrease of the seawater pH (Fig. 1.4A).

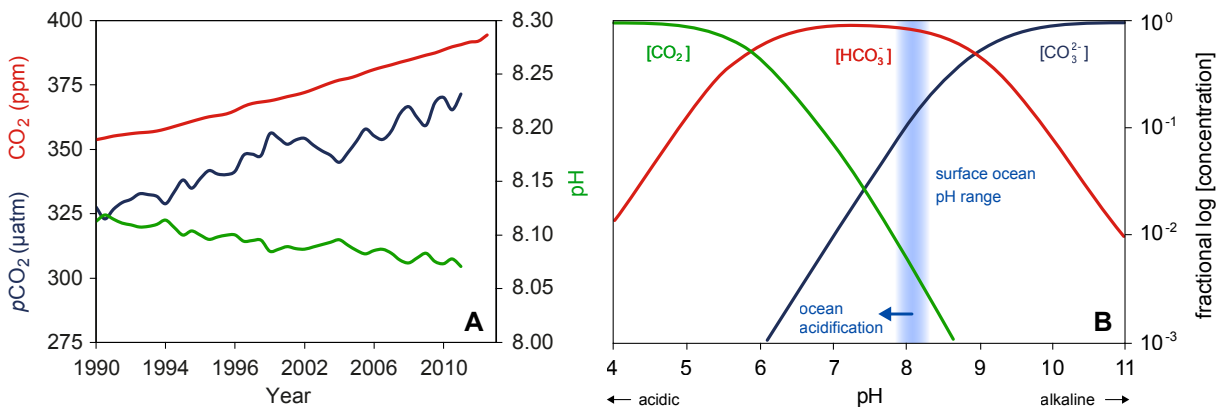


Figure 1.4. Seawater carbonate chemistry. (A) Smoothed time series of atmospheric CO_2 concentration (ppm) at the atmospheric Mauna Loa Observatory (top red line), surface ocean partial pressure of CO_2 ($p\text{CO}_2$; middle blue line) and surface ocean pH (bottom green line) at Station ALOHA in the subtropical North Pacific north of Hawaii for the period from 1990-2011. Modified after Rhein et al. (2013). (B) Bjerrum plot showing the pH depending relative proportions of the three inorganic carbon species (CO_2 , HCO_3^- , and CO_3^{2-}) dissolved in seawater. The blue area represents the present surface ocean pH range, while the blue arrow indicates the shift in inorganic carbon speciation under future ocean acidification. Modified after concepts in Raven et al. (2005).

Since the beginning of the industrial era, global surface ocean pH has dropped by about 0.1 units from ~ 8.2 to ~ 8.1 , which is equivalent to a $\sim 30\%$ increase in the concentration of H^+ ions (Feely et al., 2009; Orr et al., 2005). This drop of the ocean's pH caused by the uptake of anthropogenic CO_2 over a period of several decades is termed as 'ocean acidification' (OA) (Caldeira and Wickett, 2003; Gattuso and Hansson, 2011). By 2100 the ocean's pH is expected to drop by

another 0.1 to 0.4 units at projected atmospheric CO₂ concentrations of 421 to 936 ppm, referring to the Representative Concentration Pathways (RCPs) 2.6 and 8.5, shown in Figure 1.3B (Pörtner et al., 2014). The shift in ocean pH is also accompanied by a shift in the inorganic C speciation (i.e. the carbonate system), increasing [CO₂] and [HCO₃⁻], but decreasing [CO₃²⁻] (Fig. 1.4B) (Doney et al., 2009; Raven et al., 2005). The decrease in CO₃²⁻ concentration reduces the ocean's buffer capacity for H⁺ ions (both reacting to HCO₃⁻) and will amplify natural diurnal and seasonal variations of seawater pH e.g. due to photosynthesis (CO₂ consumption) and respiration (CO₂ release) (Egleston et al., 2010; Jury et al., 2013). Furthermore, the saturation state of CaCO₃ decreases with a corresponding shallowing of the CaCO₃ saturation horizon, the depth at which biogenic CaCO₃ becomes undersaturated and starts to dissolve (Feely et al., 2004; Orr et al., 2005).

Likewise as the CO₂ increase in the atmosphere, OA proceeds at a rate probably unprecedented in Earth's history (Hönisch et al., 2012; Zeebe, 2012). The magnitude of human impact on the environment including the global C cycle and ocean's pH, has initialised a new epoch with mankind being the major environmental force: 'The Anthropocene' (Crutzen, 2002; Lewis and Maslin, 2015).

1.2.2 Plankton responses to ocean acidification

OA is a potential stressor for all plankton organisms (Kroeker et al., 2010) and their physiological responses to increasing CO₂ concentration and decreasing pH have shown to be diverse and non-uniform even within the same taxon (see reviews by Fabry et al., 2008; Kroeker et al., 2013; Riebesell and Tortell, 2011). The enhancement of phytoplankton primary production is one of the most consistent responses with only a few exceptions of neutral or negative responses found for calcifying coccolithophores and cyanobacteria (Doney et al., 2009; Kroeker et al., 2013; Riebesell and Tortell, 2011). This 'fertilising' effect of elevated CO₂ was also found in natural phytoplankton assemblages and can be explained by reduced energy demand for C concentrating mechanisms, which actively pump CO₂ into the cells against the CO₂ concentration gradient (Riebesell and Tortell, 2011). However, this stimulating CO₂ effect is rather small and no reliable estimates of how global ocean productivity will change in the future exist so far (Joint et al., 2010). Phytoplankton growth rates (i.e. cell division rates) show a much more diverse range of responses to OA among phytoplankton groups. Two independent meta-analyses of laboratory data (Dutkiewicz et al., 2015; Kroeker et al., 2013) revealed increased growth rates of diatoms and in particular diazotrophs (i.e. N₂ fixing plankton) but no significant response by coccolithophores. However, Riebesell et al. (2017) found significantly reduced growth rates of the coccolithophore *Emiliania huxleyi* in natural plankton assemblages exposed to increased CO₂. Also the response in growth and N₂-fixation rate of diazotrophs does not seem to be entirely uniform in all taxa (Eichner et al., 2014).

It would be expected, that the impact of OA on primary producers' metabolic rates (e.g. CO₂ or N₂ fixation rates) would impact their elemental composition. In most single-strain culture studies, the cellular C:N ratio of coccolithophores and cyanobacteria significantly increased or remained unaffected at high CO₂ (see reviews by Hutchins et al., 2009; Riebesell and Tortell, 2011). Diatoms in contrast show a highly diverse response to OA in terms of the direction of changes in C:N stoichiometry, even between closely related species (Burkhardt et al., 1999; Hutchins et al., 2009; Riebesell and Tortell, 2011). However, the results from single species culture experiments are not directly transferable to natural plankton communities of several trophic levels, where complex species interactions such as concurrence for resources or grazing occur. Hutchins et al. (2009) compared several OA studies on plankton assemblages (mainly small-scale incubations) and found no general response pattern of POM C:N stoichiometry. First *in situ* OA studies in pelagic mesocosms, however, found generally increasing or stable C:N ratios of plankton communities under high CO₂ (see review in Riebesell and Tortell, 2011). This was an important finding as changes in C:N stoichiometry of the plankton biomass under OA are relevant for the future strength of the 'biological carbon pump', driving C sequestration in the deep ocean, and thus affecting atmospheric CO₂ concentrations (Passow and Carlson, 2012).

Heterotrophic bacteria are present in the ocean over a wide range of pH levels and are often already exposed to seawater pH projected for the end of the century (Joint et al., 2010). However, increasing bacterial enzyme activities and primary production, as well as bacterial community shifts were found at pH levels projected for 2100 (Endres et al., 2014; Grossart et al., 2006; Krause et al., 2012). These findings imply potential impact of OA on bacterial organic matter remineralisation rates that in turn could strongly effect elemental cycling in the ocean (see cycling of elements in Sect. 1.1.2 of this chapter).

Changing seawater chemistry under OA (mainly decreasing pH and increasing CaCO₃ solubility, see Sect. 1.2.1 of this chapter) directly affects calcifying plankton organisms in their ability to build up CaCO₃ shells and skeletons (Cyronak et al., 2016). Decreasing calcification rates, shell mass or survival rates were found for photoautotrophic coccolithophores and heterotrophic organisms such as calcareous planktonic foraminifera (amoeboid protists), shell-bearing pteropoda (pelagic sea snails), as well as larvae of crustaceans (e.g. copepods or barnacles), bivalve molluscs (mussels), and echinoderms (e.g. sea stars or sea urchins) (Dupont and Thorndyke, 2009; Fabry et al., 2008; Manno et al., 2017; Riebesell and Tortell, 2011). To date, the available data suggest that calcification rate is the metabolic process most sensitive to OA (Hendriks et al., 2010). Decreasing CaCO₃ ballasting of settling POM in the future would have substantial consequences for the efficiency of the biological pump and thus biogeochemical cycling in the ocean (Passow and Carlson, 2012).

Apart from calcifiers, evidence for direct effects of OA on micro- and adult mesozooplankton are scarce under realistic end of the century CO₂ scenarios. However, it is likely that indirect effects via the food web like changing food supply or nutritional quality of prey organisms (e.g. changing

C:nutrient ratios, biochemical stoichiometry or fatty acid composition) will play the key role for performance of zooplankton organisms under OA (Bermúdez et al., 2016; Cripps et al., 2016; Rossoll et al., 2012; Schoo et al., 2012).

All the previously described impacts on marine plankton will likely change their individual competitive fitness, which might lead to changes in community structure and functional diversity of ecosystems under future OA (Doney et al., 2009; Dutkiewicz et al., 2015; Fabry et al., 2008). There is consistent evidence for a shift to smaller phytoplankton taxa that seem to profit from increased CO₂ concentrations (Finkel et al., 2010; Sala et al., 2015; Schulz et al., 2017). However, it should be noted that recent studies have shown that certain phytoplankton taxa have the potential for evolutionary adaptation to future CO₂ levels (Collins et al., 2014; Lohbeck et al., 2012; Scheinin et al., 2015). A factor that must be considered in predictions of future plankton community structures.

1.3 Pelagic mesocosms

1.3.1 The plankton's 'world' in a test tube

Pelagic mesocosms (Greek for: medium sized worlds) are experimental enclosures designed to study natural plankton communities (Odum, 1984; Riebesell et al., 2010). The moored or even free-drifting enclosures can host multiple trophic levels of plankton organisms from autotrophic phytoplankton (primary producers) and herbivorous zooplankton (primary consumers), up to carnivorous fish larvae and jelly-fish (secondary consumers) at self-sustaining conditions. Flexible-wall mesocosms such as the 'Kiel Off-Shore mesocosms for Ocean Simulation' (Fig. 1.5; KOSMOS; Riebesell et al., 2013) or the 'Large Clean Mesocosms' (Guieu et al., 2010) have proven that environmental parameters such as light, temperature, salinity, and stratification of the surrounding water can be mimicked inside the enclosures (Guieu et al., 2010; Schulz et al., 2013).

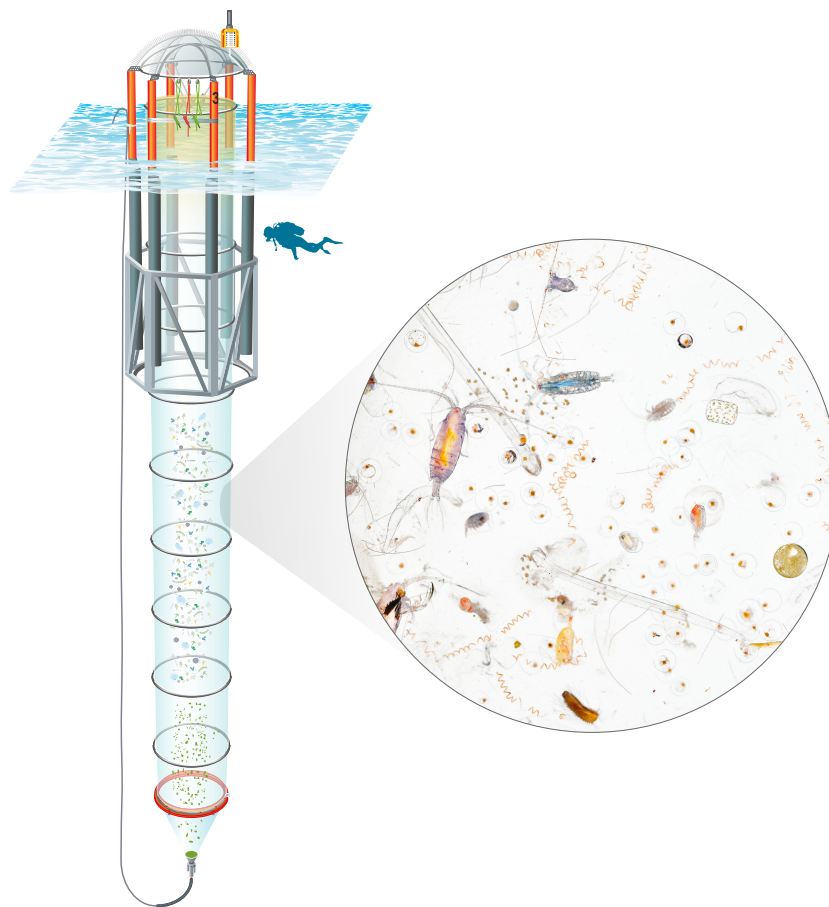


Figure 1.5. Kiel Off-Shore Mesocosm for Ocean Simulation (KOSMOS) and a natural plankton assemblage in a drop of seawater. Technical drawing modified from Rita Erven (GEOMAR). Plankton photograph by David Liittschwager.

One major advantage of isolating a water mass from the surrounding environment is the opportunity to repeatedly sample the same plankton community over long periods of time and successive phases of plankton development. Bach et al. (2016b) have shown that pelagic mesocosm systems can be maintained for more than 100 days to study natural winter-to-summer plankton successions. The possibility to set up replicate mesocosms at a given study site allows for comparison between natural (i.e. reference) conditions and *in situ* manipulated environmental parameters such as nutrients, dust deposition, pollutants or $p\text{CO}_2$ (Guieu et al., 2014; Hattori et al., 1980; Schulz et al., 2013; Taucher et al., 2017). Despite the exclusion of higher trophic levels such as adult fish or life stages of organisms with annual life cycles, pelagic mesocosms represent an experimental platform as close as possible to the real ocean. These isolated plankton ‘worlds’ are therefore ideal to investigate the impact of external stressors such as OA on entire plankton communities.

1.3.2 Pelagic mesocosm and sediment trap design and their application for biogeochemical flux measurements

The lack of exchange with the surrounding ocean (e.g. nutrients, organisms or organic matter) makes pelagic mesocosms perfectly suitable for tracking of changes in element pools over extended periods (see element pools in Fig. 1.2 in Sect. 1.1.2. of this chapter). Accordingly, they are ideal for elemental flux measurements and mass balance calculations. In contrast to the open ocean, any changes in element pools or fluxes can be directly linked with the development of the enclosed plankton community.

Previous work has highlighted three crucial points, which must be considered in mesocosm construction for biogeochemical mass balancing studies: (1) A columnar shape to ensure representative sampling with integrated water samplers for successful quantification of elemental standing stocks in the enclosed water body, (2) the exclusion of any ‘dead-volume’ with limited exchange to the sampled water body, creating a hidden source or sink for dissolved and particulate element pools, and (3) the quantitative collection of sinking PM for accurate vertical flux measurements of elements (Czerny et al., 2013; Riebesell et al., 2013). A columnar shape was adapted in almost all mesocosm designs since the ‘Large-Volume Plastic Sphere’ in the 1960’s (Strickland and Terhune, 1961) and dead-volumes inside mesocosms have been a rarity (Czerny et al., 2013). However, sinking PM inside the mesocosms was often not collected or not quantified. Cylindrical or funnel shaped particle collectors were suspended inside various mesocosm designs (von Bröckel, 1982; Svensen et al., 2001; Vadstein et al., 2012), but only covered a small fraction of the mesocosm diameter. Thus, they were prone to collection bias as observed in a mesocosm study by Schulz et al. (2008). Conical sediment traps, quantitatively collecting particles and sealing the lower end of columnar mesocosms, were implemented for the first time in the

1970s (Gamble et al., 1977; Menzel and Case, 1977) and adapted in modern pelagic mesocosm designs such as the second generation of the KOSMOS mesocosms (Riebesell et al., 2013) and the 'Large Clean Mesocosms' (Guieu et al., 2010). This sediment trap design guarantees quantitative collection of the downward particle flux and allows for accurate vertical flux measurements of elements inside mesocosm enclosures.

1.4 Thesis outline

1.4.1 Overview

The oceanic uptake of anthropogenic CO₂ slows down global warming but leads to gradual acidification of the ocean. OA is already known to affect marine biota from the organism to the ecosystem level but with largely unknown consequences for the cycling of elements. However, the ocean's ability to absorb anthropogenic C or to provide sufficient food for humankind depends on these oceanic material cycles. Therefore, it is crucial to assess how and to what extent the element cycles will be affected by OA.

Studies on the impact of OA on single plankton species or small-scale plankton assemblages have given us a first insight into how the most important cycles of C, N, and P might be influenced in the future. However, these studies largely ignored the interaction with natural stressors for plankton organisms such as competition for resources or grazing pressure that are omnipresent in the marine realm. Prediction of future biogeochemical cycling of elements requires involving as many interacting effects as possible, as the impact of OA via complex food webs can be hardly foreseen. The first studies that investigated OA effects on entire plankton communities *in situ* inside mesocosms were limited in their runtime (days to weeks) and often lacking sufficient measurement and characterisation of the biogeochemical pools and fluxes, especially the downward flux of PM.

Thus, the aim of this doctoral dissertation was to assess the impact of OA on biogeochemical cycles of C and nutrients in natural pelagic food webs of several trophic levels (up to fish larvae) and over extended time scales of several weeks to months. Large-scale pelagic mesocosms (up to 75 m³ per unit) that were deployed in different marine ecosystems were used and new methods were developed to quantify the downward flux of PM that allowed for mass balance calculations of elements under simulated OA.

This thesis focuses on results of three lead author manuscripts (Chapters 2 to 4) but also refers to several co-author papers (listed in the publication record, pp. 131 - 136) that are particularly relevant for this thesis.

Chapter 2 reports on a newly developed protocol for efficient sample recovery and processing of settling PM collected inside pelagic mesocosm sediment traps. The focus was set on quantitative collection of the downward particle flux and sample processing for highly accurate biogeochemical analysis and flux measurements. Different methods for sample concentration are described and discussed to illustrate their individual advantages and efficiencies. The developed techniques represent the basis for vertical flux measurements during the mesocosm studies of this thesis.

Chapter 3 presents an overview of the biogeochemical pools and fluxes during a long-term mesocosm study in Gullmar Fjord (Sweden). Here, the impact of OA on a coastal plankton community was assessed using ten pelagic mesocosms, each enclosing 50 m³. The natural winter-to-summer plankton succession and biogeochemical pool development was followed at ambient and realistic end-of-the-century CO₂ concentrations (~760 µatm *p*CO₂) over a time span of more than 100 days. For analysis we used a mass balance approach to investigate OA induced changes in the partitioning and cycling of C and nutrients. A particular focus was set on the transfer of biomass from primary producers to the higher trophic level of mesozooplankton and on the downward flux of the major elements.

In **Chapter 4** the C:N response of a natural plankton community to increasing CO₂ concentrations was assessed in eight pelagic mesocosms (75 m³) that were deployed in Raunefjord (Norway). We established a CO₂ gradient of up to 1615 µatm (*f*CO₂) and initiated a phytoplankton bloom. C:N ratios of suspended particle size fractions corresponding to pico-, nano-, and microplankton were measured as well as the C:N ratio of the downward particle flux collected at 25 m depth. Changes in the C:N stoichiometry were linked to the development of the enclosed plankton community and phytoplankton growth phases.

1.4.2 Thesis manuscripts and declaration of contribution

The chapters of this doctoral thesis are based on the following three manuscripts with scientific lead authorship:

Manuscript I

Boxhammer T, Bach LT, Czerny J, Riebesell U. Technical note: Sampling and processing of mesocosm sediment trap material for quantitative biogeochemical analysis. *Biogeosciences*. 2016;13:2849-2858. doi:10.5194/bg-13-2849-2016

Published in *Biogeosciences*

Idea and experimental design:	Tim Boxhammer, Jan Czerny, Ulf Riebesell
Data acquisition:	Tim Boxhammer
Data interpretation:	Tim Boxhammer with comments from Lennart T. Bach, Ulf Riebesell
Manuscript preparation:	Tim Boxhammer with comments from all co-authors

Manuscript II

Boxhammer T, Taucher J, Bach LT, Achterberg EP, Algueró-Muñiz M, Bellworthy J, Czerny J, Esposito M, Haunost M, Hellemann D, Ludwig A, Yong JC, Maren Z, Riebesell U, and Anderson LG. Enhanced transfer of organic matter to higher trophic levels caused by ocean acidification and its implications for export production: A mass balance approach.

Under revision in PLoS ONE

Idea and experimental design:	Ulf Riebesell, Tim Boxhammer, Leif G. Anderson
Data acquisition:	Tim Boxhammer, Maria Algueró-Muñiz, Jessica Bellworthy, Jan Czerny, Mario Esposito, Mathias Haunost, Dana Hellemann, Andrea Ludwig, Jan Taucher, Jaw Chuen Yong, Maren Zark, Leif G. Anderson
Data interpretation:	Tim Boxhammer with comments from Leif G. Anderson, Lennart T. Bach, Jan Taucher, Ulf Riebesell
Manuscript preparation:	Tim Boxhammer with comments from all co-authors

Manuscript III

Boxhammer T, Bach LT, Taucher J, Bellerby RGJ, Bermúdez Monsalve JR, Schulz KG, Schultz H, Sswat M, and Riebesell U. Plankton community structure controls the response of particulate organic matter stoichiometry to ocean acidification.

To be submitted

Idea and experimental design:	Ulf Riebesell, Lennart T. Bach, Tim Boxhammer
Data acquisition:	Tim Boxhammer, Richard G. J. Bellerby, J. Rafael Bermúdez Monsalve, Kai G. Schulz, Hendrik Schultz, Michael Sswat
Data interpretation:	Tim Boxhammer with comments from Lennart T. Bach, Kai G. Schulz, Jan Taucher, Ulf Riebesell
Manuscript preparation:	Tim Boxhammer with comments from all co-authors

References

- Armstrong RA, Peterson ML, Lee C, Wakeham SG. Settling velocity spectra and the ballast ratio hypothesis. *Deep Sea Res Part 2 Top Stud Oceanogr* 2009;56:1470-8. doi:10.1016/j.dsr2.2008.11.032.
- Arrigo KR. Marine microorganisms and global nutrient cycles. *Nature* 2005;437:349-55. doi:10.1038/nature04159.
- Azam F, Fenchel T, Field JG, Gray JS, Meyer-Reil LA, Thingstad F. The ecological role of water-column microbes in the sea. *Mar Ecol Prog Ser* 1983;10:257-63. doi:10.3354/meps010257.
- Bach LT, Boxhammer T, Larsen A, Hildebrandt N, Schulz KG, Riebesell U. Influence of plankton community structure on the sinking velocity of marine aggregates. *Global Biogeochem Cycles* 2016a;30:1145-65. doi:10.1002/(ISSN)1944-9224.
- Bach LT, Taucher J, Boxhammer T, Ludwig A, Achterberg EP, Algueró-Muñiz M, et al. Influence of ocean acidification on a natural winter-to-summer plankton succession: First insights from a long-term mesocosm study draw attention to periods of low nutrient concentrations. *PLoS ONE* 2016b;11:e0159068EP-. doi:10.1371/journal.pone.0159068.
- Bermúdez JR, Riebesell U, Larsen A, Winder M. Ocean acidification reduces transfer of essential biomolecules in a natural plankton community. *Sci Rep* 2016;6:27749EP. doi:10.1038/srep27749.
- von Bröckel K. Sedimentation of phytoplankton cells within controlled experimental ecosystems following launching, and implications for further enclosure studies. In: Grice GD, Reeve MR, editors. *Marine mesocosms*. New York, USA: Springer US; 1982, pp. 251-259. doi:10.1007/978-1-4612-5645-8_19.
- Bronk DA, See JH, Bradley P, Killberg L. DON as a source of bioavailable nitrogen for phytoplankton. *Biogeosciences* 2007;4:283-96. doi:10.5194/bg-4-283-2007.
- Burkhardt S, Zondervan I, Riebesell U. Effect of CO₂ concentration on C:N:P ratio in marine phytoplankton: A species comparison. *Limnol Oceanogr* 1999;44:683-90. doi:10.4319/lo.1999.44.3.0683.
- Calbet A. Mesozooplankton grazing effect on primary production: A global comparative analysis in marine ecosystems. *Limnol Oceanogr* 2001;46:1824-30. doi:10.4319/lo.2001.46.7.1824.

- Caldeira K, Wickett ME. Oceanography: Anthropogenic carbon and ocean pH. *Nature* 2003;425:365-5. doi:10.1038/425365a.
- Carlson CA, Hansell DA. DOM sources, sinks, reactivity, and budgets. In: Hansell DA, Carlson CA, editors. *Biogeochemistry of marine dissolved organic matter*. San Diego, USA: Elsevier; 2015, pp. 91-151. doi:10.1016/B978-0-12-405940-5.00003-0.
- Collins S, Rost B, Ryneerson TA. Evolutionary potential of marine phytoplankton under ocean acidification. *Evol Appl* 2014;7:140-55. doi:10.1111/eva.12120.
- Cotner JB, Wetzel RG. Uptake of dissolved inorganic and organic phosphorus compounds by phytoplankton and bacterioplankton. *Limnol Oceanogr* 1992;37:232-43. doi:10.4319/lo.1992.37.2.0232.
- Cripps G, Flynn KJ, Lindeque PK. Ocean acidification affects the phyto-zoo plankton trophic transfer efficiency. *PLoS ONE* 2016;11:e0151739. doi:10.1371/journal.pone.0151739.
- Crutzen PJ. Geology of mankind. *Nature* 2002;415:23-3. doi:10.1038/415023a.
- Cyronak T, Schulz KG, Jokiel PL. The Omega myth: What really drives lower calcification rates in an acidifying ocean. *ICES J Mar Sci* 2016;73:558-62. doi:10.1093/icesjms/fsv075.
- Czerny J, Schulz KG, Boxhammer T, Bellerby RGJ, Büdenbender J, Engel A, et al. Implications of elevated CO₂ on pelagic carbon fluxes in an Arctic mesocosm study - an elemental mass balance approach. *Biogeosciences* 2013;10:3109-25. doi:10.5194/bg-10-3109-2013.
- Doney SC, Fabry VJ, Feely RA, Kleypas JA. Ocean acidification: The other CO₂ problem. *Annu Rev Marine Sci* 2009;1:169-92. doi:10.1146/annurev.marine.010908.163834.
- Ducklow HW, Carlson CA. Oceanic bacterial production. In: Marshall KC, editor. *Advances in microbial ecology*, vol. 12. New York, USA: Springer; 1992, pp. 113-81. doi:10.1007/978-1-4684-7609-5_3.
- Dupont S, Thorndyke MC. Impact of CO₂-driven ocean acidification on invertebrates early life-history - What we know, what we need to know and what we can do. *Biogeosciences Discuss* 2009;6:3109-31. doi:10.5194/bgd-6-3109-2009.

- Dutkiewicz S, Morris JJ, Follows MJ, Scott J, Levitan O, Dyhrman ST, et al. Impact of ocean acidification on the structure of future phytoplankton communities. *Nat Clim Chang* 2015;5:1002-6. doi:10.1038/NCLIMATE2722.
- Eichner M, Rost B, Kranz SA. Diversity of ocean acidification effects on marine N₂ fixers. *J Exp Mar Bio Ecol* 2014;457:199-207. doi:10.1016/j.jembe.2014.04.015.
- Egleston ES, Sabine CL, Morel FMM. Revelle revisited: Buffer factors that quantify the response of ocean chemistry to changes in DIC and alkalinity. *Global Biogeochem Cycles* 2010;24:1-9. doi:10.1029/2008GB003407.
- Endres S, Galgani L, Riebesell U, Schulz KG, Engel A. Stimulated bacterial growth under elevated pCO₂: Results from an off-shore mesocosm study. *PLoS ONE* 2014;9:e99228-8. doi:10.1371/journal.pone.0099228.
- Fabry VJ, Seibel BA, Feely RA, Orr JC. Impacts of ocean acidification on marine fauna and ecosystem processes. *ICES J Mar Sci* 2008;65:414-32. doi:10.1093/icesjms/fsn048.
- Falkowski PG, Greene RM, Geider RJ. Physiological limitations on phytoplankton productivity in the ocean. *Oceanography* 1992;5:84-91. doi:10.5670/oceanog.1992.14.
- Falkowski PG. Rationalizing elemental ratios in unicellular algae. *J Phycol* 2000;36:3-6. doi:10.1046/j.1529-8817.2000.99161.x.
- Fenchel TM, Jørgensen BB. Detritus food chains of aquatic ecosystems: The role of bacteria. In: Alexander M, editor. *Advances in microbial ecology*, vol. 1. New York, USA: Springer; 1977, pp. 1-58. doi:10.1007/978-1-4615-8219-9_1.
- Feely RA, Sabine CL, Lee K, Berelson W, Kleypas J, Fabry VJ, et al. Impact of anthropogenic CO₂ on the CaCO₃ system in the oceans. *Science* 2004;305:362-6. doi:10.1126/science.1097329.
- Feely RA, Doney SC, Cooley SR. Ocean Acidification. *Oceanography* 2009;22:36-47. doi:10.5670/oceanog.2009.95.
- Field CB, Behrenfeld MJ, Randerson JT, Falkowski PG. Primary production of the biosphere: Integrating terrestrial and oceanic components. *Science* 1998;281:237-40. doi:10.1126/science.281.5374.237.

- Finkel ZV, Beardall J, Flynn KJ, Quigg A, Rees TAV, Raven JA. Phytoplankton in a changing world: Cell size and elemental stoichiometry. *J Plankton Res* 2010;32:119-37. doi:10.1093/plankt/fbp098.
- Francois R, Honjo S, Krishfield R, Manganini S. Factors controlling the flux of organic carbon to the bathypelagic zone of the ocean. *Global Biogeochem Cycles* 2002;16:1-20. doi:10.1029/2001GB001722.
- Gamble JC, Davies JM, Steele JH. Loch Ewe bag experiment, 1974. *Bull Mar Sci* 1977;27:146-75.
- Gattuso J-P, Hansson L. Ocean acidification: Background and history. In: Gattuso J-P, Hansson L, editors. *Ocean acidification*, New York, USA: 2011, pp. 1-20.
- Geider RJ, La Roche J. Redfield revisited: Variability of C:N:P in marine microalgae and its biochemical basis. *Eur J Phycol* 2002;37:1-17. doi:10.1017/S0967026201003456.
- Global Carbon Project. [Internet]. 2016 [cited 1 November 2017]. Available from: http://www.globalcarbonproject.org/carbonbudget/archive/2016/GCP_CarbonBudget_2016.pdf
- Granéli E, Carlsson P, Legrand C. The role of C, N and P in dissolved and particulate organic matter as a nutrient source for phytoplankton growth, including toxic species. *Aquat Ecol* 1999;33:17-27. doi:10.1023/A:1009925515059.
- Grossart H-P, Allgaier M, Passow U, Riebesell U. Testing the effect of CO₂ concentration on the dynamics of marine heterotrophic bacterioplankton. *Limnol Oceanogr* 2006;51:1-11. doi:10.4319/lo.2006.51.1.0001.
- Guieu C, Dulac F, Desboeufs K, Wagener T, Pulido-Villena E, Grisoni JM, et al. Large clean mesocosms and simulated dust deposition: A new methodology to investigate responses of marine oligotrophic ecosystems to atmospheric inputs. *Biogeosciences* 2010;7:2765-84. doi:10.5194/bg-7-2765-2010.
- Guieu C, Dulac F, Ridame C, Pondaven P. Introduction to project DUNE, a DUST experiment in a low Nutrient, low chlorophyll Ecosystem. *Biogeosciences* 2014;11:425-42. doi:10.5194/bg-11-425-2014.
- Hattori A, Koike I, Ohtsu M, Goering JJ. Uptake and regeneration of nitrogen in controlled aquatic ecosystems and the effects of copper on these processes. *Bull Mar Sci* 1980;30:431-443.

- Hendriks IE, Duarte CM, Alvarez M. Vulnerability of marine biodiversity to ocean acidification: A meta-analysis. *Estuar Coast Shelf Sci* 2010;86:157-64. doi:10.1016/j.ecss.2009.11.022.
- Henson SA, Sanders R, Madsen E. Global patterns in efficiency of particulate organic carbon export and transfer to the deep ocean. *Global Biogeochem Cycles* 2012a;26:1-14. doi:10.1029/2011GB004099.
- Henson S, Lampitt R, Johns D. Variability in phytoplankton community structure in response to the North Atlantic Oscillation and implications for organic carbon flux. *Limnol Oceanogr* 2012b;57:1591-601. doi:10.4319/lo.2012.57.6.1591.
- Ho T-Y, Quigg A, Finkel ZV, Milligan AJ, Wyman K, Falkowski PG, et al. The elemental composition of some marine phytoplankton. *J Phycol* 2003;39:1145-59. doi:10.1111/j.0022-3646.2003.03-090.x.
- Hönisch B, Ridgwell A, Schmidt DN, Thomas E, Gibbs SJ, Sluijs A, et al. The geological record of ocean acidification. *Science* 2012;335:1058-63. doi:10.1126/science.1208277.
- Hutchins DA, Mulholland MR, Fu F. Nutrient cycles and marine microbes in a CO₂-enriched ocean. *Oceanography* 2009;22:128-45. doi:10.5670/oceanog.2009.103.
- IPCC, 2014: *Climate Change 2014: Synthesis Report. Contribution of Working Groups I, II and III to the Fifth Assessment Report of the Intergovernmental Panel on Climate Change* [Core Writing Team, R.K. Pachauri and L.A. Meyer (editors)]. IPCC, Geneva, Switzerland: 2014, 151 pp.
- Joint I, Doney SC, Karl DM. Will ocean acidification affect marine microbes? *Isme J* 2010;5:1-7. doi:10.1038/ismej.2010.79.
- Joos F, Spahni R. Rates of change in natural and anthropogenic radiative forcing over the past 20,000 years. *Proc Natl Acad Sci U S A* 2008;105:1425-30. doi:10.1073/pnas.0707386105.
- Jury PC, Thomas IF, Atkinson JM, Toonen JR. Buffer capacity, ecosystem feedbacks, and seawater chemistry under global change. *Water* 2013;5:1303-25. doi:10.3390/w5031303.
- Kjørboe T. Colonization of marine snow aggregates by invertebrate zooplankton: Abundance, scaling, and possible role. *Limnol Oceanogr* 2000;45:479-84. doi:10.4319/lo.2000.45.2.0479.

- Klausmeier CA, Litchman E, Daufresne T, Levin SA. Optimal nitrogen-to-phosphorus stoichiometry of phytoplankton. *Nature* 2004;429:171-4. doi:10.1038/nature02454.
- Krause E, Wichels A, Giménez L, Lunau M, Schilhabel MB, Gerdts G. Small changes in pH have direct effects on marine bacterial community composition: A microcosm approach. *PLoS ONE* 2012;7:e47035. doi:10.1371/journal.pone.0047035.
- Kroeker KJ, Kordas RL, Crim RN, Singh GG. Meta-analysis reveals negative yet variable effects of ocean acidification on marine organisms. *Ecol Lett* 2010;13:1419-34. doi:10.1111/j.1461-0248.2010.01518.x.
- Kroeker KJ, Kordas RL, Crim R, Hendriks IE, Ramajo L, Singh GS, et al. Impacts of ocean acidification on marine organisms: Quantifying sensitivities and interaction with warming. *Glob Change Biol* 2013;19:1884-96. doi:10.1111/gcb.12179.
- Landry MR, Hassett RP. Estimating the grazing impact of marine micro-zooplankton. *Mar Biol* 1982;67:283-8. doi:10.1007/BF00397668.
- Le Quéré C, Andrew RM, Canadell JG, Sitch S, Korsbakken JI, Peters GP, et al. Global carbon budget 2016. *Earth Syst Sci Data* 2016;8:605-49. doi:10.5194/essd-8-605-2016.
- Lewis SL, Maslin MA. Defining the Anthropocene. *Nature* 2015;519:171-80. doi:10.1038/nature14258.
- von Liebig J. *Die Grundsätze der Agricultur-Chemie mit Rücksicht auf die in England angestellten Untersuchungen*. Braunschweig, Germany: Vieweg und Sohn; 1855, 152 pp.
- Lohbeck KT, Riebesell U, Reusch TBH. Adaptive evolution of a key phytoplankton species to ocean acidification. *Nat Geosci* 2012;5:1-6. doi:10.1038/ngeo1441.
- Lüthi D, Le Floch M, Bereiter B, Blunier T, Barnola J-M, Siegenthaler U, et al. High-resolution carbon dioxide concentration record 650,000-800,000 years before present. *Nature* 2008;453:379-82. doi:10.1038/nature06949.
- Manno C, Bednaršek N, Tarling GA, Peck VL, Comeau S, Adhikari D, et al. Shelled pteropods in peril: Assessing vulnerability in a high CO₂ ocean. *Earth-Science Reviews* 2017;169 IS -:132-45. doi:10.1016/j.earscirev.2017.04.005.

- Martiny AC, Pham CTA, Primeau FW, Vrugt JA, Moore JK, Levin SA, et al. Strong latitudinal patterns in the elemental ratios of marine plankton and organic matter. *Nat Geosci* 2013;6:279-83. doi:10.1038/ngeo1757.
- Martiny AC, Vrugt JA, Lomas MW. Concentrations and ratios of particulate organic carbon, nitrogen, and phosphorus in the global ocean. *Sci Data* 2014;1:140048-7. doi:10.1038/sdata.2014.48.
- Menzel DW, Case J. Concept and design: Controlled ecosystem pollution experiment. *Bull Mar Sci* 1977;27:1-7.
- Monroy P, Hernández-García E, Rossi V, López C. Modeling the dynamical sinking of biogenic particles in oceanic flow. *Nonlinear Process Geophys* 2017;24:293-305. doi:10.5194/npg-24-293-2017.
- Odum EP. The Mesocosm. *Bioscience* 1984;34:558-62. doi:10.2307/1309598.
- Orr JC, Fabry VJ, Aumont O, Bopp L, Doney SC, Feely RA, et al. Anthropogenic ocean acidification over the twenty-first century and its impact on calcifying organisms. *Nature* 2005;437:681-6. doi:10.1038/nature04095.
- Passow U, Carlson CA. The biological pump in a high CO₂ world. *Mar Ecol Prog Ser* 2012;470:249-71. doi:10.3354/meps09985.
- Petit JR, Jouzel J, Raynaud D, Barkov NI, Barnola JM, Basile I, et al. Climate and atmospheric history of the past 420,000 years from the Vostok ice core, Antarctica. *Nature* 1999;399:429-36. doi:10.1038/20859.
- Ploug H, Grossart H-P, Azam F, Jørgensen BB. Photosynthesis, respiration, and carbon turnover in sinking marine snow from surface waters of Southern California Bight: Implications for the carbon cycle in the ocean. *Mar Ecol Prog Ser* 1999;179:1-11. doi:10.2307/24851936.
- Pörtner HO, Karl D, Boyd PW, Cheung W, Lluch-Cota SE, Nojiri Y, et al. Ocean systems. In: Field CB, Barros VR, Dokken DJ, Mach KJ, Mastrandrea MD, Bilir TE, et al., editors. *Climate Change 2014: Impacts, Adaptation, and Vulnerability. Part A: Global and Sectoral Aspects. Contribution of Working Group II to the Fifth Assessment Report of the Intergovernmental Panel of Climate Change*. Cambridge, United Kingdom and New York, USA: Cambridge University Press; 2014, pp. 411-484.

- Quigg A, Finkel ZV, Irwin AJ, Rosenthal Y, Ho T-Y, Reinfelder JR, et al. The evolutionary inheritance of elemental stoichiometry in marine phytoplankton. *Nature* 2003;425:291-4. doi:10.1038/nature01953.
- Raven JA, Caldeira K, Elderfield H, Hoegh-Guldberg O, Liss PS, Riebesell U, et al. *Ocean acidification due to increasing atmospheric carbon dioxide*. London, UK: The Royal Society; 2005. ISBN 0-85403-617-2.
- Redfield AC. On the proportions of organic derivatives in sea water and their relation to the composition of plankton. In: Daniel RJ, editor. *James Johnstone memorial volume*. Universit Press of Liverpool, UK; 1934; 176-192.
- Redfield AC, Ketchum BH, Richards FA. The influence of organisms on the composition of seawater. In: Hill MN, editor. *The composition of seawater: Comparative and descriptive oceanography. The sea: Ideas and observations on progress in the study of the seas, 2*. New York, USA: Interscience Publishers; 1963, pp. 26-77.
- Rhee G-Y. Effects of N:P atomic ratios and nitrate limitation on algal growth, cell composition, and nitrate uptake. *Limnol Oceanogr* 1978;23:10-25. doi:10.4319/lo.1978.23.1.0010.
- Rhein M, Rintoul SR, Aoki S, Campos E, Chambers D, Feely RA, et al. *Observations: Ocean. Climate change the physical science basis. Contribution of working group I to the fifth assessment report of the Intergovernmental Panel on Climate Change*. [Stocker, T.F., D. Qin, G.-K. Plattner, M. Tignor, S.K. Allen, J. Boschung, et al. (editors)]. Cambridge, UK and New York, USA: Cambridge University Press; 2013.
- Riebesell U, Lee K, Nejstgaard JC. Pelagic mesocosms. In: Riebesell U, Fabry VJ, Hansson L, Gattuso J-P, editors. *Guide to best practices in ocean acidification research and data reporting*, Luxembourg: Publications Office of the European Union; 2010, pp. 95-112. doi:10.2777/58454.
- Riebesell U, Tortell D. Effects of ocean acidification on pelagic organisms and ecosystems. In: Gattuso J-P, Hansson L, editors. *Ocean acidification*, New York, USA: Oxford University Press Inc; 2011, pp. 99-121. ISBN:978-0-19-959109-1.
- Riebesell U, Czerny J, von Bröckel K, Boxhammer T, Büdenbender J, Deckelnick M, et al. *Technical Note: A mobile sea-going mesocosm system - new opportunities for ocean change research*. *Biogeosciences* 2013;10:1835-47. doi:10.5194/bg-10-1835-2013.

- Riebesell U, Bach LT, Bellerby RGJ, Bermúdez Monsalve JR, Boxhammer T, Czerny J, et al. Competitive fitness of a predominant pelagic calcifier impaired by ocean acidification. *Nat Geosci* 2017;10:19-23. doi:10.1038/NGEO2854.
- Rossoll D, Bermúdez Monsalve JR, Hauss H, Schulz KG, Riebesell U, Sommer U, et al. Ocean acidification-induced food quality deterioration constrains trophic transfer. *PLoS ONE* 2012;7:e34737-6. doi:10.1371/journal.pone.0034737.
- Sala MM, Aparicio FL, Balagué V, Boras JA, Borrull E, Cardelús C, et al. Contrasting effects of ocean acidification on the microbial food web under different trophic conditions. *ICES J Mar Sci* 2015;73:670-9. doi:10.1093/icesjms/fsv130.
- Sarmiento JL, Gruber N. *Ocean biogeochemical dynamics*. Princeton, New Jersey, USA: Princeton University Press; 2006. 503 pp. ISBN:0-691-01707-7
- Scheinin M, Riebesell U, Rynearson TA, Lohbeck KT, Collins S. Experimental evolution gone wild. *J R Soc Interface* 2015;12:20150056-6. doi:10.1098/rsif.2015.0056.
- Schoo KL, Malzahn AM, Krause E, Boersma M. Increased carbon dioxide availability alters phytoplankton stoichiometry and affects carbon cycling and growth of a marine planktonic herbivore. *Mar Biol* 2012;160:2145-55. doi:10.1007/s00227-012-2121-4.
- Schulz KG, Riebesell U, Bellerby RGJ, Biswas H, Meyerhöfer M, Müller MN, et al. Build-up and decline of organic matter during PeECE III. *Biogeosciences* 2008;5:707-18. doi:10.5194/bg-5-707-2008.
- Schulz KG, Bellerby RGJ, Brussaard CPD, Büdenbender J, Czerny J, Engel A, et al. Temporal biomass dynamics of an Arctic plankton bloom in response to increasing levels of atmospheric carbon dioxide. *Biogeosciences* 2013;10:161-80. doi:10.5194/bg-10-161-2013.
- Schulz KG, Bach LT, Bellerby RGJ, Bermúdez Monsalve JR, Büdenbender J, Boxhammer T, et al. Phytoplankton blooms at increasing levels of atmospheric carbon dioxide: Experimental evidence for negative effects on prymnesiophytes and positive on small picoeukaryotes. *Front Mar Sci* 2017;4:1-18. doi:10.3389/fmars.2017.00064.
- Stoecker DK, Hansen PJ, Caron DA, Mitra A. Mixotrophy in the marine plankton. *Annu Rev Marine Sci* 2017;9:311-35. doi:10.1146/annurev-marine-010816-060617.

- Strickland JDH, Terhune LDB. The study of *in-situ* marine photoynthesis using a large plastic bag. *Limnol Oceanogr* 1961;6:93-6. doi:10.4319/lo.1961.6.1.0093.
- Strickland JDH. Phytoplankton and marine primary production. *Annu Rev Microbiol* 1965;19:127-62. doi:10.1146/annurev.mi.19.100165.001015.
- Svensen C, Egge JK, Stiansen JE. Can silicate and turbulence regulate the vertical flux of biogenic matter? A mesocosm study. *Mar Ecol Prog Ser* 2001;217:67-80. doi:10.3354/meps217067.
- Taucher J, Bach LT, Boxhammer T, Nauendorf A, Achterberg EP, Algueró-Muñiz M, et al. Influence of ocean acidification and deep water upwelling on oligotrophic plankton communities in the subtropical North Atlantic: Insights from an *in situ* mesocosm study. *Front Mar Sci* 2017;4:1-18. doi:10.3389/fmars.2017.00085.
- The Keeling Curve. [Internet]. 2017 [cited 8 December 2017]. Available from: <https://scripps.ucsd.edu/programs/keelingcurve/>
- Thornton DCO. Dissolved organic matter (DOM) release by phytoplankton in the contemporary and future ocean. *Eur J Phycol* 2014;49:20-46. doi:10.1080/09670262.2013.875596.
- Tréguer P, Nelson DM, Van Bennekom AJ, DeMaster DJ, Leynaert A, Quéguiner B. The silica balance in the world ocean: A reestimate. *Science* 1995;268:375-9. doi:10.1126/science.268.5209.375.
- Twining BS, Baines SB. The trace metal composition of marine phytoplankton. *Annu Rev Marine Sci* 2013;5:191-215. doi:10.1146/annurev-marine-121211-172322.
- Vadstein O, Andersen T, Reinertsen HR, Olsen Y. Carbon, nitrogen and phosphorus resource supply and utilisation for coastal planktonic heterotrophic bacteria in a gradient of nutrient loading. *Mar Ecol Prog Ser* 2012;447:55-75. doi:10.3354/meps09473.
- Volk T, Hoffert MI. Ocean carbon pumps: Analysis of relative strengths and efficiencies in ocean-driven atmospheric CO₂ changes. In: Sundquist ET, Broecker WS, editors. *The carbon cycle and atmospheric CO₂: Natural variations archean to present*, vol. 35B, Washington D. C., USA: American Geophysical Union; 2013, pp. 99-110. doi:10.1029/GM032p0099.
- van Vuuren DP, Edmonds J, Kainuma M, Riahi K, Thomson A, Hibbard K, et al. The representative concentration pathways: An overview. *Clim Change* 2011;109:5-31. doi:10.1007/s10584-011-0148-z.

Zeebe RE. History of seawater carbonate chemistry, atmospheric CO₂, and ocean acidification. *Annu Rev Earth Planet Sci* 2012;40:141-65. doi:10.1146/annurev-earth-042711-105521.

2. Manuscript I

Technical note: Sampling and processing of mesocosm sediment trap material for quantitative biogeochemical analysis

T Boxhammer^{1*}, LT Bach¹, J Czerny¹, and U Riebesell¹

Published in Biogeosciences^{**}

¹GEOMAR Helmholtz Centre for Ocean Research Kiel, Kiel, Germany

*corresponding author: tboxhammer@geomar.de (T Boxhammer)

** manuscript formatted in style of journal

Biogeosciences, 13, 2849–2858, 2016
 www.biogeosciences.net/13/2849/2016/
 doi:10.5194/bg-13-2849-2016
 © Author(s) 2016. CC Attribution 3.0 License.



Technical note: Sampling and processing of mesocosm sediment trap material for quantitative biogeochemical analysis

Tim Boxhammer, Lennart T. Bach, Jan Czerny, and Ulf Riebesell

GEOMAR Helmholtz Centre for Ocean Research Kiel, Düsterbrookweg 20, 24105 Kiel, Germany

Correspondence to: Tim Boxhammer (tboxhammer@geomar.de)

Received: 28 October 2015 – Published in Biogeosciences Discuss.: 23 November 2015

Revised: 6 April 2016 – Accepted: 26 April 2016 – Published: 13 May 2016

Abstract. Sediment traps are the most common tool to investigate vertical particle flux in the marine realm. However, the spatial and temporal decoupling between particle formation in the surface ocean and particle collection in sediment traps at depth often handicaps reconciliation of production and sedimentation even within the euphotic zone. Pelagic mesocosms are restricted to the surface ocean, but have the advantage of being closed systems and are therefore ideally suited to studying how processes in natural plankton communities influence particle formation and settling in the ocean's surface. We therefore developed a protocol for efficient sample recovery and processing of quantitatively collected pelagic mesocosm sediment trap samples for biogeochemical analysis. Sedimented material was recovered by pumping it under gentle vacuum through a silicon tube to the sea surface. The particulate matter of these samples was subsequently separated from bulk seawater by passive settling, centrifugation or flocculation with ferric chloride, and we discuss the advantages and efficiencies of each approach. After concentration, samples were freeze-dried and ground with an easy to adapt procedure using standard lab equipment. Grain size of the finely ground samples ranged from fine to coarse silt (2–63 μm), which guarantees homogeneity for representative subsampling, a widespread problem in sediment trap research. Subsamples of the ground material were perfectly suitable for a variety of biogeochemical measurements, and even at very low particle fluxes we were able to get a detailed insight into various parameters characterizing the sinking particles. The methods and recommendations described here are a key improvement for sediment trap applications in mesocosms, as they facilitate the processing of large amounts of samples and allow for high-quality biogeochemical flux data.

1 Introduction

Sediment traps of various designs have been the most common tool to study vertical particle flux in the oceans since the middle of the last century (Bloesch and Burns, 1980). During this period, the impact of anthropogenic pollution and climate change on marine biogeochemical cycles has grown steadily (Doney, 2010). Pelagic mesocosm systems enclose natural plankton communities in a controlled environment (Lalli, 1990; Riebesell et al., 2011) and allow us to investigate how changing environmental factors influence elemental cycling in the ocean's surface. The closed nature of these systems makes them particularly useful to investigate plankton community processes that quantitatively and qualitatively determine particle formation and settling. Cylindrical or funnel-shaped particle traps were suspended inside various pelagic mesocosm designs (Schulz et al., 2008; Svensen et al., 2001; Vadstein et al., 2012; von Bröckel, 1982). Covering only a small section of the mesocosm's diameter, they were prone to potential collection bias also well-known from oceanic particle traps, in particular in the upper ocean (Buesseler, 1991).

To study vertical particle flux in mesocosms it is essential to achieve the collection of all particles settling to the bottom. This not only improves the measurement accuracy but also drains the material from the pelagic system, as is the case in a naturally stratified water body. Different pelagic mesocosm designs like the Controlled Ecosystem Enclosures (CEE; Menzel and Case, 1977), the “large clean mesocosms” (Guieu et al., 2010), or the Kiel Off-Shore Mesocosms for future Ocean Simulations (KOSMOS; Riebesell et al., 2013) achieved the quantitative collection of settling particles through the cone-shaped bottom of the columnar enclosures. Two different techniques were generally used to sam-

ple collected material of these sediment traps: (1) replaceable collection cups or polyethylene bottles, regularly exchanged by divers (Gamble et al., 1977; Guieu et al., 2010); (2) an extraction tube reaching down to the particle collector (Jinping et al., 1992; Menzel and Case, 1977; Riebesell et al., 2013).

The key difficulty of sediment trap applications in pelagic mesocosms is the sample processing after recovery. Depending on the setup (number of enclosures, trap design, sampling frequency, experiment duration), samples are high in number, relatively large in volume (up to several litres), and can reach extremely high particle densities during aggregation events.

In the past the collected material was usually only partly characterized to answer specific questions (e.g. Harrison and Davies, 1977; Huasheng et al., 1992; Olsen et al., 2007), while the full potential of the samples remained unexplored and the methodology of sample processing was commonly described in little detail. To fill this gap and to facilitate a broader biogeochemical analysis of the collected material, we refined methods for efficient sampling, particle concentrating, and processing of quantitatively collected mesocosm sediment trap samples. Our primary objective was the development of an efficient and easy to adopt protocol, which enables a comprehensive and accurate characterization of the vertical particle flux within pelagic mesocosms. The methods described in this paper were developed and applied during KOSMOS studies from 2010 until spring 2014 covering five different marine ecosystems at diverse stages in the succession of the enclosed plankton communities.

2 Protocol for sampling and processing

2.1 Sampling strategy

The sediment trap design of KOSMOS used since 2011 consists of a flexible thermoplastic polyurethane (TPU) funnel of 2 m in diameter, connected to the cylindrical mesocosm bag by a silicon-rubber-sealed glass fibre flange (Fig. 1a). A detailed description of the KOSMOS setup and maintenance requirements such as wall cleaning can be found in Riebesell et al. (2013). Settling particles are quantitatively collected on the 7 m² funnel surface, where they slide down at a 63° angle into the collecting cylinder, which has a volume of 3.1 L (Fig. 1b). A silicon tube of 1 cm inner diameter reaches down to the collecting cylinder outside of the mesocosm bag (Fig. 1a). A hose connector links the silicon tube to the conical bottom end of the collector, while a wire helix hose coating the first 1.5 m prevents current-related bending of the tube (Fig. 1b). The silicon tube itself is only connected to the bottom of the mesocosm and fixed to the floating frame above the sea surface to avoid any kinks (Fig. 1a). To empty the collecting cylinders, we connected 5 L Schott Duran® glass bottles via a Plexiglas® pipe to the silicon tubes attached to the floating mesocosm frames (Fig. 1b; Boxhammer et al., 2015). A slight vacuum

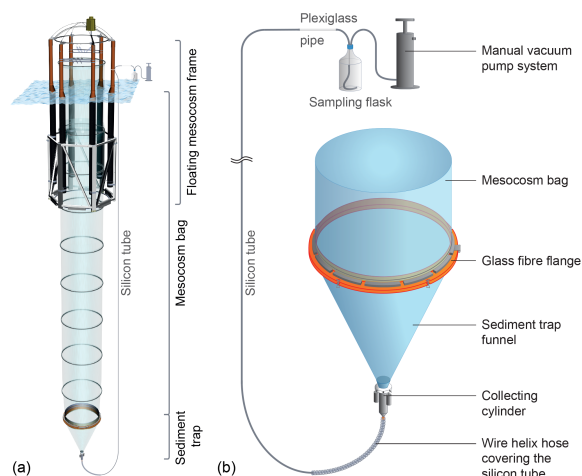


Figure 1. Panel (a): technical drawing of the KOSMOS flotation frame with unfolded TPU enclosure bag and attached funnel-shaped sediment trap. Panel (b): a silicon tube connects the collecting cylinder at the tip of the sediment trap with a 5 L sampling flask. A wire-reinforced hose prevents current-related bending of the first 1.5 m. Particles can be easily detected in the Plexiglas® pipe linking the silicon tube with the sampling flask.

of ~ 300 mbar was built up in the glass bottles by means of a manual kite surf pump to cause gentle suction of the water inside the silicon tubes (step 1 in Fig. 2). When first particles appeared in the Plexiglas® pipe, the sampling process was briefly interrupted and seawater in the bottles was screened for particles and only discarded if clear. The dense particle suspensions originating from the collecting cylinders were then vacuum-pumped into the sampling flasks until no more particles were passing through the Plexiglas® pipe in a sampled extra volume of about 0.5 L (Boxhammer et al., 2015).

Subsamples of sediment trap material for measurements such as zooplankton contribution (Niehoff et al., 2013), particle sinking velocity (Bach et al., 2012) or respiration rates of particle-colonizing bacteria were taken with a pipette after sample collection but prior to the processing of the bulk sample for biogeochemical analysis. For this the particle suspension (~ 1–4 L) was gently mixed and subsample volumes withdrawn immediately before resuspended particles were able to settle down. The total volume of all subsamples should be kept low (ideally below 5 %) in order to limit the subsampling bias on the remaining sample that is processed for quantitative biogeochemical analysis. We occasionally noticed a patchy distribution of particles within the sampling bottles despite the mixing, but we consider this subsampling bias to be rather small because the subsample volume was usually large enough to tolerate a certain degree of sample heterogeneity. Quantities of the main sample and all subsamples were gravimetrically determined with an accuracy of 0.1 g for individual share calculations.

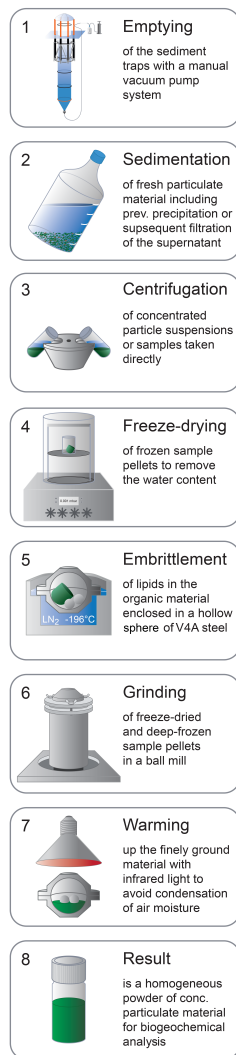


Figure 2. Protocol of mesocosm sediment trap sampling (1), particle concentration (2–3), freeze-drying (4), and grinding (5–8) to convert heterogeneous sediment trap samples into homogeneous powder for biogeochemical analysis.

2.2 Separating particles from bulk seawater

Particulate material recovered from the mesocosm sediment traps and transferred into sampling flasks needs to be separated from bulk seawater collected during the sampling procedure. In this section we describe three different methods for separating particles from bulk seawater, as this was the most critical and time-intensive step in the sampling procedure.

The particle concentration efficiency (%) of the three methods (Sects. 2.2.1–2.2.3) was determined as the percentage of total particulate carbon (TPC) concentrated in the pro-

cessed samples in relation to the sum of concentrated and residual TPC in the remaining bulk water. Residual TPC in the bulk water was determined from subsamples that were filtered on combusted GF/F filters (Whatman; $0.7\ \mu\text{m}$ pore size, $450\ ^\circ\text{C}$, 6 h) with a gentle vacuum ($< 200\ \text{mbar}$) and stored in combusted glass petri dishes ($450\ ^\circ\text{C}$, 6 h) at $-20\ ^\circ\text{C}$. Copepods, which could occasionally be found in the liquid, were carefully removed from the filters right after filtration. The filters were oven-dried at $60\ ^\circ\text{C}$ over night, packed into tin foil, and stored in a desiccator until analysis. Combusted GF/F filters without filtered supernatant were included as blanks and measured alongside with the sample filters. The carbon and nitrogen content of the concentrated and subsequently dried and ground bulk material (processing procedure described in Sects. 2.3 and 2.4) was analysed from subsamples of $2 \pm 0.25\ \text{mg}$ in tin capsules ($5 \times 9\ \text{mm}$, Hekatech). For this, subsamples were directly transferred into the tin capsules and weight was determined on a microbalance (M2P, Satorius) with an accuracy of $0.001\ \text{mg}$. All samples were measured with an elemental analyser (Euro EA–CN, Hekatech), which was calibrated with acetanilide ($\text{C}_8\text{H}_9\text{NO}$) and soil standard (Hekatech, catalogue no. HE33860101) prior to each measurement run.

2.2.1 Separating particles from bulk seawater by passive settling

Particles were allowed to settle for 2 h in 5 L glass bottles in darkness at in situ water temperature before separating the supernatant liquid. After this sedimentation period the supernatant was removed and transferred into separate vacuum bottles by means of a 10 mL pipette connected to a vacuum pump (Czerny et al., 2013; Gamble et al., 1977). We found the removal of the supernatant to be most efficient when glass bottles were stored at a 60° angle so that particles could accumulate at the bottom edge of the bottles (step 2 in Fig. 2). The dense particle suspension at the bottom of the glass bottles was concentrated in 110 mL tubes by centrifugation for 10 min at $5039 \times g$ (3K12 centrifuge, Sigma) to form compact sediment pellets (step 3 in Fig. 2). These pellets were then frozen at $-30\ ^\circ\text{C}$. A cable tie with its tip bent at a 90° angle was stuck into each sample before freezing in order to enable easy recovery of the material from the centrifugation tubes. The frozen samples were transferred to plastic screw cap jars (40–80 mL) for preservation and storage in the dark at $-30\ ^\circ\text{C}$ before freeze-drying (Sect. 2.3).

Separating particulate material from the liquid by passive gravitational settling resulted in a median concentration efficiency of 92.9%. The relatively wide range of scores (99.3–86.8%) reflects a nonideal reproducibility of this particle concentration method (Fig. 3, green). The applied sedimentation period of 2 h was occasionally not long enough for small or low-density particles to settle. To increase the concentration efficiency of passive settling, longer sedimentation periods of up to 48 h, e.g. for single plankton cells would be

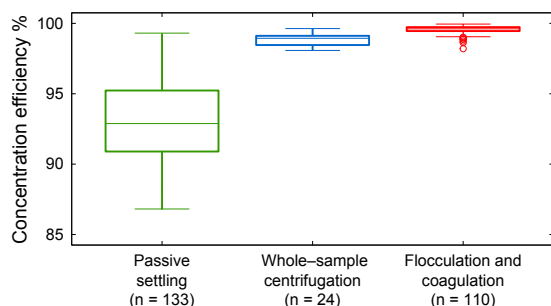


Figure 3. Box plot of the concentration efficiency (%) of three different methods for particle concentration of mesocosm sediment trap samples. Concentration of particles by passive settling (green) is compared with gravitational deposition of particulates by whole-sample centrifugation (blue). The third option of flocculation and coagulation with FeCl_3 for enhanced particle settling is presented in red. Concentration efficiency is defined as the percentage of TPC concentrated in the processed sediment trap samples in relation to the particulate carbon in the originally sampled suspensions (sum of concentrated and residual TPC in the bulk water). Outliers (circles) are defined as any data points below $1.5 \times \text{IQR}$ (interquartile range) of the first quartile hinge or above $1.5 \times \text{IQR}$ of the third quartile hinge.

required. However, this is not practical at high sampling frequencies for a set of several mesocosms and would require poisoning of the samples to inhibit microbial degradation of organic matter.

2.2.2 Separating particles from bulk seawater by whole-sample centrifugation

Centrifuging the entire sample volume, which is usually between 1 and 4 L, can considerably enhance gravitational separation of particles from bulk seawater. This procedure requires a large-volume centrifuge that is not necessarily standard lab equipment and difficult to take out into the field due to its high weight. For this approach we transferred particle suspensions originating from the sediment traps directly from the 5 L sampling flasks into 800 mL centrifuge beakers. The separation of particulate material was achieved within 10 min at $5236 \times g$ using a 6-16KS centrifuge (Sigma), followed by slow deceleration to avoid resuspension of particles (step 3 in Fig. 2). The supernatant was then carefully decanted and collected for filtration, while the sample pellets were transferred into 110 mL centrifuge tubes. This procedure was repeated until the 5 L sampling flasks were emptied. In a second step of centrifugation for 10 min at $5039 \times g$ in the small tubes (3K12, Sigma) samples were compressed into compact sediment pellets which can be frozen and stored in plastic screw cap jars as described in Sect. 2.2.1.

Whole-sample centrifugation resulted in a high concentration efficiency of particles with a median of 98.9 % and a low

variability (98.1–99.6 %), indicating the high reproducibility of this method (Fig. 3, blue).

2.2.3 Concentrating samples by flocculation and coagulation of particles

Ferric chloride (FeCl_3) is well known as a flocculant and coagulant in sewage treatment (Amokrane et al., 1997; Renou et al., 2008) but can also be used for concentrating marine viruses (John et al., 2011) or microalgae (Knuckey et al., 2006; Sukenik et al., 1988). The iron ions form a series of metal hydrolysis species aggregating to tridimensional polymeric structures (sweeping flock formation) and enhance the adsorption characteristics of colloidal compounds by reducing or neutralizing their electrostatic charges (coagulation). Best precipitation results at a salinity of 29.6 were obtained by the addition of $300 \mu\text{L}$ of 2.4 M FeCl_3 solution per litre of well-stirred particle suspension, resulting in a very clear supernatant. The disadvantage of particle precipitation with FeCl_3 , however, is that FeCl_3 is a fairly strong Lewis acid and therefore reduces the pH upon addition to a seawater sample. A pH decline in sediment trap samples needs to be avoided in order to prevent dissolution of collected calcium carbonate (CaCO_3).

To quantify the FeCl_3 -related pH reduction we added FeCl_3 to (1) a seawater sample originating from mesocosms deployed in Gullmar Fjord (Sweden 2013) and (2) a seawater sample of the same origin in which we resuspended sediment trap material. This test was carried out in 500 mL beakers at 25°C using a stationary pH meter (NBS scale, 713, METROHM) to monitor changes in the seawater pH (Fig. 4). As expected, the addition of $150 \mu\text{L}$ FeCl_3 (2.4 M) solution resulted in a distinct drop in seawater pH of about 3 units in the absence of particles (Fig. 4, blue, filled boxes) and 1.3 units in the presence of resuspended particles (Fig. 4, red, empty boxes). The pH decrease was compensated by stepwise titration with 3 M NaOH, reaching the initial seawater pH after the addition of $\sim 330 \mu\text{L}$ NaOH both in the absence and the presence of particles. In both cases the calculated aragonite saturation state, representing the more soluble form of biogenic CaCO_3 , was well above $\Omega = 1$ (Fig. 4, grey dashed line), as calculated with CO2SYS MS Excel Macro (Pierrot et al., 2006) at 25°C , 0 dbar, a salinity of 29.62, and total alkalinity (TA) of 2206.1 (Bach et al., 2016) with constants of Mehrbach et al. (1973), refitted by Dickson and Millero (1987).

According to the test, $660 \mu\text{L}$ NaOH (3 M) were simultaneously added with $300 \mu\text{L}$ FeCl_3 (2.4 M) to each litre of particle suspension to stabilize the sample pH and to achieve optimal particle precipitation (Supplement S1). The formation of dense and rapidly settling flocks allowed the separation of the supernatant and concentration of the deposit as described in Sect. 2.2.1 after only 1 h of sedimentation. Even though buffering the samples with NaOH, we still observed shifts in seawater pH. Delta pH (ΔpH) was calculated from

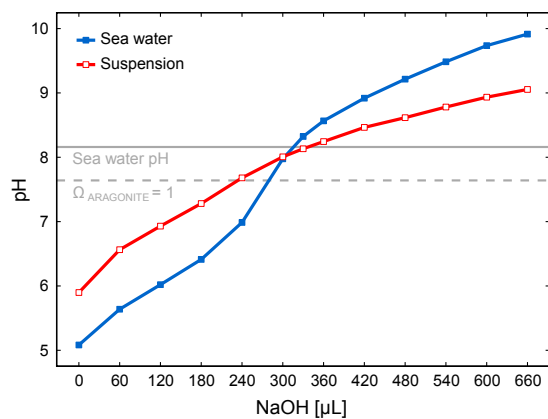


Figure 4. Titration of 500 mL sea water (blue, filled box and line) and 500 mL particle suspension (red, empty box and line) with 3 M NaOH after addition of 150 μL 2.4 M FeCl_3 solution. The grey solid line indicates the pH of seawater before any manipulation. pH (NBS scale) was measured at 25 $^\circ\text{C}$ with a stationary pH meter (713, METROHM). Calculated aragonite saturation state of $\Omega = 1$ is represented by the grey dashed line.

50 pH measurements before and after the addition of FeCl_3 and NaOH to sediment trap samples (pH meter, 3310 WTW; InLab Routine Pt1000 electrode, Mettler Toledo). The resulting ΔpH (Fig. 5) differed between individual samples of the same day as well as between sampling days over the 107 days of the experiment. A maximum spread of 0.46 pH units was observed on day 63, while the minimum difference of 0.15 units occurred on day 103. We did not detect a trend towards a positive or negative shift in pH as the variation in the data led to an average ΔpH of -0.01 . It is likely that differences in the amount and composition of particles in the samples led to the observed pattern. Aragonite and calcite saturation states of the samples after precipitation (Fig. 5) were calculated as described above using in situ storage temperature, pH measurements of the samples, and TA values from mesocosm water column measurements (Bach et al., 2016). Undersaturation of both carbonate species already occurred in several samples prior to FeCl_3 addition as ocean acidification scenarios were established inside the mesocosm bags and CO_2 released by biomass degradation likely further reduced seawater pH. In fact the number of undersaturated samples after precipitation was reduced by two and six samples with respect to aragonite and calcite. This method can therefore also be used to eliminate undersaturation of CaCO_3 in the samples as a consequence of CO_2 released by microbial degradation of the collected organic matter.

The FeCl_3 approach yielded the highest concentration efficiency among the three methods with a median of 99.6% and a narrow range of scores (98.2–99.9%), indicating a remarkable reproducibility (Fig. 3, red). The outliers seen in the box plot are likely caused by extremely high amounts

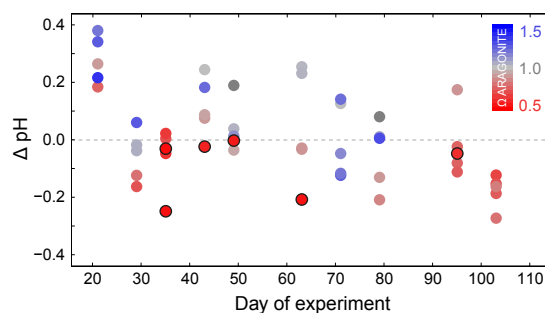


Figure 5. Delta pH of 50 sediment trap samples, calculated from pH measurements before and after addition of FeCl_3 ($300 \mu\text{L L}^{-1}$, 2.4 M) and NaOH ($660 \mu\text{L L}^{-1}$, 3 M) for precipitation of suspended particulate material. $\Omega_{\text{ARAGONITE}}$ after chemical treatment of the samples is indicated by a colour gradient from red to blue, representing undersaturated, saturated, and oversaturated samples, respectively. $\Omega_{\text{CALCITE}} < 1$ is indicated by black edging of the coloured data points.

of transparent exopolymer particles (TEP) in specific samples. We observed TEP in the supernatant of these samples in the form of strings (Alldredge et al., 1993) likely promoting buoyancy of attached particles (Azetsu-Scott and Passow, 2004) and thereby explaining the slightly decreased concentration efficiency in these samples.

2.3 Freeze-drying samples

The water content of the frozen samples was removed by freeze-drying for up to 72 h depending on pellet size (step 4 in Fig. 2). Lyophilization is preferable to drying the material in the oven for better preservation of phytoplankton pigments (McClymont et al., 2007) and a significant improvement of pigment extraction (Buffan-Dubau and Carman, 2000; van Leeuwe et al., 2006). Sedimentation rates within the mesocosms (expressed as collected dry weight per unit time) were gravimetrically determined and should be corrected for sea salt content. Residual sea salt can be estimated with the known loss of water during freeze-drying and known salinity of water in the respective samples. The alternative of removing sea salt before freeze-drying with ultra pure water has the downside of potential osmotic cell rupture and loss of intracellular compounds and should therefore be avoided.

2.4 Grinding the desiccated material

The desiccated sediment pellets were cryogenically ground into a fine powder of homogeneous composition to guarantee representative subsampling. We therefore developed a ball mill to grind sample sizes from 0.1 to 7.0 g dry weight. Hollow spheres with volumes ranging from 11.5 to 65.5 mL were cut out of blocks of stainless steel (V4A/1.4571). Each hollow sphere is divided into two hemispheres of exactly the

Table 1. Depending on the dry weight of the freeze-dried sediment trap samples, different grinding sphere volumes and numbers of grinding balls (10–20 mm) are recommended to achieve optimal grinding results at a set run time of the ball mill (5 min). The optimal combination of the different factors was determined empirically to achieve a grain size smaller than 63 μm and to minimize frictional heating of the samples.

Sample dry weight (g)	Hollow sphere volume (mL)	No. of grinding balls and size (mm)	Run time of the ball mill (min)
<1.5	11.5	1 \times 10	5
1.5–2.5	24.4	1 \times 15 + 2 \times 10	5
2.5–5.0	47.7	2 \times 15 + 2 \times 10	5
5.0–7.0	65.5	1 \times 20	5

same shape and only connected by two guide pins and sealed by a metal sealing (Fig. S1 in Supplement). The size of the grinding sphere was selected according to the dry weight of the freeze-dried sediment pellets (Table 1). A set number and size of grinding balls (stainless steel, 1.3541) ranging from 10 to 20 mm in diameter is transferred into the hemisphere containing the sample pellet (Table 1). The second hemisphere is then put on top of the other so that the two hemispheres form a hollow sphere with the sample and the grinding balls locked inside. Sediment pellets heavier than 7.0 g have to be split up into multiple spheres and require homogenization after grinding. After loading the grinding spheres we cooled them down in liquid nitrogen (step 5 in Fig. 2) until the liquid stopped boiling (-196°C). We observed that deep-freezing of the samples is essential for embrittlement of lipids in the organic matter and additionally protects phytoplankton pigments from frictional heating during the grinding process. The deep-frozen spheres (ca. -196°C) were clamped on a cell mill (Vibrogen VI 6, Edmund Bühler) and shaken at 75 Hz for 5 min (step 6 in Fig. 2), thereby grinding the material by impact and friction. Before opening the grinding spheres they needed to be warmed up to room temperature to avoid condensation of air moisture on the ground sample material. This was done by means of infrared light bulbs (150 W) installed at about 5 cm distance (step 7 in Fig. 2). The very finely ground samples were then recovered from the opened spheres with a spoon and transferred into gas tight glass vials to protect the powder from air moisture (step 8 in Fig. 2). Samples were stored in the dark at -80°C to minimize pigment degradation. All handling of the samples during the grinding process was done over a mirror for complete recovery of the ground material.

We evaluated the homogeneity of finely ground sediment trap samples by five repetitive carbon and nitrogen measurements of samples collected during experiments in different ocean regions between 2010 and 2014 (Table 2). The reproducibility of the measurements was expressed by the coefficient of variation in percent (CV %) reflecting the dispersion

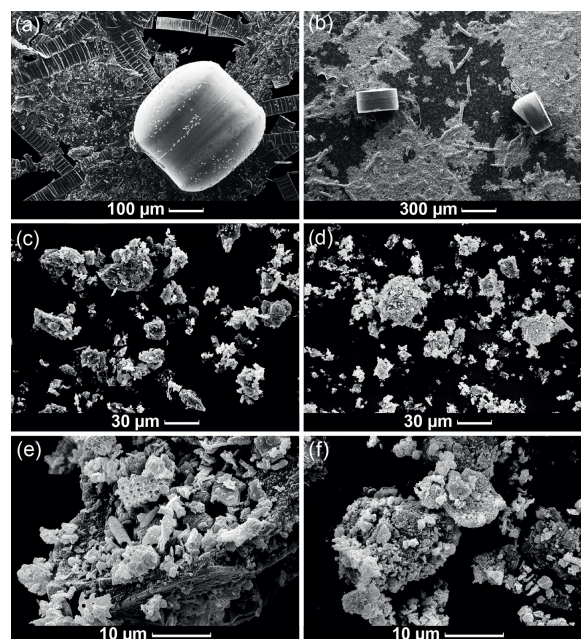


Figure 6. Scanning electron microscopy (SEM) photographs of two sediment trap samples before (a, b) and after grinding (c–f). Panels (c) and (d) represent the average grain size of the ground samples, while (e) and (f) reveal details visible at 2500-fold magnification.

of measurements relative to the mean:

$$\text{CV}\% = \frac{\text{SD}}{\text{MEAN}} \times 100. \quad (1)$$

The CV % estimates demonstrated that carbon (CV %: 0.15–0.99) and nitrogen (CV %: 0.28–1.86) measurements of the ground samples were at least equally reproducible as measurements of the two calibration standards acetanilide and a soil standard with a CV % of 0.34 and 4.17 for carbon and 0.97 and 1.55 for nitrogen, respectively (Table 2).

The homogeneity of ground samples is mainly determined by the grain size, which is therefore crucial for representative subsampling. Scanning electron microscopy (SEM) photographs of fresh sediment trap samples (Fig. 6a, b) show that the collected material consists of a heterogeneous mixture of all kind of debris particles, such as agglutinated diatom chains, faecal pellets, and macroscopic aggregates. None of these macroscopic structures were visible after the grinding procedure (Fig. 6c, d). Only at 2500-fold magnification did details such as pores of former diatom frustules become detectable in tiny fragments (Fig. 6e, f). Grain size, representing grinding quality, was in the range of fine to coarse silt (2–63 μm , international scale), independently of the sample origin and primary composition (Fig. 6c, d).

Table 2. Results from replicate carbon and nitrogen measurements of ground sediment trap material used to test its homogeneity. Powdered samples originating from different pelagic mesocosm experiments were tested and compared with commercially available standards commonly used for calibration of elemental analysers (soil standard (std), acetanilide standard (std)). Homogeneity is expressed by the coefficient of variation in percent (CV %). Also presented are the number of measured aliquots, the amount of material analysed, average carbon content, calculated standard deviation (SD), and grain size derived from scanning electron microscopy. ND: grain size not determined.

Sample origin	Measured aliquots no.	Aliquot weight (mg)	Grain size (μm)	Average carbon ($\mu\text{mol mg}^{-1}$)	SD (carbon)	CV % (carbon)	Average nitrogen ($\mu\text{mol mg}^{-1}$)	SD (nitrogen)	CV % (nitrogen)
Soil std $C = 3.429\%$	5	4 ± 0.25	ND	2.83	0.12	4.17	0.16	0.00	1.55
Acetanilide std $C = 71.089\%$	5	1 ± 0.15	ND	58.81	0.20	0.34	7.34	0.07	0.97
Svalbard 2010 No. SV106	5	2 ± 0.25	ND	22.74	0.12	0.51	3.77	0.01	0.39
Norway 2011 No. NO124	5	2 ± 0.25	≤ 63	19.57	0.09	0.48	2.53	0.01	0.54
Finland 2012 No. FI114	5	2 ± 0.25	≤ 63	22.53	0.03	0.15	3.58	0.01	0.28
Sweden 2013 No. SE502	5	2 ± 0.25	≤ 63	29.03	0.23	0.80	1.65	0.03	1.86
Gran Canaria 2014 No. GC68	5	2 ± 0.25	≤ 63	17.15	0.17	0.99	0.94	0.00	0.28

3 Conclusions and recommendations

3.1 Sediment trap design and sample recovery

The quantitative collection of settling particles, as realized in several pelagic mesocosm designs (e.g. CEE, KOSMOS, Large Clean Mesocosms), combines the advantage of sampling all settling particles produced by the enclosed plankton community with the removal of settled organic matter from the bottom of the enclosures. Collecting all settling particles avoids the potential sampling bias of suspended particle traps in mesocosm enclosures and leads to more accurate particle flux rates. Removing the accumulating material prevents resuspension and non-quantified resupply of nutrients and other dissolved compounds released by degradation back into the water column.

We applied the vacuum sampling method to allow easy sample recovery at short time intervals and to keep the systems sealed for minimal disturbance of the enclosed water bodies. Opening of the sediment traps even for a very short time can lead to water exchange due to density gradients between the enclosed and the surrounding water. The vacuum sampling method is therefore ideal to keep the mesocosm enclosures completely sealed and thereby exclude the introduction of plankton seed populations and to allow for the proper budgeting of elements. Furthermore, the extraction of the collected material from the sea surface does not require diving activities. Only in case of a nonreversible blockage of the outlet of the collecting cylinder by artificial objects do divers need to open up the collecting cylinder at the top or the bottom.

Sediment traps of mesocosms can obviously not be poisoned to prevent organic matter degradation, raising the importance of frequent sampling. Sampling intervals of the traps should be kept short – 2 days or less – to limit bacterial- and zooplankton-mediated remineralization of the settled material and to avoid or minimize the time of possible carbonate undersaturation or anoxic conditions.

3.2 Particle concentration

Centrifuging the entire sample volume (Sect. 2.2.2) as well as precipitating particles with FeCl_3 (Sect. 2.2.3) was shown to effectively concentrate sediment trap samples containing large amounts of bulk seawater without the need for separate analysis of the supernatant. In contrast, particle concentration by passive settling (Sect. 2.2.1) should be complemented by additional measurements of material remaining in the supernatant as mean concentration efficiency is much lower and more dependent on particle characteristics.

The simplest method to use in the field was centrifugation of the whole sample volume. We therefore recommend this method for sample volumes of up to 3 L, as it avoids separate supernatant analysis or readjustment of the samples' pH and undesired enrichment with iron. Concentration of samples larger than 3 L can be accelerated by precipitation of particles with FeCl_3 prior to centrifugation and is advisable during bloom and post-bloom events of high particle fluxes. If applied in the future, we strongly advise adjusting pH after FeCl_3 addition with NaOH in each sample individually to ensure CaCO_3 preservation. FeCl_3 is also known to precipitate dissolved inorganic phosphate (PO_4^{3-}) (Jenkins et al., 1971),

Table 3. List of parameters measured from ground sediment trap samples originating from KOSMOS experiments. The methods or instruments applied and the corresponding references with data sets and detailed descriptions of the methods are also provided.

Parameter	Method or instrument	Corresponding publications
Total carbon	Elemental analyser	Czerny et al. (2013), Paul et al. (2015b)
Organic carbon	Removal of inorganic carbon by direct addition of hydrochloric acid (Bisutti et al., 2004); elemental analyser	Riebesell et al. (2016)
Inorganic carbon	Calculated from total and org. carbon	Riebesell et al. (2016)
Total nitrogen	Elemental analyser	Czerny et al. (2013), Paul et al. (2015b)
Phosphorus	Spectrophotometry (Hansen and Koroleff, 1999)	Czerny et al. (2013), Paul et al. (2015b)
Biogenic silica	Spectrophotometry (Hansen and Koroleff, 1999)	Czerny et al. (2013), Paul et al. (2015b)
Isotopic tracers (^{13}C , ^{15}N)	Mass spectrometry, elemental analyser	de Kluijver et al. (2013), Paul et al. (2015a)
Phytoplankton pigments	High-pressure liquid chromatography	Paul et al. (2015a)

but the relative contribution of precipitated PO_4^{3-} to particulate phosphorus in the samples is likely to be negligible. The potential of iron to interfere with the spectrophotometric analysis of biogenic silica or particulate phosphorus leading to increased absorption at very high iron concentrations (Hansen and Koroleff, 1999) can not be confirmed based on our observations (author's unpublished data).

3.3 Sample analyses

Processing of the sediment trap material to a finely ground and homogeneous powder proved to be ideally suited for reproducible elemental composition analysis. So far we successfully measured the content of major bioactive elements such as total, organic, and inorganic carbon, nitrogen, phosphorus, and biogenic silica using standard methods for particulates in seawater (Table 3). Isotopic tracers such as ^{13}C and ^{15}N added to the mesocosms as well as natural isotope signals were additionally measured in settled organic matter (de Kluijver et al., 2013; Paul et al., 2015a). Furthermore, phytoplankton pigments extracted from the ground samples were analysed revealing the contribution of key phytoplankton groups to settling particle formation (Paul et al., 2015a). As only a few milligram of material are needed for these analyses, the measurement of further parameters such as lithogenic material or amino acids should be tested in the future.

3.4 Recommendations

This section highlights the most important recommendations for improving particle collection in pelagic mesocosms along

with sampling and processing of the collected material for biogeochemical analysis. The recommendations are as follows.

- Quantitative collection of settling particles with full-size funnel traps leads to accurate flux measurements and minimizes the impact of organic matter degradation on the enclosed water columns.
- Vacuum sampling of the sediment traps via an extraction tube allows keeping the mesocosms sealed, excluding seawater and organism exchange.
- High sampling frequency limits organic matter degradation and potential carbonate undersaturation or anoxia in the traps.
- Separation of particles and bulk seawater in the samples is highly efficient when achieved by centrifugation or chemical precipitation with FeCl_3 .
- Freeze-drying the collected material is preferable to drying the samples in the oven to better preserve phytoplankton pigments.
- Grinding of the entire samples guarantees representative subsampling for biogeochemical analysis.

Following our successfully applied protocol (Fig. 2, Sect. 2) and the above recommendations will lead to accurate biogeochemical flux data of mesocosm sediment traps, irrespective of the magnitude of the particle flux.

The Supplement related to this article is available online at doi:10.5194/bg-13-2849-2016-supplement.

T. Boxhammer et al.: Sampling and processing of mesocosm sediment trap material

2857

Author contributions. U. Riebesell conceived the mesocosm experiments between 2010 and spring 2014. T. Boxhammer and J. Czerny developed the methods for sample acquisition and material processing. T. Boxhammer carried out the practical work, while the presented data were analysed by T. Boxhammer and L. T. Bach. T. Boxhammer prepared the manuscript with contributions from all co-authors.

Acknowledgements. We thank the whole KOSMOS team for deployment and maintenance of the KOSMOS infrastructures during the five consecutive mesocosms studies between 2010 and spring 2014. In particular, we thank Andrea Ludwig and Sebastian Krug for coordinating the logistics and conducting CTD casts, Ylva Ericson and Leif Anderson for providing TA data, Allanah J. Paul for support with RStudio, Jan Taucher for supervision, Sebastian Meier from the Institute of Geology at the Kiel University for support regarding SEM analyses, Mario Deckelnick and Detlef Hoffmann for the development of the ball mill as well as Michael Sswat, Mathias Haunost, Hendrik Schultz, Saskia Audritz, Jana Meyer, Diana Gill, Kerstin Nachtigall, and Georgia Slatter for assistance during sampling, processing, and measurements. We are also grateful to the crews of *M/V Esperanza*, *R/V Alkor* (AL376, AL394, AL397, AL406, AL420), *R/V Håkan Mosby* (2011609), *R/V Heincke* (HE360), *R/V Poseidon* (POS463), and *R/V Hesperides* (29HE20140924) for transportation, deployment, and recovery of the mesocosms. This paper benefited from the constructive comments of two anonymous reviewers. The mesocosm studies were funded by the Federal Ministry of Education and Research (BMBF) in the framework of the coordinated projects BIOACID II (FKZ 03F06550) and SOPRAN II (FKZ 03F0611), as well as by the European Union in the framework of the FP7 EU projects MESOAQUA (grant agreement no. 228224) and EPOCA (grant agreement no. 211384).

Edited by: K. G. Schulz

References

- Allredge, A. L., Passow, U., and Logan, B. E.: The abundance and significance of a class of large, transparent organic particles in the ocean, *Deep-Sea Res. Pt. I*, 40, 1131–1140, 1993.
- Amokrane, A., Comel, C., and Veron, J.: Landfill leachates pretreatment by coagulation-flocculation, *Water Res.*, 31, 2775–2782, 1997.
- Azetsu-Scott, K. and Passow, U.: Ascending marine particles: Significance of transparent exopolymer particles (TEP) in the upper ocean, *Limnol. Oceanogr.*, 49, 741–748, 2004.
- Bach, L. T., Riebesell, U., Sett, S., Febiri, S., Rzepka, P., and Schulz, K. G.: An approach for particle sinking velocity measurements in the 3–400 μm size range and considerations on the effect of temperature on sinking rates, *Mar. Biol.*, 159, 1853–1864, 2012.
- Bach, L. T., Taucher, J., Boxhammer, T., Ludwig, A., The Kristineberg Kosmos Consortium, Achterberg, E. P., Algueró-Muñiz, M., Anderson, L. G., Bellworthy, J., Büdenbender, J., Czerny, J., Ericson, Y., Esposito, M., Fischer, M., Haunost, M., Hellemann, D., Horn, H. G., Hornick, T., Meyer, J., Sswat, M., Zark, M., and Riebesell, U.: Influence of ocean acidification on a natural winter-to-summer plankton succession: First insights from a long-term mesocosm study draw attention to periods of low nutrient concentrations, in review, 2016.
- Bisutti, I., Hilke, I., and Raessler, M.: Determination of total organic carbon – an overview of current methods, *Trac-Trend. Anal. Chem.*, 23, 716–726, 2004.
- Bloesch, J. and Burns, N. M.: A critical review of sedimentation trap technique, *Schweiz. Z. Hydrol.*, 42, 15–55, 1980.
- Boxhammer, T., Bach, L. T., Czerny, J., Nicolai, M., Posman, K., Sswat, M., and Riebesell, U.: Video of the sampling strategy to empty sediment traps of the “Kiel Off-Shore Mesocosms for future Ocean Simulations” (KOSMOS), 2015.
- Buesseler, K. O.: Do upper-ocean sediment traps provide an accurate record of particle flux?, *Nature*, 353, 420–423, 1991.
- Buffan-Dubau, E. and Carman, K. R.: Extraction of benthic microalgal pigments for HPLC analyses, *Mar. Ecol.-Prog. Ser.*, 204, 293–297, 2000.
- Czerny, J., Schulz, K. G., Boxhammer, T., Bellerby, R. G. J., Büdenbender, J., Engel, A., Krug, S. A., Ludwig, A., Nachtigall, K., Nondal, G., Niehoff, B., Silyakova, A., and Riebesell, U.: Implications of elevated CO_2 on pelagic carbon fluxes in an Arctic mesocosm study – an elemental mass balance approach, *Biogeosciences*, 10, 3109–3125, doi:10.5194/bg-10-3109-2013, 2013.
- de Kluijver, A., Soetaert, K., Czerny, J., Schulz, K. G., Boxhammer, T., Riebesell, U., and Middelburg, J. J.: A ^{13}C labelling study on carbon fluxes in Arctic plankton communities under elevated CO_2 levels, *Biogeosciences*, 10, 1425–1440, doi:10.5194/bg-10-1425-2013, 2013.
- Dickson, A. G. and Millero, F. J.: A comparison of the equilibrium constants for the dissociation of carbonic acid in seawater media, *Deep-Sea Res.*, 34, 1733–1743, 1987.
- Doney, S. C.: The growing human footprint on coastal and open-ocean biogeochemistry, *Science*, 328, 1512–1516, 2010.
- Gamble, J. C., Davies, J. M., and Steele, J. H.: Loch Ewe bag experiment, 1974, *B. Mar. Sci.*, 27, 146–175, 1977.
- Guiu, C., Dulac, F., Desboeufs, K., Wagener, T., Pulido-Villena, E., Grisoni, J. M., Louis, F., Ridame, C., Blain, S., Brunet, C., Bon Nguyen, E., Tran, S., Labiadh, M., and Dominici, J. M.: Large clean mesocosms and simulated dust deposition: a new methodology to investigate responses of marine oligotrophic ecosystems to atmospheric inputs, *Biogeosciences*, 7, 2765–2784, 2010.
- Hansen, H. P. and Koroleff, F.: Determination of nutrients, in: *Methods of seawater analysis*, edited by: Grasshoff, K., Kremling, K., and Ehrhardt, M., Wiley-VCH Verlag GmbH, Weinheim, Germany, 159–228, 2007.
- Harrison, W. G. and Davies, J. M.: Nitrogen cycling in a marine planktonic food chain: Nitrogen fluxes through principal components and effects of adding copper, *Mar. Biol.*, 43, 299–306, 1977.
- Huasheng, H., Laodong, G., and Jingqian, C.: Relationships between particle characteristics and biological activities in controlled ecosystems, in: *Proceedings of a symposium held in Beijing: Marine ecosystem enclosure experiments*, Beijing, People’s Republic of China, 9–14 May 1987, 230–243, 1992.
- Jenkins, D., Ferguson, J. F., and Menar, A. B.: Chemical processes for phosphate removal, *Water Res.*, 5, 369–389, 1971.
- Jinping, W., Whitney, F. A., Shumin, H., Xiaolin, C., Dongfa, Z., and Shengsan, W.: Introduction to the Xiamen Marine Ecosystem

- Enclosed Experiments, in: Proceedings of a symposium held in Beijing: Marine ecosystem enclosure experiments, Beijing, People's Republic of China, 9–14 May 1987, 158–173, 1992.
- John, S. G., Mendez, C. B., Deng, L., Poulos, B., Kauffman, A. K. M., Kern, S., Brum, J., Polz, M. F., Boyle, E. A., and Sullivan, M. B.: A simple and efficient method for concentration of ocean viruses by chemical flocculation, *Environ. Microbiol. Rep.*, 3, 195–202, 2011.
- Knuckey, R. M., Brown, M. R., Robert, R., and Frampton, D. M. F.: Production of microalgal concentrates by flocculation and their assessment as aquaculture feeds, *Aquacult. Eng.*, 35, 300–313, 2006.
- Lalli, C. M.: Introduction, in: Enclosed experimental marine ecosystems: A review and recommendations: A contribution of the scientific committee on oceanic research working group 85, edited by: Lalli, C. M., Springer US, New York, NY, 1–6, 1990.
- McClymont, E. L., Martínez-García, A., and Rosell-Melé, A.: Benefits of freeze-drying sediments for the analysis of total chlorins and alkenone concentrations in marine sediments, *Org. Geochem.*, 38, 1002–1007, 2007.
- Mehrbach, C., Culbertson, C. H., Hawley, J. E., and Pytkowicz, R. M.: Measurement of the apparent dissociation constants of carbonic acid in seawater at atmospheric pressure, *Limnol. Oceanogr.*, 18, 897–907, 1973.
- Menzel, D. W. and Case, J.: Concept and design: Controlled ecosystem pollution experiment, *B. Mar. Sci.*, 27, 1–7, 1977.
- Niehoff, B., Schmithüsen, T., Knüppel, N., Daase, M., Czerny, J., and Boxhammer, T.: Mesozooplankton community development at elevated CO₂ concentrations: results from a mesocosm experiment in an Arctic fjord, *Biogeosciences*, 10, 1391–1406, doi:10.5194/bg-10-1391-2013, 2013.
- Olsen, Y., Andersen, T., Gismervik, I., and Vadstein, O.: Protozoan and metazoan zooplankton-mediated carbon flows in nutrient-enriched coastal planktonic communities, *Mar. Ecol.-Prog. Ser.*, 331, 67–83, 2007.
- Paul, A. J., Achterberg, E. P., Bach, L. T., Boxhammer, T., Czerny, J., Haunost, M., Schulz, K.-G., Stühr, A., and Riebesell, U.: No observed effect of ocean acidification on nitrogen biogeochemistry in a summer Baltic Sea plankton community, *Biogeosciences Discuss.*, 12, 17507–17541, doi:10.5194/bgd-12-17507-2015, 2015a.
- Paul, A. J., Bach, L. T., Schulz, K. G., Boxhammer, T., Czerny, J., Achterberg, E. P., Helleman, D., Trense, Y., Nausch, M., Sswat, M., and Riebesell, U.: Effect of elevated CO₂ on organic matter pools and fluxes in a summer Baltic Sea plankton community, *Biogeosciences*, 12, 6181–6203, doi:10.5194/bg-12-6181-2015, 2015b.
- Pierrot, D., Lewis, E., and Wallace, D.: MS Excel program developed for CO₂ system calculations, ORNL/CDIAC-105a, Carbon Dioxide Information Analysis Center, Oak Ridge National Laboratory, US Department of Energy, Oak Ridge, Tennessee, 2006.
- Renou, S., Givaudan, J. G., Poulain, S., Dirassouyan, F., and Moulin, P.: Landfill leachate treatment: Review and opportunity, *J. Hazard. Mater.*, 150, 468–493, 2008.
- Riebesell, U., Lee, K., and Nejtgaard, J. C.: Pelagic mesocosms, in: Guide to best practices in ocean acidification research and data reporting, edited by: Riebesell, U., Fabry, V. J., Hansson, L., and Gattuso, J.-P., Office for Official Publications of the European Communities, Luxembourg, 95–112, 2011.
- Riebesell, U., Czerny, J., von Bröckel, K., Boxhammer, T., Bündenbender, J., Deckelnick, M., Fischer, M., Hoffmann, D., Krug, S. A., Lentz, U., Ludwig, A., Mücke, R., and Schulz, K. G.: Technical Note: A mobile sea-going mesocosm system – new opportunities for ocean change research, *Biogeosciences*, 10, 1835–1847, doi:10.5194/bg-10-1835-2013, 2013.
- Riebesell, U., Bach, L. T., Bellerby, R. G. J., Bermudez Monsalve, R. J., Boxhammer, T., Czerny, J., Larsen, A., Ludwig, A., and Schulz, K. G.: Ocean acidification can impair competitive fitness of a predominant pelagic calcifier, in review, 2016.
- Schulz, K. G., Riebesell, U., Bellerby, R. G. J., Biswas, H., Meyerhöfer, M., Müller, M. N., Egge, J. K., Nejtgaard, J. C., Neill, C., Wohlers, J., and Zöllner, E.: Build-up and decline of organic matter during PeECE III, *Biogeosciences*, 5, 707–718, doi:10.5194/bg-5-707-2008, 2008.
- Sukenik, A., Bilanovic, D., and Shelef, G.: Flocculation of microalgae in brackish and sea waters, *Biomass*, 15, 187–199, 1988.
- Svensen, C., Egge, J. K., and Stiansen, J. E.: Can silicate and turbulence regulate the vertical flux of biogenic matter? A mesocosm study, *Mar. Ecol.-Prog. Ser.*, 217, 67–80, 2001.
- Vadstein, O., Andersen, T., Reinertsen, H. R., and Olsen, Y.: Carbon, nitrogen and phosphorus resource supply and utilisation for coastal planktonic heterotrophic bacteria in a gradient of nutrient loading, *Mar. Ecol.-Prog. Ser.*, 447, 55–75, 2012.
- van Leeuwe, M. A., Villerius, L. A., Roggeveld, J., Visser, R. J. W., and Stefels, J.: An optimized method for automated analysis of algal pigments by HPLC, *Mar. Chem.*, 102, 267–275, 2006.
- von Bröckel, K.: Sedimentation of phytoplankton cells within controlled experimental ecosystems following launching, and implications for further enclosure studies, in: Marine mesocosms, edited by: Grice, G. D. and Reeve, M. R., Springer US, New York, NY, 251–259, 1982.

3. Manuscript II

Enhanced transfer of organic matter to higher trophic levels caused by ocean acidification and its implications for export production: A mass balance approach

T Boxhammer^{1*}, J Taucher¹, LT Bach¹, EP Achterberg¹, M Algueró-Muñiz², J Bellworthy³, J Czerny¹, M Esposito^{1,3}, M Haunost¹, D Hellemann¹, A Ludwig¹, JCYong¹, M Zark⁴, U Riebesell¹, and LG Anderson⁵

Under review in PLoS ONE**

¹ GEOMAR Helmholtz Centre for Ocean Research Kiel, Kiel, Germany

² Alfred Wegener Institute Helmholtz Centre for Polar and Marine Research, Biological Institute Helgoland, Helgoland, Germany

³ Ocean and Earth Sciences, University of Southampton, Southampton, United Kingdom

⁴ Institute for Chemistry and Biology of the Marine Environment (ICBM), Research Group for Marine Geochemistry (ICBM-MPI Bridging Group), Carl von Ossietzky University, Oldenburg, Germany

⁵ Department of Marine Sciences, University of Gothenburg, Gothenburg, Sweden

*corresponding author: tboxhammer@geomar.de (T Boxhammer)

** manuscript formatted in style of journal

Abstract

Ongoing acidification of the ocean through uptake of anthropogenic CO₂ is known to affect marine biota and ecosystems with largely unknown consequences for marine food webs. Changes in food web structure have the potential to alter trophic transfer, partitioning, and biogeochemical cycling of elements in the ocean. Here we investigated the impact of realistic end-of-the-century CO₂ concentrations on the development and partitioning of the carbon, nitrogen, phosphorus, and silica pools in a coastal pelagic ecosystem (Gullmar Fjord, Sweden). We covered the entire winter-to-summer plankton succession (100 days) in two sets of five pelagic mesocosms, with one set being CO₂ enriched (~760 μatm pCO₂) and the other one left at ambient CO₂ concentrations. Our key observations under high CO₂ were: (1) Enhanced carbon fixation (relative to nitrogen) that appeared in the particulate matter pool, as well as in the downward particle flux. (2) A significantly amplified transfer of carbon, nitrogen, and phosphorus from primary producers to higher trophic levels, particularly during times of regenerated primary production. (3) A prolonged retention of all three elements in the water column that significantly reduced nitrogen and phosphorus sedimentation by about 11 and 9%, respectively. Our findings highlight the potential for ocean acidification to alter partitioning and cycling of carbon and nutrients in the surface ocean but also show that impacts are temporarily variable and likely depending upon the structure of the plankton food web.

3.1 Introduction

The ocean is a major sink for anthropogenic carbon dioxide (CO₂) by absorbing more than 2 Pg carbon per year from the atmosphere [1,2]. This uptake of atmospheric CO₂ leads to both carbonation (increasing CO₂ concentration) and acidification (decreasing seawater pH) of the surface ocean [3,4]. Changes of both environmental factors are expected to impact marine biota from the organism [5] to the ecosystem level [6,7]. Phytoplankton groups belonging to the picoeukaryotes will likely benefit from increased inorganic carbon availability [8,9], while calcifying phyto- and zooplankton groups such as coccolithophores or pteropods will likely be impaired by decreasing seawater pH [10,11]. Presumed shifts in plankton community composition, e.g. to smaller (medium-sized) phytoplankton organisms [12] with different elemental stoichiometry can modify marine element cycling [13-15]. Recent studies have further revealed the potential of CO₂ to alter the partitioning of carbon between dissolved and particulate organic matter pools in the euphotic ocean zone [16-18]. Increasing proportions of dissolved organic carbon can stimulate bacterial growth and recycling of organic matter [17,19,20], but are also known to promote particle

formation and organic matter export by increasing particle stickiness [19,21]. While our knowledge about the impact of CO₂ on carbon cycling in the ocean is continuously growing, the potential effects on cycling of macronutrients (inorganic nitrogen, phosphorus, and silica) through changes in the marine food webs require more in-depth investigation. In fact, the partitioning of macronutrients between different pools and trophic levels determines their turnover rates and can thereby feedback on ecosystem structure and functioning [22]. For instance changes in stoichiometry and fatty acid composition of primary producers as a consequence of increasing CO₂ have already been shown to impact mesozooplankton reproduction and development [23,24]. This implies direct consequences for element cycling within the ocean's food webs.

Calculating the mass balance of carbon and macronutrients is one of the best approaches to estimate their partitioning and cycling. However, such approaches are prone to high uncertainties in open ocean regions. Availability of essential parameters (e.g. gas exchange of CO₂ or settling particulate matter) is often limited, while vertical mixing and lateral advection permanently exchange the investigated water masses. Pelagic mesocosms have the advantage of isolating a water mass from the surrounding ocean and hence allow us to investigate natural plankton assemblages of several trophic levels at close to natural conditions. The enclosed water bodies can be characterised with respect to element pools and plankton community, while repetitive sampling of the same water parcel allows monitoring of changes over long timescales and successive phases of plankton development.

Here we present results from a pelagic *in situ* mesocosm CO₂ perturbation study in Gullmar Fjord (Sweden) covering the full winter-to-summer plankton succession typical for the coastal sea in mid-latitudes. The mid-latitude regions are of particular importance to global element cycling due to the annual formation of large phytoplankton spring blooms characterised by high export efficiency [25]. We monitored the enclosed plankton communities (from viruses to fish larvae) over more than 100 days in two sets of five mesocosms representing ambient and projected year 2100 *p*CO₂ (partial pressure of CO₂), respectively [26]. Element pools of carbon, nitrogen, phosphorus, and silica (C, N, P, and Si) were measured to compute mass balances and estimates of net community production, thereby assessing the impact of ocean acidification on the partitioning and cycling of major elements within the ocean surface layer.

3.2 Materials and methods

3.2.1 Mesocosm setup and maintenance

Ten ‘Kiel Off-Shore Mesocosms for Ocean Simulations’ (KOSMOS; [27]) were deployed on January 29, 2013 in Gullmar Fjord on the west coast of Sweden (58.26635 °N, 11.47832 °E). Sea ice drift and technical problems described in Bach et al. [26] delayed the start of the experiment until March 7 (day 2 = t_2 , i.e. 2 days before homogenization of the water column; see Sect. 3.2.2). Each cylindrical mesocosm bag (2 m diameter) enclosed a 17 m deep water column, sealed at the bottom end by a two meter long, funnel-shaped sediment trap (Fig 3.1A).

Enclosed nekton and large mesozooplankton (e.g. fish larvae or jelly fish) were removed during the initial period of the study by a full-diameter-size net (1 mm mesh) that was pulled through each mesocosm (t_6 ; Fig 3.2). Samples relevant for mass balancing of elements were taken over a period of more than 100 days until June 22 (t_{105} ; Fig 3.2). Biofilm formation on the inner and outer walls of the cylindrical mesocosm bags was prevented by regular cleaning [26] (Fig 3.2). Settled material adhering to the inner surface of the sediment trap funnels was removed at the very end of the experiment (t_{102}). A detailed description of the study site, the initiation of the experiment, and mesocosm cleaning can be found in Bach et al. [26].

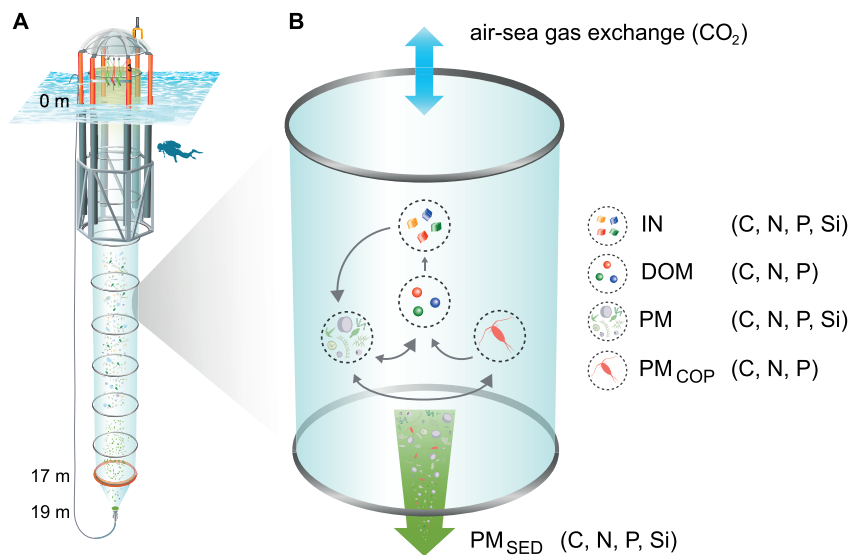


Fig 3.1. KOSMOS mesocosm unit and conceptual figure of element pools and fluxes. (A) Schematic illustration of a KOSMOS unit, including the floatation frame at the sea surface and the enclosure bag reaching down to the sediment trap at the bottom. (B) Element pools (IN, DOM, PM, PM_{COP}) and fluxes (air-sea gas exchange of CO₂, sedimentation of PM_{SED}) included in the mass balances of carbon, nitrogen, phosphorus, and silica (C, N, P, and Si). Grey arrows indicate exchange between the individual element pools in the water column. Illustration of the KOSMOS unit modified from Rita Erven (GEOMAR).

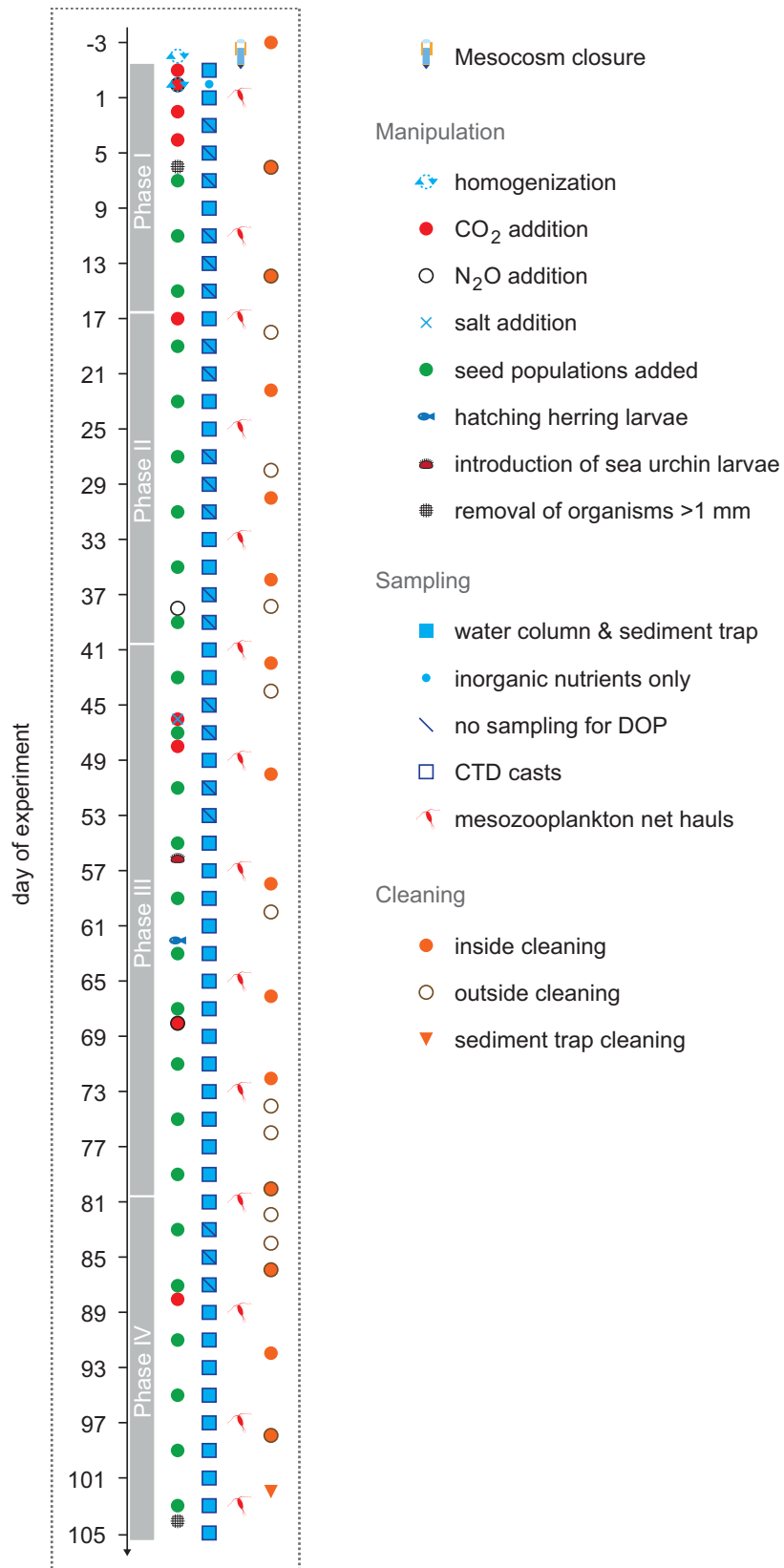


Fig 3.2. Manipulation, sampling, and maintenance schedule. Days of experiment are relative to the day of water column homogenization (day 0 = t_0).

3.2.2 System manipulations and volume determination

The natural salinity gradient enclosed inside the mesocosms was homogenized by injecting air to the bottom of the enclosures in two stages (t_2 and t_0 ; Fig 3.2; [26]). A ‘high CO₂ treatment’ of initially 961 $\mu\text{atm } p\text{CO}_2$ (t_5) was established in five of the ten mesocosms (M2, M4, M6, M7, M8) by stepwise addition of CO₂-saturated seawater (t_1, t_0, t_2, t_4). The other five mesocosms served as untreated controls (M1, M3, M5, M9, M10), representing ambient CO₂ conditions. $p\text{CO}_2$ levels were re-adjusted four times in the high CO₂ mesocosms ($t_{17}, t_{46} + t_{48}, t_{68}, t_{88}$; Fig 3.2) to counteract the loss from outgassing and biological uptake.

Seed populations of organisms from the surrounding fjord were introduced to the mesocosms by adding 22 L of fjord water on every fourth day (Fig 3.2). In total, the regular fjord water additions summed up to about 1% of the mesocosms’ volume [26]. In early May, we introduced green sea-urchin larvae (*Strongylocentrotus droebachiensis*; t_{56}) and herring eggs (*Clupea harengus*; t_{48}), that hatched two weeks later on t_{62} .

The volume of each mesocosm was determined by adding a known amount of calibrated sodium chloride brine solution and by measuring the salinity increase as described in Czerny et al. [28]. The brine solution was evenly dispersed inside the mesocosms on April 24 (t_{46}), elevating salinity by about 0.1 units from on average 29.2 to 29.3. Mesocosm volumes were converted from kilograms of seawater to litres using individual seawater density of each mesocosm on t_{46} .

3.2.3 Sampling procedures and CTD operations

The mesocosm water columns and sediment traps were sampled every second day starting at t_{-1} with the exception of one additional inorganic nutrient sampling on t_2 (Fig 3.2). The sediment traps at 19 m water depth were emptied with a vacuum system following Boxhammer et al. [29]. Water column samples were taken with depth-integrating water samplers (IWS, Hydro-Bios) which collected equal amounts of water from all depth levels between 0 and 17 m. Samples sensitive for contamination or gas exchange such as inorganic nutrients (including dissolved inorganic nitrogen (DIN = nitrate (NO_3^-) + nitrite (NO_2^-) + ammonium (NH_4^+)), phosphorus (DIP = phosphate (PO_4^{3-})) and silica (DSi = $\text{Si}(\text{OH})_4$)), dissolved organic matter (DOM; DOC (carbon), DON (nitrogen), DOP (phosphorus)) and carbonate chemistry samples (dissolved inorganic carbon (DIC), pH) were directly transferred from the IWS samplers into corresponding sample bottles. DOC/DON samples were gravity filtered through glass fibre filters (pore size 0.7 μm , Whatman) during transfer into pre-combusted glass vials on board of the sampling boats and acidified in the lab (HCl, 25%, analysis grade, Carl Roth) to pH 2 as described in Zark et al. [30]. DOP samples were collected in acid-rinsed

polycarbonate bottles (Nalgene) and filtered in the lab through 0.7 μm (GF/F, Whatman) into low-density polyethylene vials (LDPE, Roth) using gentle vacuum filtration (<200 mbar). Until t_{55} DOP samples were only collected on 12 out of 30 sampling days (see Fig 3.2) and were poisoned with mercury chloride following Kattner [31]. DOP samples collected after t_{55} were taken alongside the 48 hours sampling routine (apart from t_{83} - t_{87}) and stored frozen at 20°C .

Carbonate chemistry samples were taken as described in Bach et al. [26] and sterile-filtered ($0.2 \mu\text{m}$) for a maximum of three days storage (dark and cold) before analysis.

Particulate matter (PM) was sampled from seawater pooled in 10 L carboys that were subsampled within a few hours at *in-situ* water temperatures. Water from these carboys was used for analysis of biogenic silica (BSi), total particulate carbon (TPC), nitrogen (TPN), and phosphorus (TPP), as well as Chlorophyll *a* (Chl *a*) concentrations.

Mesozooplankton was collected with an Apstein net (55 μm mesh size, 17 cm diameter opening) by vertical net hauls (17 to 0 m water depth), representing a sampled volume of about 386 L. We restricted the sampling frequency to every eighth day to minimize the impact on the mesozooplankton community (Fig 3.2). A subsample of 4% was used for high-resolution plankton imaging with the ZooScan method (see Sect. 3.2.4.6), while the majority of the sample was preserved with sodium tetraborate-buffered formalin (4% v/v) for taxonomic abundance analyses [32].

CTD casts, providing salinity and temperature profiles, were performed with a CTD60M (Sea & Sun Technology) on every sampling day between 11 a.m. and 3 p.m. (local time; Fig 3.2), covering a water depth from 0.3 to 18 m.

3.2.4 Sample analysis

3.2.4.1 Carbonate chemistry measurements and calculations

DIC was determined by colorimetric titration following Johnson et al. [33], with an estimated precision of $3 \mu\text{mol kg}^{-1}$ (standard deviation of duplicate measurements). Measurement accuracy was ensured by calibration against certified reference materials (CRM, supplied by A. Dickson, Scripps Institution of Oceanography, USA). pH_T (total scale) was determined spectrophotometrically, based on the absorption ratio of the sulphonephthalien dye, *m*cresol purple [34], with a precision of ~ 0.002 pH units (SD of duplicates), while the accuracy was set by the equilibrium constants of the indicator. pCO_2 was calculated from the combination of pH_T and DIC using CO2SYS [35] with the carbonate dissociation constants (K_1 and K_2) of Lueker et al. [36]. The input data included salinity, temperature, and inorganic nutrient concentrations (PO_4^{3-} and $\text{Si}(\text{OH})_4$).

3.2.4.2 Inorganic nutrient measurements

Inorganic nutrient samples ($\text{NO}_3^- + \text{NO}_2^-$, PO_4^{3-} , and $\text{Si}(\text{OH})_4$) were filtered as triplicates through 0.45 μm cellulose acetate syringe filters (Whatman) before measuring them with a QuAatro AutoAnalyzer (Seal Analytical) as described in Bach et al. [26]. When concentrations of $\text{NO}_3^- + \text{NO}_2^-$ and PO_4^{3-} dropped below 0.1 $\mu\text{mol L}^{-1}$ (t_{37} and t_{35} , respectively) we switched to using the nanomolar system described by Patey et al. [37]. NH_4^+ concentrations were determined according to Holmes et al. [38]. Inorganic nutrient measurements were stopped after t_{95} as concentrations were close to or below their detection limits.

3.2.4.3 DOM measurements

Concentrations of DOC and total dissolved nitrogen (TDN) were analysed of duplicate samples using high-temperature catalytic oxidation on a Shimadzu TOC-VCPH/CPN Total Organic Carbon Analyser, equipped with an ASI-V autosampler and a TNM-1 module for TDN determination as described in Zark et al. [30]. Samples with concentrations of DOC and TDN exceeding the measurement of their duplicate by 30% or more were considered being contaminated and were excluded from the dataset. Measurements from the high and ambient CO_2 mesocosms were subsequently pooled for identification and removal of outliers using the Dixon-Dean test ($p < 0.05$). DON concentrations were calculated by subtracting the concentration of DIN (see Sect. 3.2.4.2) from average TDN values.

DOP was converted to orthophosphate by autoclaving for 30 minutes in an oxidizing decomposition solution (Merck, catalogue no. 112936). Concentration of total dissolved phosphate (TDP) was then determined from triplicate subsamples with a QuAatro AutoAnalyzer (Seal Analytical) as described for PO_4^{3-} in Sect. 3.2.4.2. DOP concentrations were calculated by subtracting DIP from TDP concentrations. DON and DOP datasets ended on t_{95} because measurements of DIN and DIP were discontinued after this day.

3.2.4.4 Particulate matter and Chlorophyll a measurements

Size fractions of PM smaller and greater than 200 μm (separated with a 200 μm mesh) were collected using gentle vacuum filtration (≤ 200 mbar) on pre-combusted (6 h at 450°C) glass fibre filters (GF/F, 0.7 μm pore size, Whatman) or cellulose acetate filters (0.65 μm , Whatman) for analysis of TPC, TPN, TPP or BSi, respectively. Glass fibre filters were stored at 20°C in pre-combusted

(6 h at 450°C) glass petri dishes until analysis, while cellulose acetate filters were also frozen at 20°C but stored in plastic petri dishes. TPC/TPN filters were oven-dried over night at 60°C, packed in tin foil and analysed alongside blank filters on an acetanilide calibrated CN analyser following Sharp [39]. We refrained from acidifying the filters to remove inorganic C, as pelagic calcifying organisms were very low in abundance. Accordingly, all particulate C data are presented as TPC but are assumed to represent particulate organic carbon (POC). TPP collected on the filters was converted to orthophosphate as described for TDP in Sect. 3.2.4.3. Concentration of inorganic phosphate was then determined spectrophotometrically according to Hansen and Koroleff [40]. BSi was leached from the collected particulate matter by alkaline pulping with 0.1 M NaOH at 85°C. After 135 minutes the leaching process was terminated with 0.05 M H₂SO₄ and DSi was measured by spectrophotometry following Hansen and Koroleff [40]. If not indicated differently, presented PM values are the sum of the two measured size fractions (< and > 200 µm). Exceptions are TPP and BSi samples that were filtered as bulk samples before t_7 and t_{29} , respectively. BSi data of t_{29} were removed from the dataset due to a systematic error made during size fractionation on this specific day.

Water column samples for Chl *a* concentration analysis were filtered as described for PM, taking care to minimize light exposure during filtration. Chl *a* content of the collected particles was extracted and analysed by high-performance liquid chromatography (HPLC) as described in Bach et al. [26].

3.2.4.5 Elemental analysis of sediment trap samples

The sediment trap samples were collected in 5 L Schott Duran glass bottles. To separate PM from bulk seawater, particles were concentrated by flocculation and coagulation with ferric chloride (FeCl₃) as described by Boxhammer et al. [29]. Briefly, FeCl₃ and NaOH (for pH stabilisation) were added simultaneously to the well-stirred samples. The clear supernatant water was removed after one hour of particle sedimentation. Mean concentration efficiency of this method was 99.6% with respect to samples' TPC content [29]. The concentrated samples were centrifuged, deep-frozen at 30°C and lyophilised for 72 hours. The desiccated material was then ground in a ball mill to a homogeneous powder of 2 - 60 µm particle size [29]. TPC, TPN, TPP, and BSi content of the finely ground sample material was determined from subsamples of 1 - 2 mg as described for PM of water column samples (see Sect. 3.2.4.4). The cumulative mass flux of all four elements was expressed in µmol L⁻¹ by dividing the summed up mass flux by the calculated mesocosm volumes (Sect. 3.2.2).

From May 25 (t_{77}) onwards we screened the freshly taken samples for dead herring larvae that hatched inside the mesocosms on t_{62} (see Sect. 3.2.2). All larvae found were removed for separate analysis, thus they did not contribute to the vertical flux.

3.2.4.6 Calculation of mesozooplankton biomass

Biomass of the mesozooplankton community was calculated based on abundance data obtained from counting with a stereomicroscope [32]. The community was strongly dominated by the copepod species *Pseudocalanus acuspes*, which represented about 97% of the mesozooplankton counts. Therefore, we only considered copepod biomass for mesozooplankton PM. Copepod nauplii were sufficiently abundant (up to 100 ind. L⁻¹) to be sampled quantitatively on PM filters (Sect. 3.2.4.4). Adult copepods and copepodites, however, were much lower in abundance and naturally escape sampling by the IWS. Thus they were not represented in PM analysis. To avoid double counting of nauplii biomass, only adult copepod and copepodite biomass were included in the calculation of copepod PM (PM_{COP}). We applied the image-based ZooScan approach to estimate biomass for the different copepod size classes [41], since biomass measurements of individual organisms have not been conducted. Therefore, subsamples from the mesozooplankton net tows (4% of the total sample) were evenly distributed on a flat-bed scanner (Perfection Pro V750, Epson) to provide high-resolution images (10.6 µm pixel size) of all particles and organisms in the sample. Subsequent image processing with ZooProcess [41] provided a large number of variables for object characterization, including several measures of size such as length or area. For estimation of copepod biomass we then converted measured area of each individual imaged organism to dry-weight (dw) by applying the empirical relationship of [42]:

$$dw = 43.97 * area^{1.52} \quad (3.1)$$

The dry-weight was subsequently converted to C and N content (µmol) using the data for body mass composition of zooplankton from Kiørboe [43]. For copepods, the applied C:dw and N:dw ratios were 0.48 and 0.10, respectively. The resulting conversion factors for C and N biomass per individual organism were applied to the complete time series of abundance data for adult copepods and copepodites. P content was calculated using a conversion factor of C:P of 52:1 derived from *Pseudocalanus* sp. caught in Oslofjord (Norway) during the same time of the year (average ratio of individuals caught between March and May) by Gismervik [44].

Similar procedures for image-based biomass estimation of mesozooplankton have been applied in previous studies and showed generally reliable results [45-47]. It should be noted, however, that this approach assumes constant size ranges of copepod life stages and can thus not account for shifts in size structure within a community or population.

3.2.5 Calculation of net changes in element pools and net community production

The relevant pools for mass balancing C, N, P, and Si are dissolved inorganic nutrients ($IN_{C/N/P/Si}$), dissolved organic matter ($DOM_{C/N/P}$), suspended particulate matter ($PM_{C/N/P/Si}$), and the sum of particulate matter collected in the sediment traps ($\Sigma PM_{SED(C/N/P/Si)}$). Mesozooplankton, strongly dominated by copepods, was treated as a separate PM pool (Sect. 3.2.4.6), and defined as $PM_{C/N/P(COP)}$. A summary of all pools and fluxes considered in the mass balances are shown in the conceptual Fig 3.1B. Net changes of the element pools (IN, DOM, PM, and PM_{COP}) were calculated as delta (Δ) values relative to conditions at the start of the experiment. We defined the starting conditions as the average value of the first seven sampling days ($t_1 - t_{11}$). Averaging over this relatively long period was necessary to minimize the influence of data variability. This was well justifiable as relative changes of the element pools were small before t_{13} (Sect. 3.3.1). However, some exceptions (listed in the following text) had to be made for distinct element pools. The first two data points of DSi (t_1 and t_1) were excluded due to a methodological measurement problem. The reference value of ΔDIC in the high CO_2 treatment is based on a single sampling day t_5 , since before DIC was increased by stepwise CO_2 additions (Sect. 3.2.2) and afterwards CO_2 rapidly outgassed to the atmosphere (super-saturation of the water column). DOC and DON data of t_1 were removed from the datasets as measurements displayed substantial unexplainable variability with strong impact on calculated starting conditions. Reference values for DOP were calculated from three data points (t_1 , t_1 and t_9), as those days were the only days when DOP was sampled during the initial phase of the experiment (Fig 3.2). The first mesozooplankton sampling on t_1 served as the reference point for net changes in $PM_{C/N/P(COP)}$. The start and end point of the individual reference periods, as well as the calculated reference values of each element pool within the water column are summarized in Table S3.1.










Net community production (NCP) is most commonly estimated by measuring the biological draw-down of DIC or NO_3^- [48,49]. In the present study, we derived NCP from the actual build-up of biogenic C, N, P, and Si following Hansell and Carlson [48] and Spilling et al. [18]. This total NCP theoretically equals the cumulative drawdown of inorganic nutrients (ΔIN) and is therefore given in moles per litre and not as a rate. We calculated net community production in (1) high temporal resolution lacking mesozooplankton contribution (eq. 3.2) and (2) in reduced temporal resolution but including mesozooplankton contribution (eq. 3.3):

$$NCP_{C/N/P/Si} = \Delta PM_{C/N/P/Si} + \Delta DOM_{C/N/P} + \Sigma PM_{SED(C/N/P/Si)} \quad (3.2)$$

$$NCP_{C/N/P(COP)} = \Delta PM_{C/N/P} + \Delta PM_{C/N/P(COP)} + \Delta DOM_{C/N/P} + \Sigma PM_{SED(C/N/P)} \quad (3.3)$$

Thus, $NCP_{C/N/Si}$ was calculated for every second day (Table 3.1), while NCP_p followed the irregular sampling of DOP described in Sect. 3.2.3 and illustrated in Fig 3.2. $NCP_{C/N/P (COP)}$ was calculated for usually every 8th day (Table 3.1) following the mesozooplankton sampling regime (Fig 3.2).

Table 3.1. Colour code, symbols, and abbreviations of the different element pools and their calculated net community production.

Colour	Symbol	Abbreviation	Element pool / net community production	Elements	SF (days)
dark grey		IN	inorganic nutrients	C, N, P, Si	2
orange		DOM	dissolved organic matter	C, N, P	*2
green		PM	suspended particulate matter	C, N, P, Si	2
brown		PM _{SED}	sedimented particulate matter	C, N, P, Si	2
light red		PM _{COP}	calculated copepod organic matter	C, N, P	8
blue		$NCP_{C/N/P (COP)}$ ambient CO ₂	net community production of the element at ambient CO ₂ incl. PM _{COP}	C, N, P	*8
blue (dotted)		$NCP_{C/N/P/Si}$ ambient CO ₂	net community production of the element at ambient CO ₂ excl. PM _{COP}	C, N, P, Si	*2
dark red		$NCP_{C/N/P (COP)}$ high CO ₂	net community production of the element at high CO ₂ incl. PM _{COP}	C, N, P	*8
dark red (dotted)		$NCP_{C/N/P/Si}$ high CO ₂	net community production of the element at high CO ₂ excl. PM _{COP}	C, N, P, Si	*2

Sampling frequency (SF) indicates the time resolution of the respective data set. *Samples for DOP determination were taken irregularly, reducing the time resolution of DOP, NCP_p , and $NCP_{P (COP)}$ (see Sect. 3.2.3).

3.2.6 Data analysis and statistics

Data shown in tables and figures represent average treatment values (ambient and high CO₂) of the five treatment replicates. Datasets of C and Si pools encompassed the entire duration of the experiment until t_{103} and t_{105} , respectively. Datasets of N and P, however, ended on t_{95} as this was the last day where DON and DOP data were available (see Sect. 3.2.4.3).

Two sample t-tests using *R* software [50] were performed for detection of differences in the initial concentrations of element pools between ambient and high CO₂ mesocosms (average values used for delta calculations; Table S3.1).

For detection of CO₂ treatment effects on net changes of element pools and calculated net community production, univariate permutational analysis of variance (PERMANOVA) tests were run in *R* software [50], using Euclidean distances matrices with 99,999 permutations [51,52]. PERMANOVA was chosen, as assumption of homogeneity of variances was not met for all analysed parameters in all experimental phases. CO₂ effects were evaluated for average values of each experimental phase (see Sect. 3.3) or in the case of sedimented PM for cumulative values at the end of the four experimental phases.

3.3 Results and discussion

The experiment was divided into four phases based on the development of Chl *a* concentrations (Fig 3.3A; [26]): Phase I ($t_1 - t_{16}$), Phase II ($t_{17} - t_{40}$), Phase III ($t_{41} - t_{80}$), Phase IV ($t_{81} - t_{105}$). These phases were used for the interpretation of net changes in the C, N, P and Si pools inside the mesocosms (Fig 3.1B). Average $p\text{CO}_2$ values of the four experimental phases and the entire experiment at ambient and high CO_2 ($t_1 - t_{105}$) are given in Table 3.2.

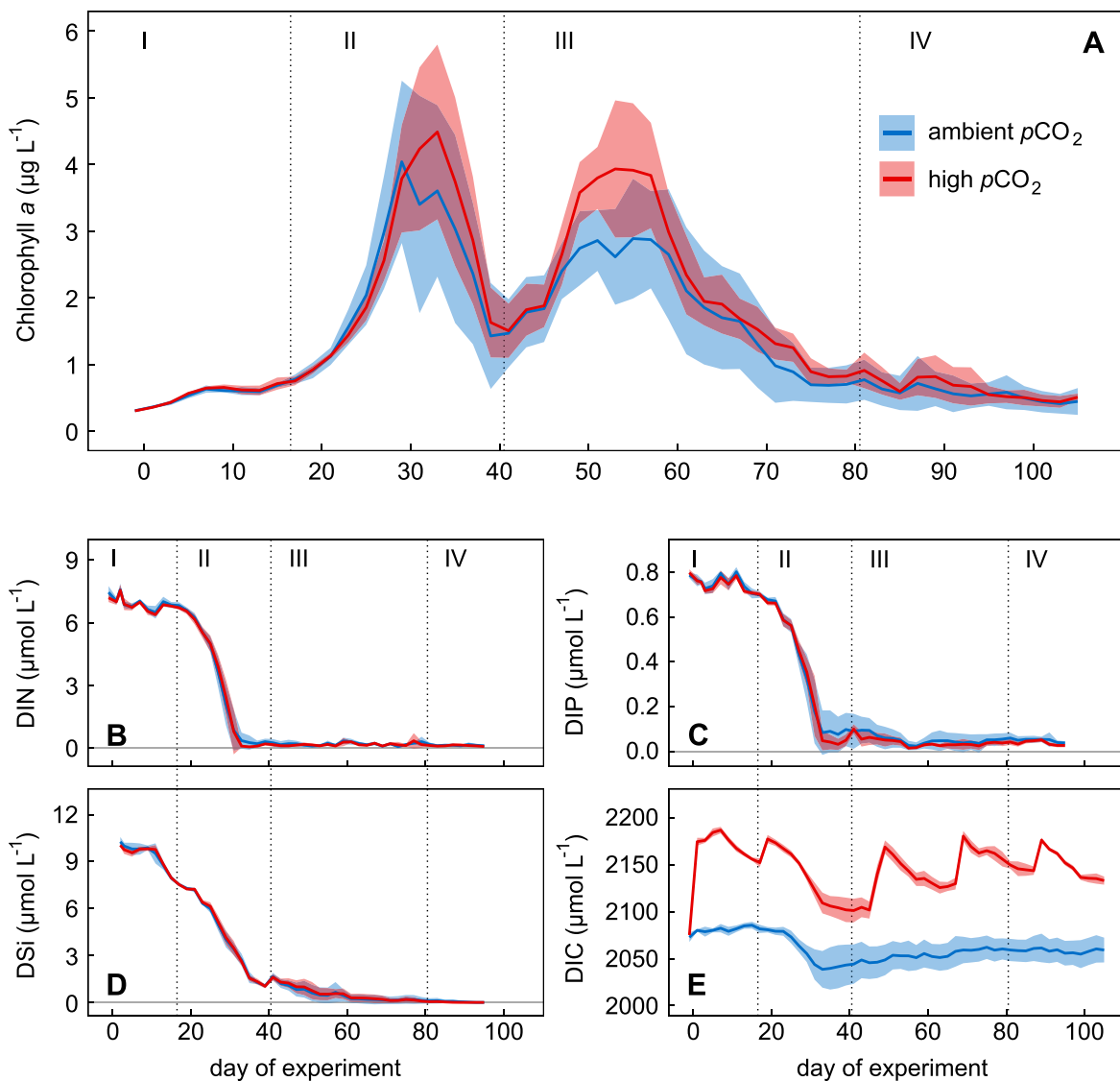


Fig 3.3. Temporal development of Chlorophyll *a*, inorganic nutrients, and dissolved inorganic carbon. Solid lines show mean values of (A) Chlorophyll *a* (Chl *a*), (B) dissolved inorganic nitrogen (DIN), (C) dissolved inorganic phosphorus (DIP), (D) dissolved silica (DSi), and (E) dissolved inorganic carbon (DIC) in the ambient (blue) and high (red) CO_2 treatment. Coloured areas indicate the standard deviation of the five treatment replicates. Roman numerals denote the different phases of the experiment.

Table 3.2. Overview of the CO₂ treatments.

Color code	Volume	$p\text{CO}_2$		$p\text{CO}_2$		$p\text{CO}_2$		$p\text{CO}_2$		$p\text{CO}_2$	
		I	II	III	IV	I - IV	I - IV	I - IV	I - IV	I - IV	I - IV
	$\text{m}^3 \pm \text{SD}$	$t_{-1} - t_{16}$	$t_{17} - t_{40}$	$t_{41} - t_{80}$	$t_{81} - t_{105}$	$t_{-1} - t_{105}$					
ambient CO ₂	48.2 ± 1.5	366	329	367	447	377	↻	↻	↻	↻	↻
high CO ₂	51.0 ± 2.4	762	641	747	878	756	↻	↻	↻	↻	↻

Average mesocosm volume was determined on t_{46} of the experiment. $p\text{CO}_2$ values are averages of the four phases and of the entire experiment. The two symbols ↻ and ↻ represent out- and in-gassing conditions of CO₂, respectively (presumed atmospheric $p\text{CO}_2$ of 395 μatm).

3.3.1 Temporal development of the C, N, P, and Si pools during the phytoplankton spring-bloom

The first (pre-bloom) phase of the experiment was characterised by relatively stable environmental conditions with high concentrations of DIN, DIP, and DSi (~ 7.0 , ~ 0.76 , and $\sim 9.8 \mu\text{mol L}^{-1}$, respectively; Fig 3.3B-D) and short day length [26]. The enclosed water columns were entirely mixed due to thermal convection inside the mesocosm bags [26]. Enclosed plankton assemblages were relatively similar among the ten mesocosms although small differences were detected [26]. No significant differences in initial concentrations of inorganic nutrients as well as the other element pools (PM, PM_{COP}, DOM) were found between CO₂ treatments apart from DIC, as a direct consequence of the CO₂ manipulation (see reference values in Table S3.1). Net changes in the pools of all four elements (C, N, P, Si) were relatively small underlining the pre-bloom character of Phase I (Fig 3.4). The decline of DOC in this early phase was not reflected in changes of any other C pool and is therefore more likely associated with sampling induced artefacts than with real changes in the DOC pool. Thus, we do not draw any conclusion from this trend.

The second phase covers the first major build-up and decrease of Chl *a* during the phytoplankton spring-bloom (Fig 3.3A). Primary production was fuelled by inorganic nutrients that rapidly decreased during the bloom development (Fig 3.3B-D). Small silicifiers (2 - 5 μm , mostly diatoms) as well as the large diatom *Coscinodiscus concinnus* ($>200 \mu\text{m}$) dominated the bloom-forming autotrophic community during this phase. Low DIN and DIP concentrations limited primary production after t_{31} and thus terminated the exponential growth of phytoplankton (Fig 3.3B, C). The decrease of DSi, however, just slowed down according to uptake kinetics of diatoms [53,54]. Thus, DSi was still available in low concentrations after the first bloom ($>1 \mu\text{mol L}^{-1}$ at the end of Phase II; Fig 3.3D).

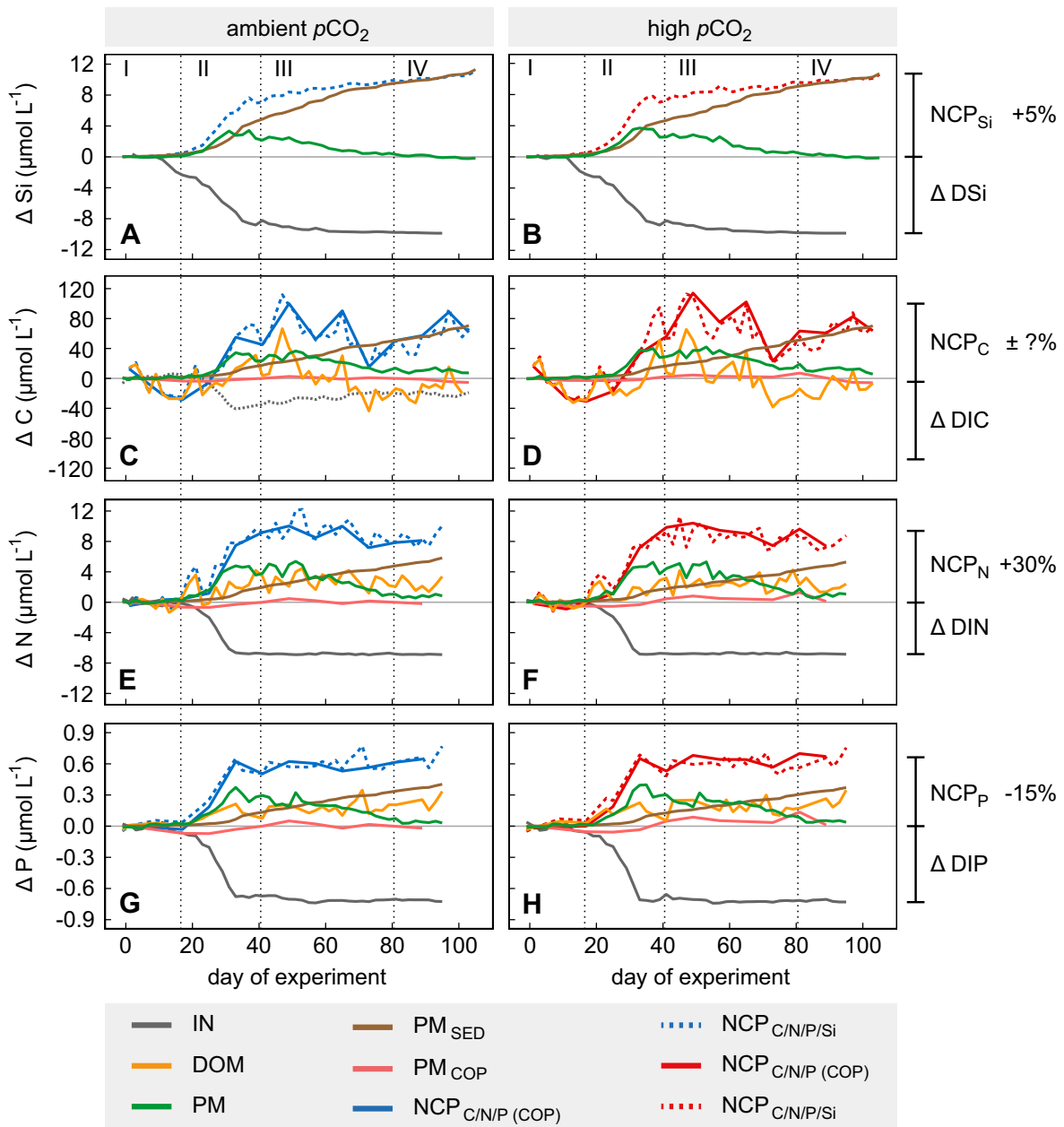


Fig 3.4. Mass balances of silica, carbon, nitrogen, and phosphorus. Solid lines indicate temporal net changes of the silica, carbon, nitrogen, and phosphorus (Si, C, N, and P) pools and of their respective net community production as average values of ambient and high CO₂ mesocosms respectively (see Table 3.1 for a detailed symbol description). DIC is only included at ambient CO₂ (grey, dotted line), lacking correction for CO₂ air-sea gas exchange (see Sect. 3.3.2). Roman numbers denote the different phases of the experiment. Percentages indicate the approximate discrepancy between net community production and inorganic nutrient consumption during Phases III and IV.

Peak values of PM were reached between t_{31} and t_{37} with average net build-up of TPC, TPN, TPP, and BSi of ~ 33.6 , ~ 4.7 , ~ 0.33 and $\sim 3.3 \mu\text{mol L}^{-1}$, respectively (Fig 3.4). Sedimentation of PM of all four elements and build-up of $\text{DOM}_{\text{C/N/P}}$ started to increase right from the onset of the first phytoplankton bloom (Fig 3.4). Highest sedimentation rates were observed during the bloom peak, implying a close temporal coupling between primary production and sinking particle flux. In contrast to particulate C, N, and P, the amount of BSi removed from the water column during this period equalled the net build-up in the water column (Fig 3.4). BSi:C ratios in the sediment trap samples were four times higher than those in the water column (Fig S3.1), suggesting a strong decoupling of the two elements when it comes to settling from the productive surface layer. A phenomenon also observed in the open ocean [55,56].

The strong decline of Chl *a* concentrations at the end of Phase II was much less pronounced in the PM pools (compare Figs 3A and 4). TPC, TPN, and TPP remained relatively high even though Chl *a* strongly decreased. This suggests a highly efficient transfer of autotrophic into heterotrophic biomass and/or non-sinking phytodetritus accumulating in the water column. Indeed, bacterial as well as micro- and mesozooplankton abundances increased parallel to the Chl *a* decrease [32,57]. Phase III encompassed the second and slightly less pronounced build-up and decrease of Chl *a* during the spring-bloom (Fig 3.3A). Small diatoms and flagellates (2 - 5 μm), but mainly the giant diatom *C. concinnus* (up to 50% Chl *a* contribution) dominated the phytoplankton community during this phase. The shift in dominance from small diatom species (< 200 μm) to the large cells of *C. concinnus* (> 200 μm) is clearly reflected in the temporal development of the two size fractions of BSi (Fig S3.2). Regenerated N and P, as well as the remaining DSi likely fueled primary production during this second bloom. Peak values of PM were reached between t_{49} and t_{53} with average net build-up of TPC, TPN, and TPP of ~ 36.8 , ~ 5.1 , and $\sim 0.25 \mu\text{mol L}^{-1}$, respectively (Fig 3.4C-H). A peak in net build-up of BSi was absent due to the high loss through sedimentation and only very low DSi concentrations available (Figs 4A, B and 3D). The high variability in DON and DOP concentrations likely masked consumption of both pools by the plankton community (Fig 3.4E-H). We suspect that considerable proportions of DON and DOP were rather refractory and only a small fraction of these pools, composed of labile compounds, was used and turned over by bacteria and phytoplankton on time scales that could not be resolved by our 48 h sampling regime. This assumption is consistent with field observations [58,59] and is supported by relatively high background concentrations of (likely refractory) DON and DOP right after mesocosm closure (see Table S3.1). Labile DOP is known to be recycled within hours to days [58,60], therefore often fuelling primary production under DIP depletion. In contrast to the relatively stable concentrations of DON and DOP (Phases III and IV), DOC concentrations showed a decreasing trend during the second phytoplankton bloom, reaching values lower than the initial ones by the end of Phase III.

Adult copepod and copepodite biomass ($\text{PM}_{\text{C/N/P (COP)}}$) decreased directly after mesocosm closure (Fig 3.4C-H), but increased again during the phytoplankton blooms with highest values reached

during and after the second bloom peak in Phase III. Predation by herring larvae that hatched inside the mesocosms (t_{62} ; see Sect. 3.2.2) and started feeding on larger mesozooplankton around t_{80} were most likely responsible for the decline of $PM_{C/N/P(COP)}$ in the post-bloom Phase IV. The relative change in the PM_{COP} pool was most pronounced in the P mass balance due to the relatively high P content of copepods. With abundances much lower than those of primary producers and usually relatively small sample volumes for PM analysis the pool of mesozooplankton is likely often not accounted for in mass balance approaches. We observed a temporal contribution of up to 20% to TPP build-up, which emphasizes that this pool should not be neglected.

The fourth phase (post-bloom) was characterized by typical summer conditions in the coastal mid-latitudes. Inorganic nutrient concentrations were depleted (Fig 3.3B-D), the water column was stratified [26], and PM concentrations had almost declined to those of the pre-bloom phase (Fig 3.4).

3.3.2 Mass balances of Si, C, N, and P

The NCP of all four investigated elements (see eqs. 2 and 3) should in theory match the consumption of their inorganic nutrients over time. This worked out well for Si, where NCP was only slightly overestimated with on average ~5% during Phases III and IV (2nd bloom and post-bloom; Fig 3.4A, B). This is well within the range one would expect from combining measurement uncertainties of three different pools (DSi, BSi, BSi_{SED} ; Fig 3.1B). Interestingly, we observed a temporal mismatch of DSi consumption and NCP_{Si} shortly before and during the onset of the spring-bloom (between Phases I and II). Wall growth, a common artefact in enclosure experiments [61-63], can be excluded as a sink for DSi, as mesocosm inside walls were frequently cleaned (see Sect. 3.2.1; Fig 3.2) and we have not observed a comparable pattern in the mass balances of N or P (Fig 3.4E-H). Thus, we assume that this mismatch at the end of Phase I can be explained by the internal storage of DSi in diatoms. We observed that the dominating diatom taxon *Arcocellulus* sp. during that time has very fragile frustules that potentially released internal DSi through breakage, during the filtration process for BSi analysis. Apart from this specific period the Si mass balance was virtually closed.

When attempting to calculate the mass balance of C, we faced two major difficulties. These were (1) the unexplainable day-to-day variability in DOC data (up to ~50 $\mu\text{mol L}^{-1}$ within 48 hours; Fig 3.4C, D) and (2) the poorly constrained gas exchange of CO_2 with the atmosphere. Both made it ultimately impossible to calculate a reasonable mass balance of C. Achieving accurate DOC data in an experimental setup like pelagic mesocosms has shown to be challenging [63], but not impossible [9,64]. Measurement precision and accuracy in the present study was high [30], so that the variability is more likely to originate from artifacts which were induced during sampling.

We refrained from smoothing the data by calculating moving averages since potential contaminations can only increase not decrease the mean and would have led to an overestimation of DOC build-up and NCP_C (see Fig S3.3).

To correct DIC for the air-sea flux of CO_2 we have followed the approach described by Czerny et al. [65], using the injected tracer gas N_2O to infer the exchange rate ('gas transfer velocity') of CO_2 . This technique has been shown to yield good estimates of CO_2 transfer velocity in past mesocosm experiments under relatively stable physical conditions [18,63]. However, in the present study, the hydrographic situation within the mesocosms was highly dynamic with initial thermal circulation of the entire water columns, followed by variable thermal stratification and surface layer mixing depth [26]. The complex physical conditions impeded reasonable estimates of N_2O and consequently CO_2 gas transfer velocities. Hence, DIC concentrations could not be corrected appropriately for CO_2 air-sea gas exchange. To illustrate the discrepancy of un-corrected DIC data with NCP_C we have included the measured net change in DIC into Figure 4C (dotted grey line, ambient treatment). In Phase IV the cumulative sedimentation of C alone exceeds net drawdown of DIC by a factor of three. Including CO_2 gas exchange with the atmosphere is therefore clearly crucial for mass balance calculations of C or when net organic C build-up is calculated from DIC drawdown. Hence, the exclusion of the CO_2 air-sea gas exchange in DIC drawdown [66] should be seen as very critical.

Balancing the NCP of N and P with DIN and DIP drawdown was not as easy as for Si but not as difficult as for C. The offset between inorganic nutrient consumption and NCP during build-up of the first bloom (Phase II) was highly variable in the case of N (40% to +13%) and relatively constant for P (approx. 7%; Fig 3.4E-H). The offset stabilised during Phases III and IV at values of about +30% and 15% for N and P, respectively, when the phytoplankton community had taken up all inorganic nutrients. NCP_N can theoretically be increased above DIN consumption by N_2 -fixation, a significant external N source in the close-by Baltic Sea [67-69]. However, this explanation for the overestimated NCP_N was excluded in the present study, as the corresponding organisms (diazotrophic cyanobacteria) were not present in the mesocosms. The pronounced overestimation of NCP_N is therefore more likely a result of accumulated measurement inaccuracies of the N pools. Similar to DOC, build-up of DON showed strong variability of up to $4 \mu\text{mol L}^{-1}$ within 48 hours, not reflected in any other N pool (Fig 3.4E, F). Thus, the DON pool was the source of the largest uncertainty within the N mass balance.

The underestimation of NCP_P was unexpected as uncertainties in sampling of DOM and PM (e.g. clogging of filters or bursting phytoplankton cells) rather result in a certain overestimation of the two pools, than leading to their underestimation (Fig 3.4G, H). The discrepancy in DIP consumption and NCP_P might be caused by variability in DIP measurements during the reference period used for calculation of net changes (see Table S3.1 and Sect. 3.2.5). During this period, DIP concentrations varied by about $0.1 \mu\text{mol L}^{-1}$ within 48 hours with only low primary production going

on [70]. A potential overestimation of the background concentration of DIP by about $0.1 \mu\text{mol L}^{-1}$ could have led to an overestimated consumption of DIP, possibly explaining the observed offset in the P mass balance.

Altogether, our study has shown that mass balance calculations of elements in marine ecosystems are challenging even in enclosed mesocosm systems with discrete measurements of all relevant parameters. Precise determination of the DOM pools and in the case of C the accurate correction of DIC by the CO_2 air-sea gas exchange turned out to be most critical. This highlights the enormous challenge of mass balancing elements in open systems (e.g. the coastal ocean, estuaries or eddies) where even more uncertainties emerge due to permanent exchange of water masses.

3.3.3 Impact of CO_2 on partitioning of C, N, and P

TPC was the only PM pool influenced by increased CO_2 (Fig 3.5A, F, and K). We observed enhanced TPC build-up at high CO_2 during both phytoplankton blooms (up to 7 and $9 \mu\text{mol L}^{-1}$, respectively), although this observation was statistically non-significant in all phases due to high within-treatment variability (Table 3.3).

The tendency of increased C-fixation was likely caused by enhanced ‘carbon overconsumption’ [71,72], which was also indicated by an elevated C:N ratio of particulate matter at high CO_2 (Fig 3.6A; non-significant in all Phases, see Table 3.4). This trend was most prominent in the size fraction larger than $200 \mu\text{m}$, which was mainly constituted by the diatom *C. concinnus* (Fig 3.6C, D). The CO_2 -dependent C:N signal in the water column was also found in sedimented PM, indicating that the excess C fixed by *C. concinnus* was not transferred into higher trophic levels or re-mineralized by bacteria in the water column (Fig 3.6B). In contrast to other plankton community CO_2 perturbation studies [16,17], we have not detected an increase in DOC build-up at high CO_2 , although the high variability in the present data set may have masked small differences (Fig 3.5B).

Surprisingly, we found that copepod biomass was significantly elevated under high CO_2 during times of regenerated production (Phase III; Table 3.3). Between the peak of the first phytoplankton bloom and mid of the post-bloom Phase IV ($t_{35} - t_{89}$), PM_{COP} was increased on average by 2.7, 0.5 and $0.05 \mu\text{mol L}^{-1}$ with respect to C, N, and P (Fig 3.5C, H, M). Enhanced primary production at high CO_2 [70] must have caused this amplified transfer of biomass from primary producers (phytoplankton) to the higher trophic level of mesozooplankton [73]. A potential further transfer into biomass of herring larvae, showing higher survival rates at high CO_2 , can likely explain the disappearance of the CO_2 effect on copepod biomass towards the end of the study (Phase IV). The amplified transfer of C, N, and P to higher trophic levels at high CO_2 has caused a prolonged retention of biomass in the water column, which significantly reduced the downward flux of N and P (Table 3.3).

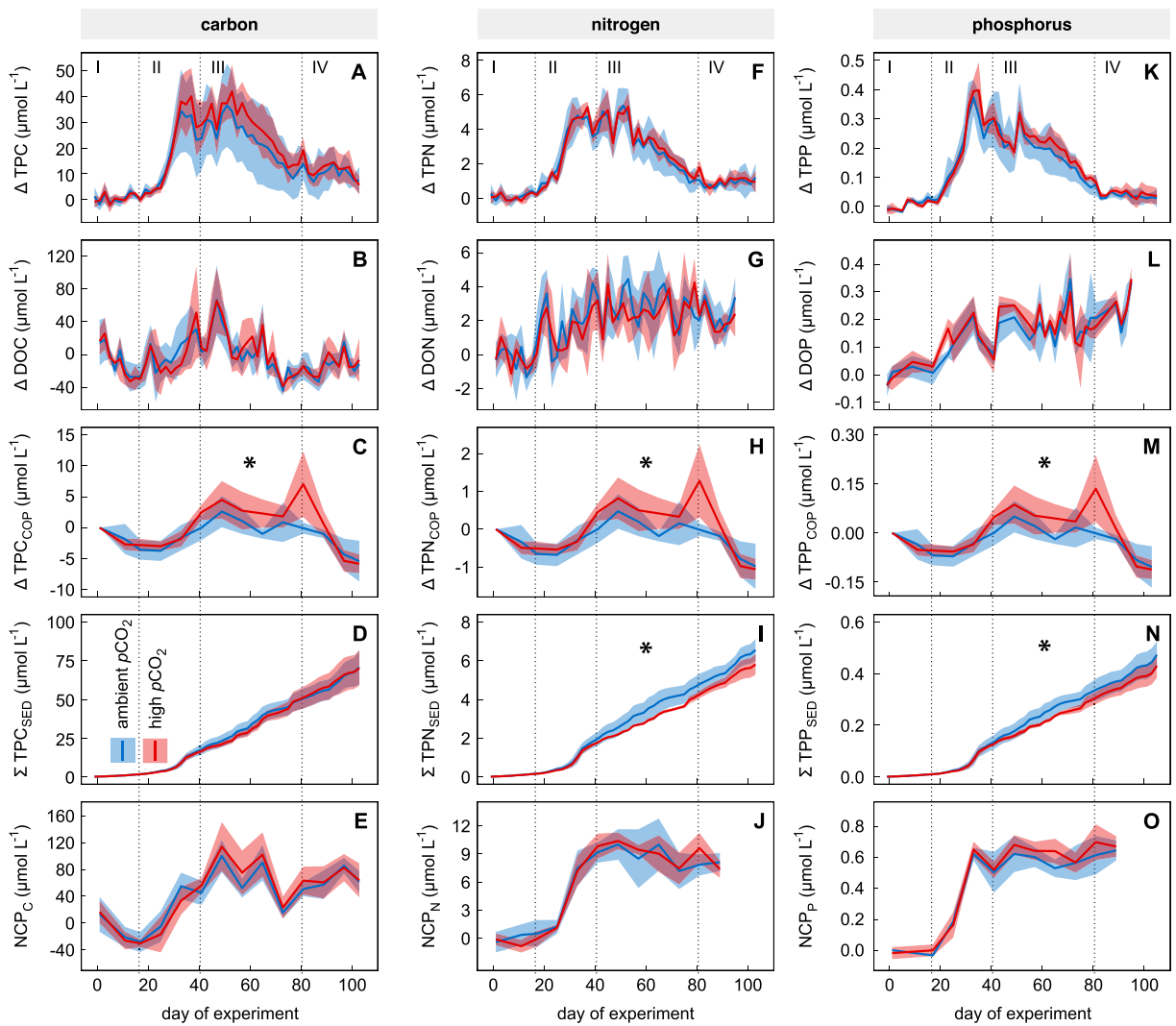


Fig 3.5. Time course of net changes of the element pools at ambient and high CO_2 . Solid lines show average values of the element pools and net community production (see Table 3.1) of (A - E) carbon, (F - J) nitrogen, and (K - O) phosphorus in the ambient (blue) and high (red) CO_2 treatments. Coloured areas indicate the standard deviation of replicated ($n = 5$) treatments. Roman numerals denote the four different phases of the experiment. Black asterisks identify significant CO_2 effects (PERMANOVA, $p < 0.05$).

Table 3.3. Tested CO₂ effects on selected pools and net community production.

Parameter	ambient CO ₂ μmol L ⁻¹ ± SD	high CO ₂ μmol L ⁻¹ ± SD	SS	Pseudo-F	p (perm)
ΔTPC					
I	0.6 ± 0.4	0.5 ± 0.3	0.001	0.010	0.897
II	16.4 ± 7.1	17.6 ± 4.6	3.536	0.100	0.755
III	22.9 ± 12.4	27.6 ± 7.1	55.450	0.540	0.477
IV	10.3 ± 5.0	11.8 ± 4.3	6.015	0.280	0.587
ΔTPC_{COP}					
I	-0.9 ± 1.2	-1.4 ± 0.5	0.478	0.561	0.595
II	-3.0 ± 1.7	-2.5 ± 0.9	0.496	0.277	0.619
III	0.7 ± 1.0	2.8 ± 1.6	10.588	5.946	⁽⁺⁾ 0.047
t ₃₅ - t ₈₉	0.4 ± 0.8	3.1 ± 1.8	18.399	9.145	⁽⁺⁾ 0.016
IV	-2.7 ± 1.7	-0.9 ± 1.3	8.187	3.507	0.087
ΔTPN_{COP}					
I	-0.2 ± 0.2	-0.3 ± 0.1	0.016	0.561	0.595
II	-0.5 ± 0.3	-0.5 ± 0.2	0.016	0.277	0.621
III	0.1 ± 0.2	0.5 ± 0.3	0.351	5.946	⁽⁺⁾ 0.047
t ₃₅ - t ₈₉	0.1 ± 0.1	0.6 ± 0.3	0.589	9.014	⁽⁺⁾ 0.016
IV	-0.5 ± 0.3	-0.2 ± 0.2	0.272	3.507	0.088
ΔTPP_{COP}					
I	-0.02 ± 0.02	-0.03 ± 0.01	<0.001	0.561	0.595
II	-0.06 ± 0.03	-0.05 ± 0.02	<0.001	0.277	0.618
III	0.01 ± 0.02	0.05 ± 0.03	0.004	5.946	⁽⁺⁾ 0.046
t ₃₅ - t ₈₉	0.01 ± 0.02	0.06 ± 0.04	0.007	9.145	⁽⁺⁾ 0.015
IV	-0.05 ± 0.03	-0.02 ± 0.03	0.003	3.507	0.088
ΣTPN_{SED}					
t ₁₅	0.1 ± <0.1	0.1 ± <0.1	<0.001	0.939	0.358
t ₃₉	1.8 ± 0.3	1.7 ± 0.1	0.065	1.074	0.355
t ₆₉	4.1 ± 0.5	3.4 ± 0.1	1.116	8.352	⁽⁻⁾ 0.047
t ₇₉	4.6 ± 0.5	4.1 ± 0.2	0.725	4.883	0.063
t ₁₀₅	7.0 ± 0.6	6.3 ± 0.6	1.438	4.367	0.088
ΣTPP_{SED}					
t ₁₅	0.01 ± <0.01	0.01 ± <0.01	<0.001	0.083	0.786
t ₃₉	0.12 ± 0.03	0.12 ± 0.01	<0.001	0.196	0.683
t ₆₉	0.29 ± 0.03	0.25 ± 0.01	0.004	7.903	⁽⁻⁾ 0.040
t ₇₉	0.33 ± 0.04	0.30 ± 0.02	0.002	2.297	0.174
t ₁₀₅	0.47 ± 0.05	0.43 ± 0.05	0.005	1.844	0.189
NCP_c					
I	-4.5 ± 14.4	-5.1 ± 13.6	1.040	0.005	0.939
II	7.0 ± 16.0	-4.9 ± 12.3	352.050	1.741	0.239
III	60.6 ± 9.3	74.1 ± 17.6	456.040	2.305	0.152
IV	63.7 ± 6.8	67.6 ± 15.9	36.600	0.245	0.653

Values are average values of the different phases (I - IV) in the ambient and high CO₂ treatments ± standard deviation (SD). Effects of CO₂ were assessed by PERMANOVA, giving the sum of squares (SS), the F value by permutation (Pseudo-F), and the p-value (p (perm)). Significant effects detected are highlighted in bold, while positive or negative trends are indicated by ⁽⁺⁾ and ⁽⁻⁾, respectively.

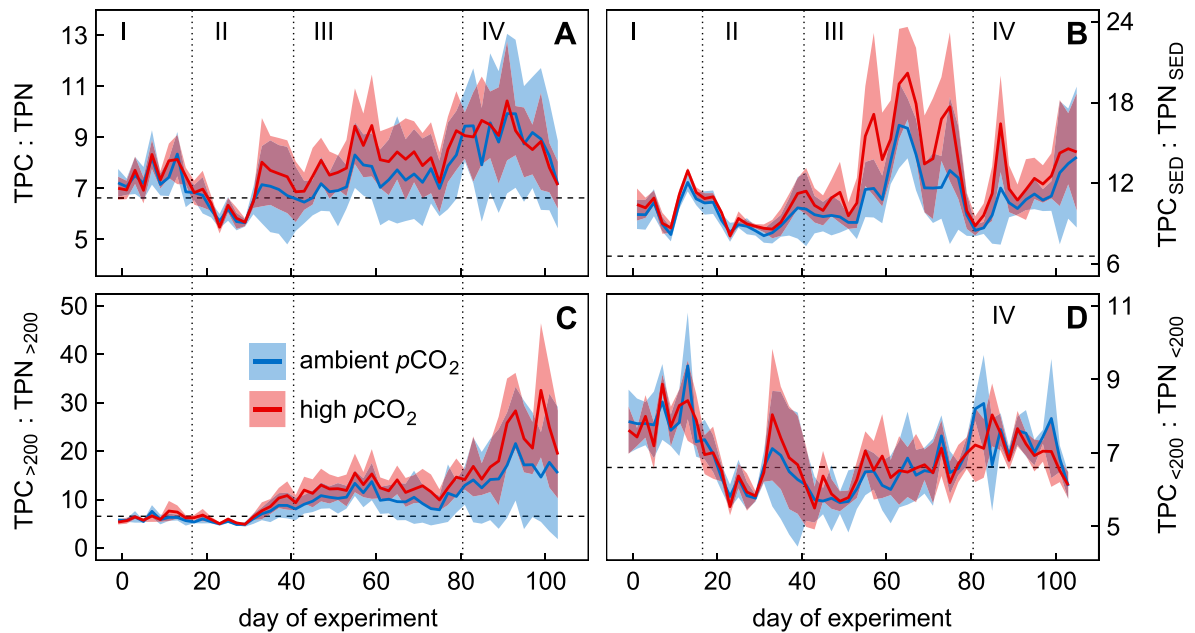


Fig 3.6. Time course the particulate carbon to nitrogen ratio at ambient and high CO_2 . Solid lines show mean values of the particulate carbon (TPC) to nitrogen (TPN) ratio in (A) the water column, (B) collected sediment trap samples, and of the suspended particle size fractions (C) larger and (D) smaller than $200 \mu\text{m}$ in the ambient (blue) and high (red) CO_2 treatment. Coloured areas indicate standard deviation of replicated ($n = 5$) treatments. Roman numbers denote the four different phases of the experiment. Vertical dashed lines represent the Redfield ratio of carbon to nitrogen (6.6).

Cumulative sedimentation of both elements started to differ between treated and control mesocosms at the same time when CO_2 driven trends in PM_{COP} occurred (Fig 3.5H, I, M, N). The observed difference between treatments constantly increased until t_{69} (0.7 and $0.04 \mu\text{mol L}^{-1}$ for N and P, respectively) and remained at this level until the end of the experiment. On t_{105} the deposition of N and P at high CO_2 was reduced by about 11 and 9%, respectively. Due to increasing within-treatment variability, cumulative sedimentation of both elements was significantly different on t_{69} but not on the last day of experiment (t_{105} ; Table 3.3). In the case of C, increased relative C content of settling *C. concinnus* cells under high CO_2 compensated for a theoretically reduced sedimentation of C analogue to N and P (Figs 5D and 6B). The large cell size of *C. concinnus* ($> 200 \mu\text{m}$) prevented grazing by the dominating copepod species *P. acuspes* and therefore likely excluded transition of its biomass into higher trophic levels.

Our findings show that increased retention of N and P within the pelagic food web under high CO_2 can lead to a significant and equivalent reduction of their sedimentation. The plankton community composition in the present study has furthermore shown that a mismatch between phyto- and mesozooplankton taxa can strongly impact element cycling. Together with changes of phytoplankton C:N ratios, the observed impacts of ocean acidification on element partitioning have the potential to alter cycling of carbon and nutrients in the marine realm.

Table 3.4. Tested CO₂ effects on the total particulate carbon to nitrogen ratio.

Parameter	ambient CO ₂ mol:mol ± SD	high CO ₂ mol:mol ± SD	SS	Pseudo-F	p (perm)
C:N_{BULK}					
P I	7.4 ± 0.2	7.5 ± 0.3	0.027	0.433	0.515
P II	6.4 ± 0.5	6.7 ± 0.4	0.198	0.909	0.353
P III	7.3 ± 1.3	8.1 ± 1.1	1.438	1.042	0.324
P IV	8.9 ± 2.3	8.9 ± 1.2	0.001	<0.001	0.984
C:N_{<200 μm}					
P I	8.0 ± 0.3	7.9 ± 0.3	0.002	0.029	0.864
P II	6.5 ± 0.5	6.6 ± 0.4	0.055	0.250	0.614
P III	6.3 ± 0.5	6.4 ± 0.4	0.029	0.132	0.634
P IV	7.4 ± 0.5	7.1 ± 0.2	0.155	1.241	0.315
C:N_{>200 μm}					
P I	6.2 ± 0.3	6.4 ± 0.4	0.110	1.035	0.332
P II	6.3 ± 0.7	7.0 ± 0.6	1.242	2.685	0.158
P III	10.2 ± 3.0	12.5 ± 2.7	12.757	1.583	0.302
P IV	15.8 ± 9.6	21.2 ± 5.8	74.100	1.183	0.308
C:N_{SED}					
P I	10.1 ± 0.5	10.6 ± 0.4	0.661	3.409	0.105
P II	9.2 ± 0.4	9.6 ± 0.4	0.399	2.683	0.143
P III	11.6 ± 1.6	13.9 ± 2.5	14.315	3.139	0.135
P IV	10.8 ± 1.1	12.2 ± 1.1	4.699	3.759	0.095

Values are average values of the different phases (I - IV) in the ambient and high CO₂ treatments ± standard deviation (SD). Effects of CO₂ were assessed by PERMANOVA, giving the sum of squares (SS), the F value by permutation (Pseudo-F), and the p-value (p (perm)). Significant effects detected are highlighted in bold, while positive or negative trends are indicated by ⁽⁺⁾ and ⁽⁻⁾, respectively.

3.4 Conclusions

In this study we investigated the influence of simulated ocean acidification on the development and partitioning of the C, N, P, and Si pools in a coastal pelagic ecosystem. Our mass balance approach over 100 days, covering a natural winter-to-summer plankton succession, has highlighted important challenges and uncertainties in elemental mass balance calculations, but also revealed significant changes of element pool partitioning under realistic end-of-the-century CO₂ concentrations (~760 $\mu\text{atm } p\text{CO}_2$):

- Even in a closed mesocosm system we experienced high uncertainties and methodological challenges for our mass balance approach that highlight potential uncertainties in balance calculations of major biogeochemical elements in the open ocean. Accurate determination of the DOM pools and the CO₂ air-sea gas exchange were most critical in the current study.
- C-fixation relative to N was slightly enhanced at high CO₂, correlating with the time of inorganic nutrient depletion and the bloom of the large diatom *C. concinnus*. The excess C fixed by *C. concinnus* was not available for higher trophic levels due to its large cell size (>200 μm) and was removed from the water column by settling of the diatom cells.
- Transfer of C, N, and P from primary producers to higher trophic levels during times of regenerated production was significantly amplified at high CO₂, leading to prolonged retention of biomass in the water column. Retention of N and P within the pelagic food web resulted in reduced sedimentation of both elements by about 11 and 9%, respectively.

Even though the observed impacts were temporarily variable and likely dependant on the food web structure, our findings show that ocean acidification has the potential to change the biogeochemical cycles of C, N, and P by retaining C and nutrients in the sea surface food web.

Acknowledgments

We thank all participants of the KOSMOS 2013 study for deployment, maintenance and sampling of the mesocosms. In particular, we thank Jana Meyer and Georgia Slatter for support with sediment trap sample processing and analysis. We would also like to thank the Sven Lovén Centre for Marine Sciences, Kristineberg for providing excellent infrastructure, exceptional support and warm hospitality. We gratefully acknowledge the captains and crews of RV ALKOR (AL406 and AL420) and RV OSCAR VON SYDOW for transportation, deployment and recovery of the mesocosms and sediment traps.

References

1. Sabine CL, Feely RA, Gruber N, Key RM, Lee K, Bullister JL, et al. The oceanic sink for anthropogenic CO₂. *Science*. 2004;305: 367-371. doi:10.1126/science.1097403
2. Le Quéré C, Andrew RM, Canadell JG, Sitch S, Korsbakken JI, Peters GP, et al. Global carbon budget 2016. *Earth Syst Sci Data*. 2016;8: 605-649. doi:10.5194/essd-8-605-2016
3. Caldeira K, Wickett ME. Oceanography: Anthropogenic carbon and ocean pH. *Nature*. 2003;425: 365-365. doi:10.1038/425365a
4. Doney SC, Fabry VJ, Feely RA, Kleypas JA. Ocean acidification: The other CO₂ problem. *Annu Rev Marine Sci*. 2009;1: 169-192. doi:10.1146/annurev.marine.010908.163834
5. Kroeker KJ, Kordas RL, Crim RN, Singh GG. Meta-analysis reveals negative yet variable effects of ocean acidification on marine organisms. *Ecology Letters*. 2010;13: 1419-1434. doi:10.1111/j.1461-0248.2010.01518.x
6. Fabry VJ, Seibel BA, Feely RA, Orr JC. Impacts of ocean acidification on marine fauna and ecosystem processes. *ICES J Mar Sci*. 2008;65: 414-432. doi:10.1093/icesjms/fsn048
7. Kroeker KJ, Micheli F, Gambi MC. Ocean acidification causes ecosystem shifts via altered competitive interactions. *Nature Clim Change*. 2012;3: 156-159. doi:10.1038/nclimate1680
8. Crawford KJ, Alvarez-Fernandez S, Mojica KDA, Riebesell U, Brussaard CPD. Alterations in microbial community composition with increasing fCO₂: A mesocosm study in the eastern Baltic Sea. *Biogeosciences*. 2017;14: 3831-3849. doi:10.5194/bg-14-3831-2017
9. Schulz KG, Bach LT, Bellerby RGJ, Bermúdez Monsalve JR, Büdenbender J, Boxhammer T, et al. Phytoplankton blooms at increasing levels of atmospheric carbon dioxide: Experimental evidence for negative effects on prymnesiophytes and positive on small picoeukaryotes. *Front Mar Sci*. 2017;4: 7193-18. doi:10.3389/fmars.2017.00064
10. Lischka S, Büdenbender J, Boxhammer T, Riebesell U. Impact of ocean acidification and elevated temperatures on early juveniles of the polar shelled pteropod *Limacina helicina*: Mortality, shell degradation, and shell growth. *Biogeosciences*. 2011;8: 919-932. doi:10.5194/bg-8-919-2011
11. Riebesell U, Bach LT, Bellerby RGJ, Bermúdez Monsalve JR, Boxhammer T, Czerny J, et al. Competitive fitness of a predominant pelagic calcifier impaired by ocean acidification. *Nature Geosci*. 2017;10: 19-23. doi:10.1038/ngeo2854

12. Sala MM, Aparicio FL, Balagué V, Boras JA, Borrull E, Cardelús C, et al. Contrasting effects of ocean acidification on the microbial food web under different trophic conditions. *ICES J Mar Sci.* 2015;73: 670-679. doi:10.1093/icesjms/fsv130
13. Riebesell U, Schulz KG, Bellerby RGJ, Botros M, Fritsche P, Meyerhöfer M, et al. Enhanced biological carbon consumption in a high CO₂ ocean. *Nature.* 2007;450: 545-548. doi:10.1038/nature06267
14. Bellerby RGJ, Schulz KG, Riebesell U, Neill C, Nondal G, Heegaard E, et al. Marine ecosystem community carbon and nutrient uptake stoichiometry under varying ocean acidification during the PeECE III experiment. *Biogeosciences.* 2008;5: 1517-1527. doi:10.5194/bg-5-1517-2008
15. Finkel ZV, Beardall J, Flynn KJ, Quigg A, Rees TAV, Raven JA. Phytoplankton in a changing world: Cell size and elemental stoichiometry. *J Plankton Res.* 2010;32: 119-137. doi:10.1093/plankt/fbp098
16. Kim J-M, Lee K, Shin K, Yang EJ, Engel A, Karl DM, et al. Shifts in biogenic carbon flow from particulate to dissolved forms under high carbon dioxide and warm ocean conditions. *Geophys Res Lett.* 2011;38: L08612. doi:10.1029/2011GL047346
17. Engel A, Borchard C, Piontek J, Schulz KG, Riebesell U, Bellerby R. CO₂ increases ¹⁴C primary production in an Arctic plankton community. *Biogeosciences.* 2013;10: 1291-1308. doi:10.5194/bg-10-1291-2013
18. Spilling K, Schulz KG, Paul AJ, Boxhammer T, Achterberg EP, Hornick T, et al. Effects of ocean acidification on pelagic carbon fluxes in a mesocosm experiment. *Biogeosciences.* 2016;13: 6081-6093. doi:10.5194/bg-13-6081-2016
19. Engel A, Piontek J, Grossart HP, Riebesell U, Schulz KG, Sperling M. Impact of CO₂ enrichment on organic matter dynamics during nutrient induced coastal phytoplankton blooms. *J Plankton Res.* 2014;36: 641-657. doi:10.1093/plankt/fbt125
20. Endres S, Galgani L, Riebesell U, Schulz KG, Engel A. Stimulated bacterial growth under elevated pCO₂: Results from an off-shore mesocosm study. Dupont S, editor. *PLoS ONE.* 2014;9: e99228-8. doi:10.1371/journal.pone.0099228
21. Passow U. Transparent exopolymer particles (TEP) in aquatic environments. *Prog Oceanogr.* 2002;55: 287-333. doi:10.1016/S0079-6611(02)00138-6

22. Thornton DCO. Dissolved organic matter (DOM) release by phytoplankton in the contemporary and future ocean. *Eur J Phycol.* 2014;49: 20-46. doi:10.1080/09670262.2013.875596
23. Rossoll D, Bermúdez Monsalve JR, Hauss H, Schulz KG, Riebesell U, Sommer U, et al. Ocean acidification-induced food quality deterioration constrains trophic transfer. Thrush S, editor. *PLoS ONE.* 2012;7: e34737-6. doi:10.1371/journal.pone.0034737
24. Schoo KL, Malzahn AM, Krause E, Boersma M. Increased carbon dioxide availability alters phytoplankton stoichiometry and affects carbon cycling and growth of a marine planktonic herbivore. *Mar Biol.* 2012;160: 2145-2155. doi:10.1007/s00227-012-2121-4
25. Sanders R, Henson SA, Koski M, La Rocha De CL, Painter SC, Poulton AJ, et al. The biological carbon pump in the North Atlantic. *Prog Oceanogr.* 2014;129, Part B IS -: 200-218. doi:10.1016/j.pocean.2014.05.005
26. Bach LT, Taucher J, Boxhammer T, Ludwig A, Achterberg EP, Algueró-Muñiz M, et al. Influence of ocean acidification on a natural winter-to-summer plankton succession: First insights from a long-term mesocosm study draw attention to periods of low nutrient concentrations. Anil AC, editor. *PLoS ONE.* 2016;11: e0159068 EP -. doi:10.1371/journal.pone.0159068
27. Riebesell U, Czerny J, Bröckel von K, Boxhammer T, Büdenbender J, Deckelnick M, et al. Technical Note: A mobile sea-going mesocosm system - new opportunities for ocean change research. *Biogeosciences.* 2013;10: 1835-1847. doi:10.5194/bg-10-1835-2013
28. Czerny J, Schulz KG, Krug SA, Ludwig A, Riebesell U. Technical Note: The determination of enclosed water volume in large flexible-wall mesocosms 'KOSMOS'. *Biogeosciences.* 2013;10: 1937-1941. doi:10.5194/bg-10-1937-2013
29. Boxhammer T, Bach LT, Czerny J, Riebesell U. Technical note: Sampling and processing of mesocosm sediment trap material for quantitative biogeochemical analysis. *Biogeosciences.* 2016;13: 2849-2858. doi:10.5194/bg-13-2849-2016
30. Zark M, Riebesell U, Dittmar T. Effects of ocean acidification on marine dissolved organic matter are not detectable over the succession of phytoplankton blooms. *Science Advances.* 2015;1: e1500531-e1500531. doi:10.1126/sciadv.1500531
31. Kattner G. Storage of dissolved inorganic nutrients in seawater: Poisoning with mercuric chloride. *Mar Chem.* 1999;67: 61-66. doi:10.1016/S0304-4203(99)00049-3

32. Algueró-Muñiz M, Alvarez-Fernandez S, Thor P, Bach LT, Esposito M, Horn HG, et al. Ocean acidification effects on mesozooplankton community development: Results from a long-term mesocosm experiment. *PLoS ONE*. 2017;12: e0175851. doi:10.1371/journal.pone.0175851
33. Johnson KM, Sieburth JM, Williams PJL, Brändström L. Coulometric total carbon dioxide analysis for marine studies: Automation and calibration. *Mar Chem*. 1987;21: 117-133. doi:10.1016/0304-4203(87)90033-8
34. Clayton TD, Byrne RH. Spectrophotometric seawater pH measurements: Total hydrogen ion concentration scale calibration of m-cresol purple and at-sea results. *Deep-Sea Res PT I*. 1993;40: 2115-2129. doi:10.1016/0967-0637(93)90048-8
35. van Heuven S, Pierrot D, Rae JWB, Lewis E, Wallace DWR. CO2SYS v 1.1. MATLAB Program Developed for CO₂ System Calculations. ORNL/CDIAC-105b. Oak Ridge National Laboratory; 2011.
36. Lueker TJ, Dickson AG, Keeling CD. Ocean *p*CO₂ calculated from dissolved inorganic carbon, alkalinity, and equations for K₁ and K₂: validation based on laboratory measurements of CO₂ in gas and seawater at equilibrium. *Mar Chem*. 2000;70: 105-119. doi:10.1016/S0304-4203(00)00022-0
37. Patey MD, Rijkenberg MJA, Statham PJ, Stinchcombe MC, Achterberg EP, Mowlem M. Determination of nitrate and phosphate in seawater at nanomolar concentrations. *Trac-Trend Anal Chem*. 2008;27: 169-182. doi:10.1016/j.trac.2007.12.006
38. Holmes RM, Aminot A, Kérouel R, Hooker BA, Peterson BJ. A simple and precise method for measuring ammonium in marine and freshwater ecosystems. *Can J Fish Aquat Sci*. 1999;56: 1801-1808. doi:10.1139/f99-128
39. Sharp JH. Improved analysis for 'particulate' organic carbon and nitrogen from seawater. *Limnol Oceanogr*. 1974;19: 984-989. doi:10.4319/lo.1974.19.6.0984
40. Hansen HP, Koroleff F. Determination of nutrients. *Methods of Seawater Analysis*. Weinheim, Germany: Wiley-VCH Verlag GmbH; 1999. pp. 159-228. doi:10.1002/9783527613984.ch10
41. Gorsky G, Ohman MD, Picheral M, Gasparini S, Stemmann L, Romagnan J-B, et al. Digital zooplankton image analysis using the ZooScan integrated system. *J Plankton Res*. 2010;32: 285-303. doi:10.1093/plankt/fbp124

42. Lehette P, Hernández-León S. Zooplankton biomass estimation from digitized images: A comparison between subtropical and Antarctic organisms. *Limnol Oceanogr Methods*. 2009;7: 304-308. doi:10.4319/lom.2009.7.304
43. Kiørboe T. Zooplankton body composition. *Limnol Oceanogr*. 2013;58: 1843-1850. doi:10.4319/lo.2013.58.5.1843
44. Gismervik I. Stoichiometry of some marine planktonic crustaceans. *J Plankton Res*. 1997;19: 279-285. doi:10.1093/plankt/19.2.279
45. Hernández-León S, Montero I. Zooplankton biomass estimated from digitalized images in Antarctic waters: A calibration exercise. *J Geophys Res*. 2006;111: 307-6. doi:10.1029/2005JC002887
46. Garijo JC, Hernández-León S. The use of an image-based approach for the assessment of zooplankton physiological rates: A comparison with enzymatic methods. *J Plankton Res*. 2015;37: 923-938. doi:10.1093/plankt/fbv056
47. Biard T, Stemmann L, Picheral M, Mayot N, Vandromme P, Hauss H, et al. *In situ* imaging reveals the biomass of giant protists in the global ocean. *Nature*. 2016;532: 504-507. doi:10.1038/nature17652
48. Hansell DA, Carlson CA. Net community production of dissolved organic carbon. *Global Biogeochem Cycles*. 1998;12: 443-453. doi:10.1029/98GB01928
49. Silyakova A, Bellerby RGJ, Schulz KG, Czerny J, Tanaka T, Nondal G, et al. Pelagic community production and carbon-nutrient stoichiometry under variable ocean acidification in an Arctic fjord. *Biogeosciences*. 2013;10: 4847-4859. doi:10.5194/bg-10-4847-2013
50. R Core Team 2015. R: A language and environment for statistical computing [Internet]. Vienna, Austria. Available from: <http://www.R-project.org/>
51. Anderson MJ. A new method for non-parametric multivariate analysis of variance. *Austral Ecol*. 2001;26: 32-46. doi:10.1111/j.1442-9993.2001.01070.pp.x
52. Anderson MJ, Walsh DCI. PERMANOVA, ANOSIM, and the Mantel test in the face of heterogeneous dispersions: What null hypothesis are you testing? *Ecol Monogr*. 2013;83: 557-574. doi:10.1890/12-2010.1
53. Amo YD, Brzezinski MA. The chemical form of dissolved Si taken up by marine diatoms. *J Phycol*. 1999;35: 1162-1170. doi:10.1046/j.1529-8817.1999.3561162.x

54. Thametrakoln K, Hildebrand M. Silicon uptake in diatoms revisited: A model for saturable and nonsaturable uptake kinetics and the role of silicon transporters. *Plant Physiol.* 2008;146: 1397-1407. doi:10.1104/pp.107.107094
55. DeMaster DJ, Dunbar RB, Gordon LI, Leventer AR, Morrison JM, Nelson DM, et al. Cycling and accumulation of biogenic silica and organic matter in high-latitude environments: The Ross Sea. *Oceanography.* 1992;5: 146-153. doi:10.5670/oceanog.1992.03
56. Nelson DM, DeMaster DJ, Dunbar RB, Smith WO. Cycling of organic carbon and biogenic silica in the Southern Ocean: Estimates of water-column and sedimentary fluxes on the Ross Sea continental shelf. *J Geophys Res.* 1996;101: 18519-18532. doi:10.1029/96JC01573
57. Horn HG, Sander N, Stühr A, Algueró-Muñiz M, Bach LT, Löder MGJ, et al. Low CO₂ sensitivity of microzooplankton communities in the Gullmar Fjord, Skagerrak: Evidence from a long-term mesocosm study. *PLoS ONE.* 2016;11: e0165800. doi:10.1371/journal.pone.0165800
58. Benitez-Nelson CR, Buesseler KO. Variability of inorganic and organic phosphorus turnover rates in the coastal ocean. *Nature.* 1999;398: 502-505. doi:10.1038/19061
59. Bronk DA, See JH, Bradley P, Killberg L. DON as a source of bioavailable nitrogen for phytoplankton. *Biogeosciences.* 2007;4: 283-296. doi:10.5194/bg-4-283-2007
60. White AE, Watkins-Brandt KS, Engle MA, Burkhardt B, Paytan A. Characterization of the rate and temperature sensitivities of bacterial remineralization of dissolved organic phosphorus compounds by natural populations. *Front Microbiol.* 2012;3: 276-13. doi:10.3389/fmicb.2012.00276/abstract
61. Chen CC, Petersen JE, Kemp WM. Spatial and temporal scaling of periphyton growth on walls of estuarine mesocosms. *Mar Ecol-Prog Ser.* 1997;155: 1-15. doi:10.3354/meps155001
62. Riebesell U, Lee K, Nejstgaard JC. Pelagic mesocosms. In: Riebesell U, Fabry VJ, Hansson L, Gattuso J-P, editors. *Guide to best practices in ocean acidification research and data reporting.* Luxembourg; 2010. pp. 95-112. doi:10.2777/58454
63. Czerny J, Schulz KG, Boxhammer T, Bellerby RGJ, Büdenbender J, Engel A, et al. Implications of elevated CO₂ on pelagic carbon fluxes in an Arctic mesocosm study - an elemental mass balance approach. *Biogeosciences.* 2013;10: 3109-3125. doi:10.5194/bg-10-3109-2013

64. Paul AJ, Bach LT, Schulz KG, Boxhammer T, Czerny J, Achterberg EP, et al. Effect of elevated CO₂ on organic matter pools and fluxes in a summer Baltic Sea plankton community. *Biogeosciences*. 2015;12: 6181-6203. doi:10.5194/bg-12-6181-2015
65. Czerny J, Schulz KG, Ludwig A, Riebesell U. Technical Note: A simple method for air-sea gas exchange measurements in mesocosms and its application in carbon budgeting. *Biogeosciences*. 2013;10: 1379-1390. doi:10.5194/bg-10-1379-2013
66. Strong AL, Lowry KE, Brown ZW, Mills MM, van Dijken GL, Pickart RS, et al. Mass balance estimates of carbon export in different water masses of the Chukchi Sea shelf. *Deep Sea Res Part 2 Top Stud Oceanogr*. 2016;130 IS -: 88-99. doi:10.1016/j.dsr2.2016.05.003
67. Howarth RW, Marino R, Lane J, Cole JJ. Nitrogen fixation in freshwater, estuarine, and marine ecosystems. 1. Rates and importance. *Limnol Oceanogr*. 1988;33: 669-687. doi:10.4319/lo.1988.33.4part2.0669
68. Stal LJ, Albertano P, Bergman B, Bröckel von K, Gallon JR, Hayes PK, et al. BASIC: Baltic Sea cyanobacteria. An investigation of the structure and dynamics of water blooms of cyanobacteria in the Baltic Sea-responses to a changing environment. *Cont Shelf Res*. 2003;23: 1695-1714. doi:10.1016/j.csr.2003.06.001
69. Ohlendieck U, Gundersen K, Meyerhöfer M, Fritsche P, Nachtigall K, Bergmann B. The significance of nitrogen fixation to new production during early summer in the Baltic Sea. *Biogeosciences*. 2007;4: 63-73. doi:10.5194/bg-4-63-2007
70. Eberlein T, Wohlrab S, Rost B, John U, Bach LT, Riebesell U, et al. Effects of ocean acidification on primary production in a coastal North Sea phytoplankton community. Vopel KC, editor. *PLoS ONE*. 2017;12: e0172594-15. doi:10.1371/journal.pone.0172594
71. Sambrotto RN, Savidge G, Robinson C, Boyd P, Takahashi T, Karl DM, et al. Elevated consumption of carbon relative to nitrogen in the surface ocean. *Nature*. 1993;363: 248-250. doi:10.1038/363248a0
72. Toggweiler JR. Carbon overconsumption. *Nature*. 1993;363: 210-211. doi:10.1038/363210a0
73. Taucher J, Haunost M, Boxhammer T, Bach LT, Alguer Mu iz MA, Riebesell U. Influence of ocean acidification on plankton community structure during a winter-to-summer succession: An imaging approach indicates that copepods can benefit from elevated CO₂ via indirect food web effects. Ianora A, editor. *PLoS ONE*. 2017;12: e0169737-23. doi:10.1371/journal.pone.0169737

Supporting information

Table S3.1. Conditions of the element pools during the reference period of the experiment.

	ambient CO ₂			high CO ₂			t-test	
	reference period		reference value	reference period		reference value	p-value	
	start	end	μmol L ⁻¹ ± SD	start	end	μmol L ⁻¹ ± SD		
IN	DIC	t ₋₁	t ₁₁	2079.3 ± 3.2	t ₅	t ₅	2184.3 ± 4.3	<0.001
	DIN	t ₋₁	t ₁₁	7.0 ± 0.1	t ₋₁	t ₁₁	6.9 ± 0.1	0.380
	DIP	t ₋₁	t ₁₁	0.76 ± 0.01	t ₋₁	t ₁₁	0.76 ± 0.01	0.242
	Si	t ₂	t ₁₁	9.9 ± 0.3	t ₂	t ₁₁	9.8 ± 0.1	0.572
DOM	DOC	t ₁	t ₁₁	189.0 ± 10.8	t ₁	t ₁₁	190.1 ± 5.7	0.840
	DON	t ₁	t ₁₁	8.8 ± 0.6	t ₁	t ₁₁	8.9 ± 0.4	0.804
	DOP	t ₋₁	t ₁₁	0.16 ± 0.02	t ₋₁	t ₁₁	0.14 ± 0.02	0.238
PM	TPC	t ₋₁	t ₁₁	14.4 ± 0.7	t ₋₁	t ₁₁	14.7 ± 0.8	0.613
	TPN	t ₋₁	t ₁₁	1.9 ± 0.1	t ₋₁	t ₁₁	2.0 ± <0.1	0.554
	TPP	t ₋₁	t ₁₁	0.08 ± 0.01	t ₋₁	t ₁₁	0.09 ± 0.01	0.665
	BSi	t ₋₁	t ₁₁	0.4 ± <0.1	t ₋₁	t ₁₁	0.4 ± <0.1	0.679
PM _{COP}	TPC _{COP}	t ₁	t ₁	7.5 ± 2.5	t ₁	t ₁	6.8 ± 0.9	0.590
	TPN _{COP}	t ₁	t ₁	1.4 ± 0.5	t ₁	t ₁	1.2 ± 0.2	0.590
	TPP _{COP}	t ₁	t ₁	0.14 ± 0.05	t ₁	t ₁	0.13 ± 0.02	0.590

Reference values of both CO₂ treatments are average values ± standard deviation (SD) of the indicated reference periods for calculation of net changes in the respective element pools (see Table 3.1 for abbreviations of the element pools). If start and end point of the reference period are identical, reference period is limited to only one data point. t-tests performed on average values of all ambient and high CO₂ mesocosms are indicated by p-values (bold values indicate significant difference, p ≤ 0.05).

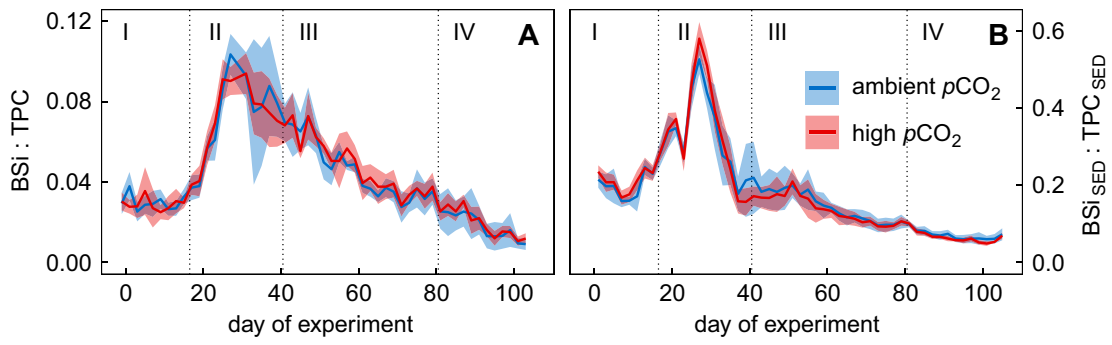


Fig S3.1. Time course of the biogenic silica to total particulate carbon ratio. Solid lines show mean values of the biogenic silica (BSi) to particulate carbon (TPC) ratio in (A) the water column and (B) sediment trap samples of the ambient (blue) and high (red) CO_2 treatment. Coloured areas indicate standard deviation of the replicated ($n = 5$) treatments. Roman numbers denote the different phases of the experiment.

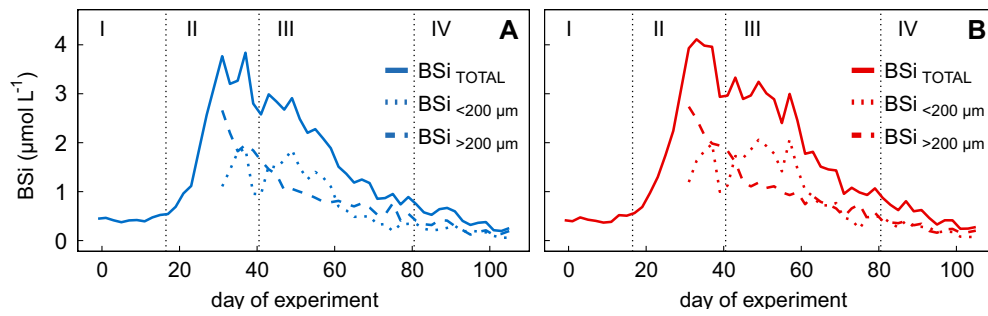


Fig S3.2. Time course of different size classes of biogenic silica. Solid lines, dotted lines, and dashed lines represent the three size classes of total biogenic silica (BSi), the fraction $> 200 \mu\text{m}$, and the fraction $< 200 \mu\text{m}$ respectively. All lines represent mean values of the (A) ambient and (B) high CO_2 treatment. Roman numerals denote the different phases of the experiment.

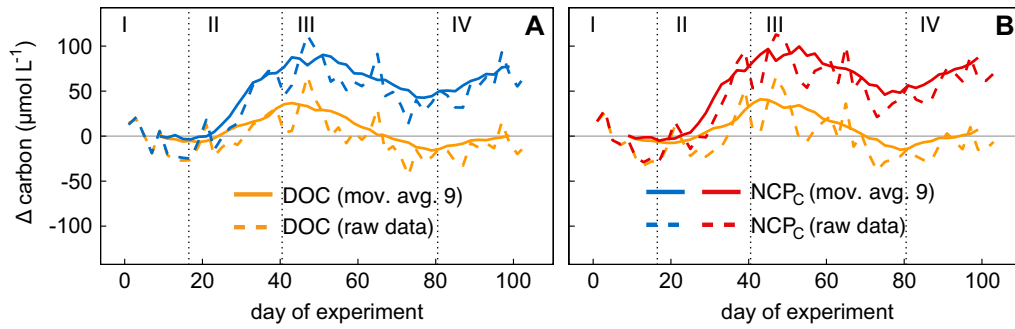


Fig S3.3. Moving average of dissolved organic carbon and net community production. Dashed lines show net changes of dissolved organic carbon (DOC, yellow) and net community production of carbon (NCP, blue/red) as average values of (A) ambient and (B) high CO₂ mesocosms. Solid lines of the same colour code show strongly smoothed data (moving average of nine), with an adjusted reference period for calculation of net changes to $t_1 - t_{17}$. Accordingly, smoothed data sets do not start before day 9. Roman numbers denote the different phases of the experiment.

4. Manuscript III

Plankton community structure controls the response of particulate organic matter stoichiometry to ocean acidification

Tim Boxhammer^{1*}, Lennart T. Bach¹, Jan Taucher¹, Richard G. J. Bellerby^{2,3}, J. Rafael Bermúdez Monsalve^{1,4}, Kai G. Schulz^{1,5}, Hendrik Schultz^{1,6}, Michael Sswat¹, and Ulf Riebesell¹

To be submitted**

¹ GEOMAR Helmholtz Centre for Ocean Research Kiel, Kiel, Germany.

² Norwegian Institute for Water Research, Bergen, Norway.

³ SKLEC-NIVA Centre for Marine and Coastal Climate Research, East China Normal University, Shanghai, China.

⁴ Galapagos Marine Research and Exploration, GMaRE. Joint ESPOL-CDF program, Charles Darwin Research Station, Puerto Ayora, Galapagos Islands, Ecuador.

⁵ Centre for Coastal Biogeochemistry, Southern Cross University, Lismore, NSW, Australia.

⁶ University of Auckland, Auckland, New Zealand.

*Correspondence to: tboxhammer@geomar.de

** manuscript formatted in style of Science (reports)

Abstract

The carbon to nitrogen (C:N) ratio of particulate organic matter plays a central role in ocean biogeochemistry. Previous *in situ* plankton community studies reported an increase of C:N ratios with rising seawater CO₂ concentrations. Here, we present results from an *in-situ* mesocosm CO₂ perturbation study with natural plankton communities, which call for a reconsideration of this concept. Instead of a positive correlation between C:N and CO₂, we find shifting correlations depending on the plankton community structure and phytoplankton growth phase. The observation is consistent with elemental ratios in settling particulate matter and results from similar experiments in different ocean regions. Our results show that C:N ratios in a high CO₂ ocean will be depending on the composition of future plankton communities and their inherent C:N signatures rather than increasing linearly with CO₂.

Main Text

The Redfield ratio, the global average elemental stoichiometry of marine plankton (106C : 16N : 1P) (1), is commonly used for calculating nutrient-based primary production, potential carbon sequestration, as well as global distribution and cycling of biogeochemical tracers. The elemental composition of phytoplankton is known, however, to vary among ocean regions, phytoplankton taxa, and even growth conditions of the same taxon (2-4). Excess carbon fixation above the Redfield ratio by phytoplankton has been observed in response to nutrient limitation, increasing temperature, as well as rising carbon dioxide (CO₂) concentrations (5-7). As the ocean is a major sink for anthropogenic CO₂ emissions, CO₂ will likely become one of the most important factors modulating marine organic matter stoichiometry in the future (8, 9). Enhanced carbon fixation of plankton communities observed under high CO₂ suggested significant implications for future ocean sequestration of anthropogenic carbon emissions with consequences for global carbon cycling and oxygen consumption in subsurface ocean layers (10, 11).

To assess the C:N response at the community level under close to natural conditions, we conducted a large scale mesocosm CO₂ perturbation study in Raunefjord, Norway (60.265° N, 5.205° E) in 2011 (12, 13). We used eight pelagic mesocosms, each enclosing about 75 m³ of seawater, containing natural plankton assemblages from viruses to mesozooplankton (14). The initial *f*CO₂ gradient (fugacity of CO₂) of 300 to 3050 μatm between mesocosms continuously decreased in response to CO₂ air-sea gas exchange and biological activity, leading to average values of 300 to 1615 μatm (Fig. 4.1A). The two highest CO₂ treatments are well above projected CO₂ scenarios and were

chosen as a ‘proof of concept’ (15). Based on the plankton biomass development and the day of significant CO_2 manipulation (day 3) we divided the experiment into five consecutive phases (13).

A phytoplankton bloom, based on nutrients present in the enclosed water, developed right from the beginning of the study (Phase 0, Fig. 4.1B-D). The bloom was dominated by pico- and nano-phytoplankton, mostly chlorophytes and small diatoms (12), which contributed most to particulate organic carbon and nitrogen (POC and PON, Fig. 4.2A and B).

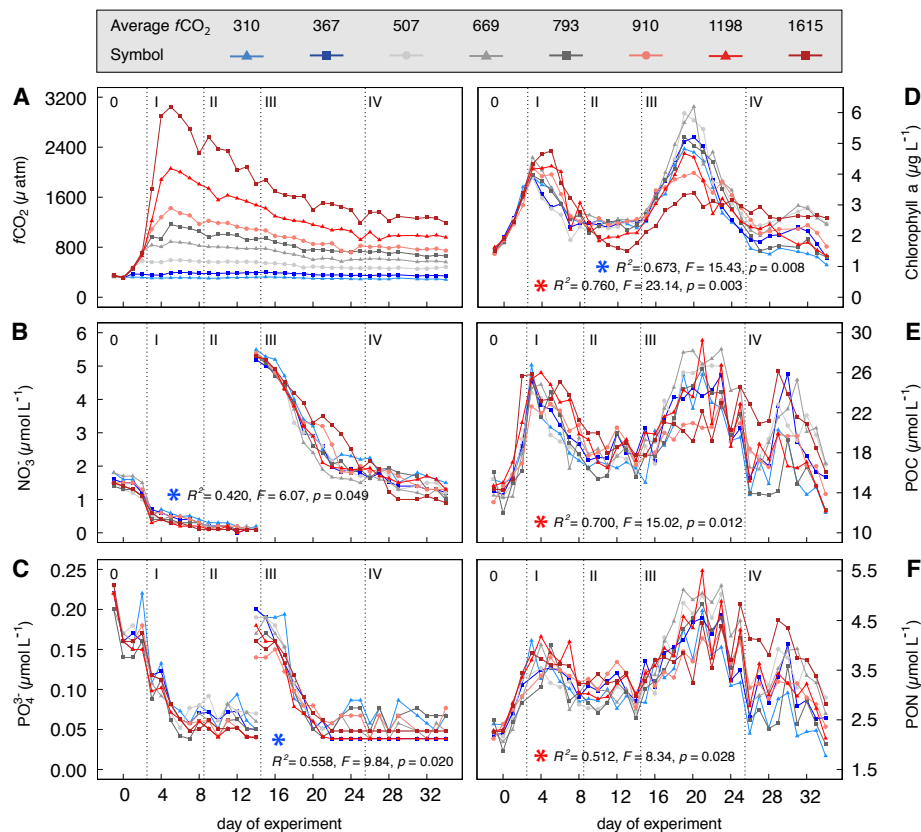


Fig. 4.1. Time course of key parameters in the mesocosms. (A) $f\text{CO}_2$, (B) NO_3^- = Nitrate concentration, (C) PO_4^{3-} = phosphate concentration, (D) Chlorophyll *a* concentration, (E) POC = particulate organic carbon concentration, and (F) PON = particulate organic nitrogen concentration. Colours and symbols indicate the CO_2 treatment. Roman numbers denote the different phases of the experiment (13). On day 14, panel B and C show two data points of each mesocosm, one before and one after the addition of inorganic nitrate and phosphorus. Red and blue asterisks denote a significantly positive or negative CO_2 effect of phase specific average values, respectively, published in (12).

Significantly higher build-up of POC and PON at elevated CO_2 during this bloom (Phase I, Fig. 4.1E and F) can be attributed to elevated pico-phytoplankton abundances (12). Fourteen days after the first CO_2 addition (day 14, Fig. S4.1), we added inorganic nitrate and phosphate to the systems to induce a second phytoplankton bloom (Phase III, Fig. 4.1B-D). As before, POC and PON build-up was driven by growth of pico- and nano-plankton, mainly small diatoms, cryptophytes, and chlorophytes (12),

but in contrast to the first bloom biomass build-up was not significantly stimulated by CO_2 (Fig. 4.2A and B). A subsequent bloom by coccolithophores at ambient CO_2 and cyanobacteria at elevated CO_2 levels (12) had only a moderate impact on plankton biomass (Phase IV, Fig. 4.1E and F).

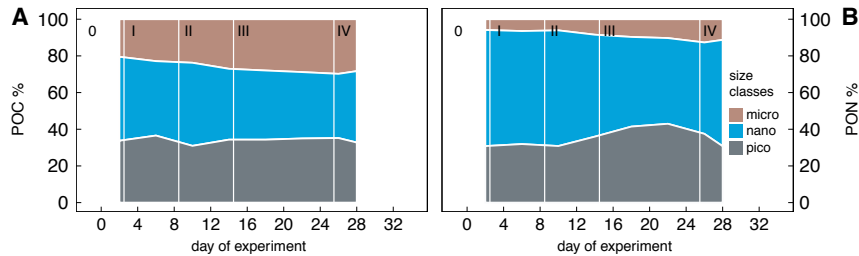


Fig. 4.2. Particle size class contribution to POC and PON. Average relative contribution of pico- (0.3 - 2.7 μm), nano- (2.7 - 10 μm), and microplankton-sized (10 - 100 μm) particles to (A) particulate organic carbon (POC) and to (B) particulate organic nitrogen (PON). Roman numerals denote the different phases of the experiment (13).

The stoichiometry of particulate organic matter was tightly coupled to phytoplankton growth phases and changing phytoplankton community composition. Substantially elevated carbon to nitrogen (C:N) ratios of microplankton-sized particles at elevated CO_2 initially determined the trend of bulk C:N (Phase I, Table 4.1, Fig. 4.3A and E). This is consistent with increased inorganic C to nitrogen consumption at high CO_2 during a former study by Riebesell et al. (10) in the same Norwegian fjord where microplankton-sized diatoms dominated.

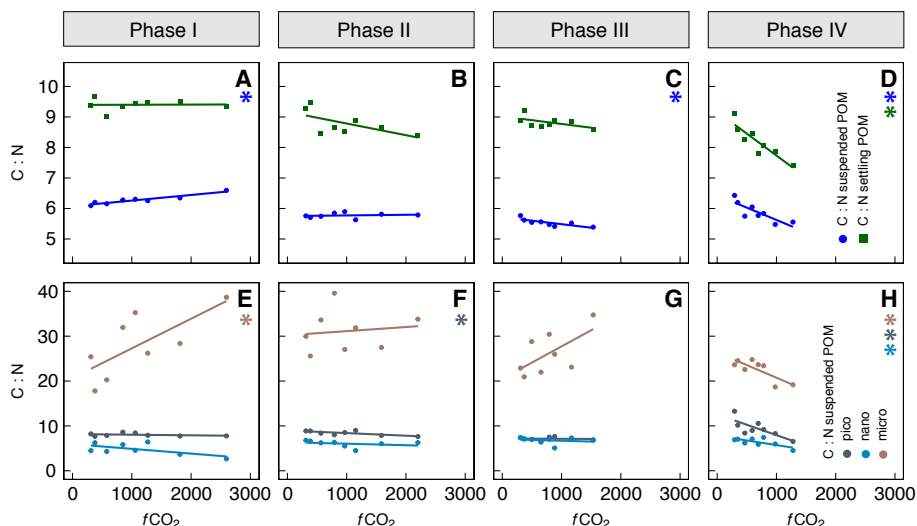


Fig. 4.3. Correlation of carbon to nitrogen ratios with $f\text{CO}_2$. Phase specific average carbon to nitrogen (C:N) ratios of (A-D) suspended and settling particulate organic matter (POM), as well as (E-H) suspended POM size fractions of pico- (0.3 - 2.7 μm), nano- (2.7 - 10 μm), and microplankton (10 - 100 μm) are correlated with the average $f\text{CO}_2$ of the respective experimental phase (Table S4.1) (13). Asterisks denote a statistically significant CO_2 effect ($p < 0.05$; Table 4.1).

Table 4.1. Summary of linear regression analysis. Statistical significance of potential CO₂ effects on elemental stoichiometry of suspended and sedimented particulate organic matter was tested for each experimental phase (0 - IV) (13) using a linear model. Size classes of pico-, nano-, and microplankton represent particulate matter of 0.3 - 2.7 μm, 2.7 - 10 μm, and 10 - 100 μm, respectively. Significant effects detected are highlighted in bold, while the positive or negative trends are indicated by ⁽⁺⁾ and ⁽⁻⁾, respectively. Degrees of freedom = 6.

	Phase	Suspended POM			Settling POM		
		Multiple R ²	F-statistic	<i>p</i>	Multiple R ²	F-statistic	<i>p</i>
C:N	0	0.095	0.629	0.458	0.067	0.430	0.536
	I	0.894	50.630	⁽⁺⁾ <0.001	<0.001	0.003	0.959
	II	0.027	0.165	0.699	0.387	3.791	0.099
	III	0.635	10.430	⁽⁻⁾ 0.018	0.308	2.671	0.153
	IV	0.694	13.640	⁽⁻⁾ 0.010	0.818	26.870	⁽⁻⁾ 0.002
C:P	0	0.078	0.507	0.503	0.011	0.065	0.807
	I	0.097	0.645	0.453	0.593	8.755	⁽⁻⁾ 0.025
	II	0.616	9.616	⁽⁻⁾ 0.021	0.812	25.830	⁽⁻⁾ 0.002
	III	0.120	0.818	0.401	0.663	11.790	⁽⁻⁾ 0.014
	IV	0.796	23.360	⁽⁻⁾ 0.003	0.600	8.986	⁽⁻⁾ 0.024
C:N _{PICO}	0	<0.001	<0.001	0.996			
	I	0.093	0.619	0.461			
	II	0.527	6.691	⁽⁻⁾ 0.041			
	III	0.004	0.025	0.881			
	IV	0.595	8.830	⁽⁻⁾ 0.025			
C:N _{NANO}	0	0.018	0.091	0.775			
	I	0.398	3.973	0.093			
	II	0.087	0.573	0.478			
	III	0.041	0.259	0.629			
	IV	0.522	6.543	⁽⁻⁾ 0.043			
C:N _{MICRO}	0	0.222	1.715	0.238			
	I	0.521	6.527	⁽⁺⁾ 0.043			
	II	0.017	0.102	0.761			
	III	0.387	3.794	0.099			
	IV	0.641	10.700	⁽⁻⁾ 0.017			

The picture progressively changed during the post-bloom phase and with the shift of dominating phytoplankton groups and their individual responses to increasing CO₂ levels during the second phytoplankton bloom (Phases II and III, Fig. 4.3B, C, F, and G). From the second bloom on, bulk C:N correlated negatively with CO₂, which we consider to be due to a reduced dominance of diatoms at high CO₂ (12) (Table 4.1, Fig. 4.3C). The subsequent CO₂-controlled intensity of the coccolithophore and cyanobacteria blooms further amplified the negative correlation of C:N with CO₂,

now consistent in all three particle size classes (Table 4.1, Fig. 4.3D and H). A corresponding trend in settling particulate matter, collected in sediment traps at the bottom of the mesocosms, was already visible since the post-bloom phase (II), but only got significant in the presence of blooming coccolithophores and cyanobacteria (Table 4.1, Fig. 4.3B-D). However, about one third of the measured vertical POC flux occurred in this last phase, emphasizing the relevance of this observation for potential future ocean carbon sequestration (16). Carbon to phosphorus (C:P) ratios of bulk suspended as well as settling particulate matter mirror the observed pattern of C:N ratios, with significant negative correlation in settling particles throughout the experiment (Table 4.1, Fig. S4.2A-D). Previous studies have shown enhanced production of carbon rich transparent exopolymer particles (TEP) at increased CO_2 concentrations, which were thought to potentially increase carbon load of settling particles (17). Surprisingly, enhanced production of TEP at increased CO_2 levels in the present study (18) did not increase the relative carbon content of settling POM.

Our findings indicate that under close to natural conditions, elevated CO_2 does not necessarily enhance carbon consumption and C:N ratios of marine organic matter. In contrast, we show that the POM stoichiometry is tightly linked to plankton community structure and can even result in lower C:N ratios under high CO_2 levels. However, individual responses of phytoplankton groups or species cannot be totally excluded. Indeed, CO_2 perturbation studies with natural plankton assemblages during the last decade have shown diverse responses of plankton community structure and POM stoichiometry to increasing CO_2 (19-24). Furthermore, we have shown that the shifting C:N signal of suspended organic matter carries on to settling POM, likely impacting carbon sequestration. These results call for reconsidering the concept that natural plankton communities show a unidirectional response of elevated C:N to increasing CO_2 , especially with respect to global biogeochemical models. Therefore we emphasize the need to understand CO_2 -driven plankton community shifts in order to predict the response of elemental ratios and biogeochemical cycling in a high CO_2 ocean.

References and Notes

1. A. C. Redfield, B. H. Ketchum, F. A. Richards, in *The Sea*, M. N. Hill, Ed. (The Sea, ed. 2, 1963), pp. 26-77.
2. R. J. Geider, J. La Roche, Redfield revisited: Variability of C:N:P in marine microalgae and its biochemical basis. *Eur J Phycol.* **37**, 1-17 (2002).
3. T.-Y. Ho *et al.*, The elemental composition of some marine phytoplankton. *J Phycol.* **39**, 1145-1159 (2003).
4. A. C. Martiny *et al.*, Strong latitudinal patterns in the elemental ratios of marine plankton and organic matter. *Nat Geosci.* **6**, 279-283 (2013).
5. M. S. Wetz, P. A. Wheeler, Production and partitioning of organic matter during simulated phytoplankton blooms. *Limnol Oceanogr.* **48**, 1808-1817 (2003).
6. J. Taucher *et al.*, Combined effects of CO₂ and temperature on carbon uptake and partitioning by the marine diatoms *Thalassiosira weissflogii* and *Dactyliosolen fragilissimus*. *Limnol Oceanogr.* **60**, 901-919 (2015).
7. Z. V. Finkel *et al.*, Phytoplankton in a changing world: Cell size and elemental stoichiometry. *J Plankton Res.* **32**, 119-137 (2010).
8. C. L. Sabine *et al.*, The oceanic sink for anthropogenic CO₂. *Science.* **305**, 367-371 (2004).
9. D. B. Van de Waal, A. M. Verschoor, J. M. Verspagen, E. van Donk, J. Huisman, Climate-driven changes in the ecological stoichiometry of aquatic ecosystems. *Frontiers in Ecology and the Environment.* **8**, 145-152 (2010).
10. U. Riebesell *et al.*, Enhanced biological carbon consumption in a high CO₂ ocean. *Nature.* **450**, 545-548 (2007).
11. A. Oschlies, K. G. Schulz, U. Riebesell, A. Schmittner, Simulated 21st century's increase in oceanic suboxia by CO₂-enhanced biotic carbon export. *Global Biogeochem Cycles.* **22** (2008), doi:10.1029/2007GB003147.
12. K. G. Schulz *et al.*, Phytoplankton blooms at increasing levels of atmospheric carbon dioxide: Experimental evidence for negative effects on prymnesiophytes and positive on small picoeukaryotes. *Front Mar Sci.* **4**, 7193-18 (2017).

13. Materials and methods are available as supplementary materials at the Science website.
14. T. Boxhammer, L. T. Bach, M. Nicolai, U. Riebesell, Video of a plankton community enclosed in a 'Kiel Off-Shore Mesocosm for future Ocean Simulations' (KOSMOS) during the SOPRAN study in Raunefjord (Norway) 2011 (GEOMAR, 2015; <http://oceanrep.geomar.de/29400/>).
15. IPCC, 2014: Climate Change 2014: Synthesis Report. Contribution of Working Groups I, II and III to the Fifth Assessment Report of the Intergovernmental Panel on Climate Change [Core Writing Team, R.K. Pachauri and L.A. Meyer (eds.)]. IPCC, Geneva, Switzerland, 151 pp.
16. U. Riebesell *et al.*, Competitive fitness of a predominant pelagic calcifier impaired by ocean acidification. *Nat Geosci.* **10**, 19-23 (2017).
17. A. Engel, S. Thoms, U. Riebesell, E. Rochelle-Newall, I. Zondervan, Polysaccharide aggregation as a potential sink of marine dissolved organic carbon. *Nature.* **428**, 929-932 (2004).
18. S. Endres, L. Galgani, U. Riebesell, K. G. Schulz, A. Engel, Stimulated bacterial growth under elevated $p\text{CO}_2$: Results from an off-shore mesocosm study. *PLoS ONE.* **9**, e99228-8 (2014).
19. K. G. Schulz *et al.*, Temporal biomass dynamics of an Arctic plankton bloom in response to increasing levels of atmospheric carbon dioxide. *Biogeosciences.* **10**, 161-180 (2013).
20. J. Czerny *et al.*, Implications of elevated CO_2 on pelagic carbon fluxes in an Arctic mesocosm study - an elemental mass balance approach. *Biogeosciences.* **10**, 3109-3125 (2013).
21. A. J. Paul *et al.*, Effect of elevated CO_2 on organic matter pools and fluxes in a summer Baltic Sea plankton community. *Biogeosciences.* **12**, 6181-6203 (2015).
22. D. A. Hutchins, M. R. Mulholland, F. Fu, Nutrient cycles and marine microbes in a CO_2 -enriched ocean. *Oceanography.* **22**, 128-145 (2009).
23. T. Boxhammer *et al.*, Enhanced transfer of organic matter to higher trophic levels caused by ocean acidification and its implications for export production: A mass balance approach. *In review.*
24. P. Stange *et al.*, Ocean acidification-induced restructuring of the plankton food-web can influence the degradation of sinking particles. *Accepted.*
25. U. Riebesell *et al.*, Technical Note: A mobile sea-going mesocosm system - new opportunities for ocean change research. *Biogeosciences.* **10**, 1835-1847 (2013).

26. T. Boxhammer, L. T. Bach, J. Czerny, U. Riebesell, Technical note: Sampling and processing of mesocosm sediment trap material for quantitative biogeochemical analysis. *Biogeosciences*. **13**, 2849-2858 (2016).
27. J. R. Bermúdez, U. Riebesell, A. Larsen, M. Winder, Ocean acidification reduces transfer of essential biomolecules in a natural plankton community. *Sci Rep*. **6**, 27749 EP (2016).
28. J. H. Sharp, Improved analysis for 'particulate' organic carbon and nitrogen from seawater. *Limnol Oceanogr*. **19**, 984-989 (1974).
29. H. P. Hansen, F. Koroleff, in *Methods of Seawater Analysis, Third Edition* (Wiley-VCH Verlag GmbH, Weinheim, Germany, 1999), pp. 159-228.
30. R. G. Barlow, D. G. Cummings, S. W. Gibb, Improved resolution of mono- and divinyl chlorophylls *a* and *b* and zeaxanthin and lutein in phytoplankton extracts using reverse phase C-8 HPLC. *Mar Ecol Prog Ser*. **161**, 303-307 (1997).
31. K. M. Johnson, J. M. Sieburth, P. J. L. Williams, L. Brändström, Coulometric total carbon dioxide analysis for marine studies: Automation and calibration. *Mar. Chem.* **21**, 117-133 (1987).
32. B. R. Carter, J. A. Radich, H. L. Doyle, A. G. Dickson, An automated system for spectrophotometric seawater pH measurements. *Limnol. Oceanogr. Methods*. **11**, 16-27 (2013).
33. C. Mehrbach, C. H. Culberson, J. E. Hawley, R. M. Pytkowicz, Measurement of the apparent dissociation constants of carbonic acid in seawater at atmospheric pressure. *Limnol Oceanogr*. **18**, 897-907 (1973).
34. T. J. Lueker, A. G. Dickson, C. D. Keeling, Ocean $p\text{CO}_2$ calculated from dissolved inorganic carbon, alkalinity, and equations for K_1 and K_2 : validation based on laboratory measurements of CO_2 in gas and seawater at equilibrium. *Mar. Chem.* **70**, 105-119 (2000).
35. J. Taucher *et al.*, Influence of ocean acidification on plankton community structure during a winter-to-summer succession: An imaging approach indicates that copepods can benefit from elevated CO_2 via indirect food web effects. *PLoS ONE*. **12**, e0169737-23 (2017).
36. R Core Team 2015, R: A language and environment for statistical computing, (available at <http://www.R-project.org/>).

Acknowledgments

We thank all participants of the 2011 mesocosm study for deployment, maintenance and sampling of the mesocosm infrastructure. Furthermore, we gratefully acknowledge the captain and the crews of RV ALKOR (AL376), RV Heincke (HE360), and Håkan Mosby (2011609) for transportation, deployment, and recovery of the mesocosm units. This project was funded by the German Ministry for Education and Research (BMBF) in the framework of the coordinated projects SOPRAN (Surface Ocean Processes in the ANthropocene) and BIOACID (Biological Impacts of Ocean ACIDification). Richard G. J. Bellerby received financial support from the EU Framework 7 EuroBASIN (EUROpean Basin-scale Analysis, Synthesis and Integration) project no. 264933.

The data reported in this paper are archived on PANGEA and can be accessed via the following link: DOI from PANGEA to be inserted

Supplementary materials

Materials and Methods

Table S4.1

Figs. S4.1 to S4.5

Materials and Methods

Experimental design

Nine 'Kiel Off-Shore Mesocosms for Ocean Simulations' (KOSMOS; (25)) were deployed in Raunefjord at the west coast of Norway (60.265° N, 5.205° E) on April 30 2011 (day -8; Fig. S4.1). The cylindrical mesocosm bags were initially covered with a 3 mm screen on both ends and were left open fully submerged for free water exchange for four days. On May 4 (day -4) the screens were removed, the top of the bags pulled above sea surface and the bottoms sealed by two meter long, conical sediment traps. After mesocosm closure, each unit enclosed a 25 m long and two meter in diameter water column of on average volume of 74.5 m³ (12). A salinity gradient present inside the mesocosms was homogenized by injecting air to the bottom of the mesocosms in two consecutive steps (days -4 and -3).

For the CO₂ treatment, we established an *f*CO₂ gradient between mesocosms of initially 311 to 3045 µatm (day 5; Table S4.1), by stepwise addition of CO₂ saturated seawater over five consecutive days (days 0 to 4) following procedures described in Riebesell et al. (25). One mesocosm (M4) served as an untreated control, while a second 'control mesocosm' (M2) was excluded from the current data set due to water exchange of several cubic meters with the surrounding fjord (12). After initial addition, the *f*CO₂ was left free drifting in response to air-sea CO₂ gas exchange and biological activity. On day 14 inorganic nutrients were added to all mesocosms to induce a phytoplankton bloom based on new production. We only increased nitrate and phosphate concentrations (5 and 0.16 µmol L⁻¹ respectively) to favor a bloom of the coccolithophore *Emiliana huxleyi* (16). A detailed description of the experiment setup, manipulations and maintenance can be found in Schulz et al. (12), while a timeline of the experiment is shown in Fig. S1.

Sampling and processing

Sampling procedures of the mesocosm water columns and sediment traps were carried out as described in Schulz et al. (19) and Boxhammer et al. (26), respectively. Briefly, water samples from 0 - 23 m were taken on a daily basis using depth-integrating water samplers (IWS, HYDROBIOS). Suspended particulate mater (PM) for organic carbon, nitrogen, and phosphorus (POC, PON, POP) analysis were collected on pre-combusted glass fibre filters (GF/F, Whatman) using gentle vacuum filtration (≤ 200 mbar). Water samples for carbon and nitrogen analysis of fractionated particle size classes were only taken on every fourth day between day 2 and 26 and additionally on day 28 (Fig. S4.1). Each of these water samples passed three filters, connected in series that

were corresponding approximately to the size classes of micro (10 - 100 μm), nano (2.7 - 10), and pico (0.3 - 2.7 μm) plankton. A detailed description can be found in Bermúdez et al. (27). Inorganic carbon on filters was removed by fuming with 37% HCl in a desiccator for 2 h prior to drying them over night at 60°C and packing them into tin foil.

The sediment traps were also emptied on a daily basis by a vacuum pump system connected to silicon tubes reaching down to the collecting cylinders of the traps. The collected material was concentrated via passive sedimentation and centrifugation, freeze-dried and ground to fine and homogeneous powder (grain size $\leq 63 \mu\text{m}$) following methods described in Boxhammer et al. (26). Subsamples of the supernatant after sedimentation were collected on filters as described for water column samples. The inorganic carbon fraction in ground sediment trap samples was removed by direct exposure of 2 mg subsamples to 50 μL 1 M HCl inside silver cartridges.

Particulate matter and Chl *a* analysis

POC and PON collected on filters and of the ground sediment trap subsamples was analysed with an acetanilide calibrated CN analyser following Sharp (28). TPP of both sample types was converted to orthophosphate by autoclaving the samples for 30 minutes in an oxidizing decomposition solution (Merck, catalogue no. 112936). Inorganic phosphate concentration was then determined spectrophotometrically according to Hansen and Koroleff (29). Water column samples for Chl *a* concentration analysis were collected and filtered as described for PM, minimizing light exposure during filtration. Chl *a* content of the collected PM was extracted and analysed by high-performance liquid chromatography (HPLC) following Barlow et al. (30).

Nutrient measurements

Dissolved inorganic nutrients including nitrate (NO_3^-), phosphate (PO_4^{3-}), and silicate ($\text{Si}(\text{OH})_4$) were analysed from integrated water samples using standard methods described in Hansen and Koroleff (29).

Carbonate system analysis

Samples for dissolved inorganic carbon (DIC) and pH measurements were taken and analysed as described in Schulz et al. (12). Shortly, samples were directly drawn from the integrated water samplers without gas exchange and filled headspace free into sample bottles. DIC was then measured coulometrically following Johnson et al. (31), while seawater pH was determined spectrophotometrically as described by Carter et al. (32). Seawater $f\text{CO}_2$ for *in-situ* temperature and salinity was calculated from DIC and pH measurements using the dissociation constants of carbonic acid from Mehrbach et al. (33) as refitted by Lueker et al.(34).

Data analysis and statistics

Based on the CO_2 and nutrient manipulation, as well as the Chlorophyll *a* (Chl *a*) development, we divided the experiment into five consecutive phases described in detail in Schulz et al. (12) (Table S4.1; Fig. 4.1B). Briefly, Phase 0 encompasses the time before a significant CO_2 gradient was established (days -1 to 2), Phase I covers the peak and decline of the first phytoplankton bloom (days 3 - 8), Phase II represents the first post-bloom phase (days 9 - 14), Phase III includes the second phytoplankton bloom, while the last Phase IV covers the second post-bloom.

Similar to other mesocosm CO_2 perturbation studies with a CO_2 gradient established (19, 21, 35), we applied linear regression analysis to detect significant correlations between average $f\text{CO}_2$ and average elemental ratio during each experimental phase. *R* software (36) was used to perform statistical analysis.

Additional author notes:

UR designed and coordinated the mesocosm experiment that was carried out by TB, LTB, RGJB, JRBM, KGS, HS, MS, and UR. Dissolved inorganic carbon, and pH were measured and carbonate chemistry calculated by RGJB and KGS. JRBM, HS, and MS measured elemental stoichiometry of bulk and size fractionated suspended particulate matter. Settling organic matter composition was analysed by TB, who also visualized the data and wrote the manuscript. All authors contributed to the data analysis and commented on the manuscript.

Supplementary tables and figures

Table S4.1. Phase specific mesocosm CO₂ treatments. $f\text{CO}_2$ represents average values of each of the five experimental phases (0 - IV, (13) and the initial CO₂ levels on day 5. Mesocosm 2 was excluded from the current data set due to water exchange of several cubic meters with the surrounding fjord through an un-mendable hole (12).

Mesocosm	$f\text{CO}_2$	$f\text{CO}_2$	$f\text{CO}_2$	$f\text{CO}_2$	$f\text{CO}_2$	$f\text{CO}_2$
	initial	Phase 0	Phase I	Phase II	Phase III	Phase IV
#	on day 5	day -1 - 2	day 3 - 8	day 9 - 14	day 15 - 25	day 26 - 34
4	311	326	310	312	306	293
6	393	351	378	387	369	348
8	593	427	578	565	497	467
1	888	460	850	792	653	590
3	1164	453	1059	968	792	693
5	1425	462	1270	1152	884	784
7	2058	443	1813	1586	1167	980
9	3045	462	2596	2202	1534	1279

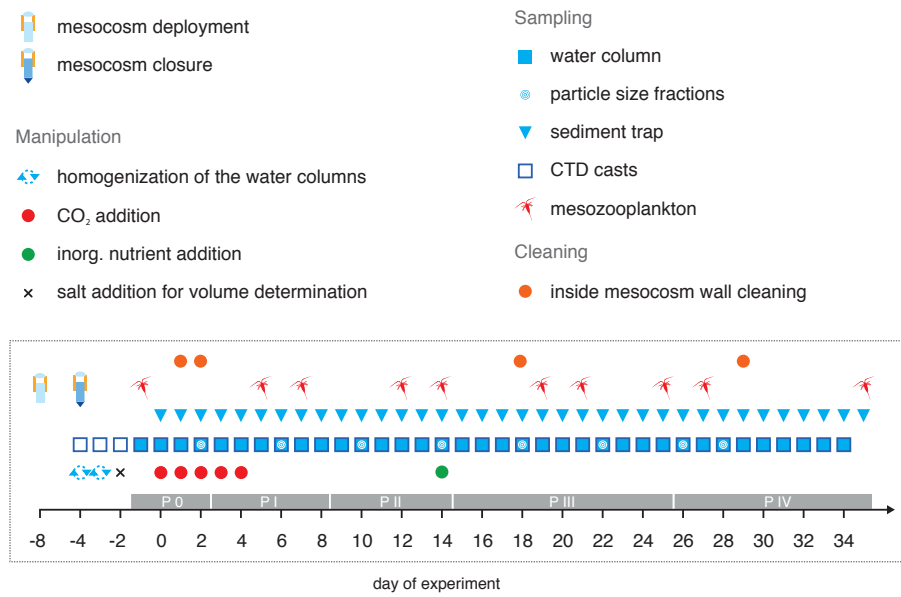


Fig. S4.1. Manipulation, sampling and maintenance schedule. Days of experiment are related to the day of the first CO₂ addition (day 0 = 8 May 2011). P 0 - IV, indicate the four consecutive phases of the experiment (13).

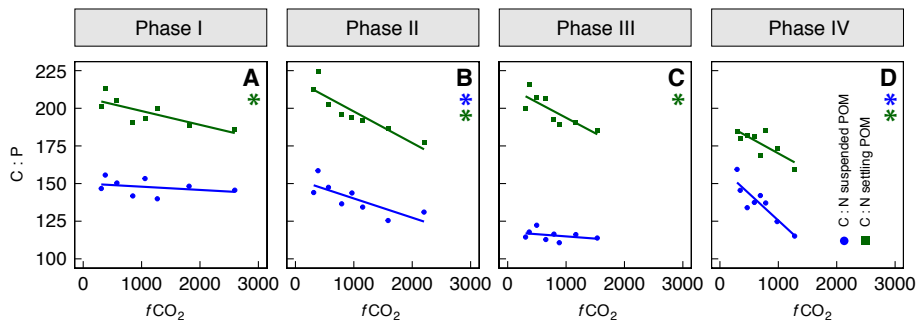


Fig. S4.2. Correlation of carbon to phosphorus ratios with $f\text{CO}_2$. (A-D) Phase specific average ratios of carbon to phosphorus (C:P) in suspended and settling particulate organic matter (POM) are correlated with the average $f\text{CO}_2$ of the respective experimental phase (Table S4.1) (13). Asterisks denote a statistically significant CO_2 effect ($p < 0.05$; Table 4.1).

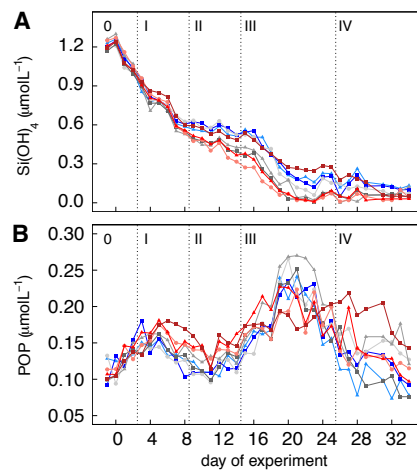


Fig. S4.3. Time course of additional key parameters in the mesocosms. (A) Si(OH)_4 = dissolved silicate and **(B)** POP = particulate organic phosphorus. Colours and symbols of the CO_2 treatments and the control mesocosm as described in Fig. 4.1. Roman numbers denote the different phases of the experiment (13).

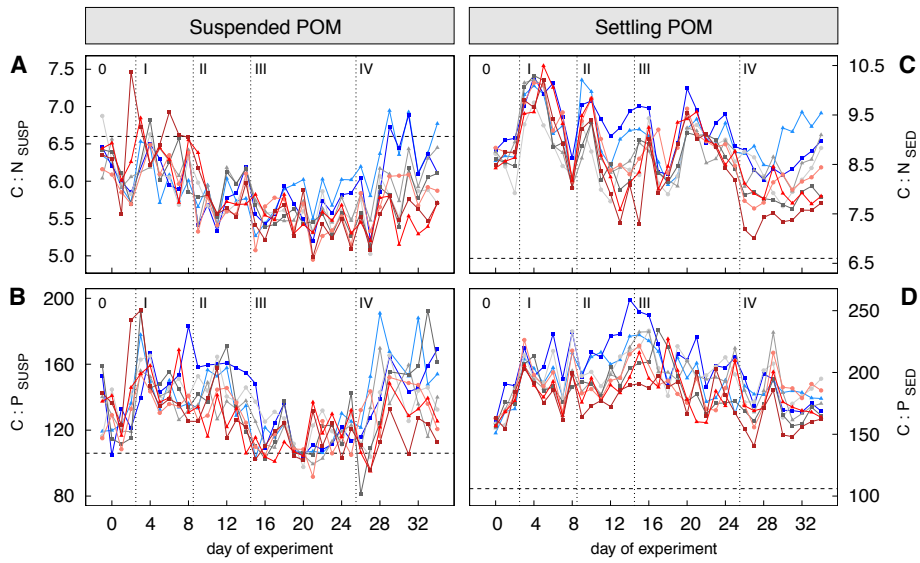


Figure S4.4. Time course of elemental ratios. Ratios of suspended particulate (A) C:N = carbon to nitrogen and (B) C:P = carbon to phosphorus, as well as ratios of settling particulate (C) C:N = carbon to nitrogen and (D) C:P = carbon to phosphorus. The horizontal dashed line indicates the Redfield ratio of 106C : 16N : 1P. CO₂ treatments are indicated by colours and symbols shown in Fig. 4.1. Roman numbers denote the different phases of the experiment (13).

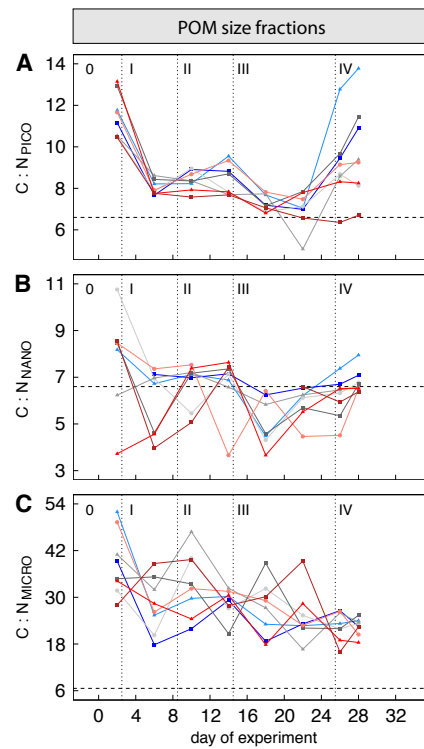


Fig. S4.5. Time course of the carbon to nitrogen ratio in different particle size classes. Ratio of carbon to nitrogen (C:N) of particles corresponding to the size class of (A) pico-, (B) nano-, and (C) microplankton. The horizontal dashed line indicates the Redfield ratio of 106C : 16N : 1P. CO₂ treatments are indicated by colours and symbols shown in Fig. 4.1. Roman numbers denote the different phases of the experiment (13).

5. Synthesis

In this chapter, I synthesize methodological insights from eight years of biogeochemical research with pelagic mesocosms and discuss impacts of OA on C:N stoichiometry of POM and transfer of biomass to higher trophic levels. Based on this, I then suggest methodological improvements for mesocosm research and highlight open questions and perspectives of future OA research focusing on the biogeochemical impact of entire plankton communities with multi-trophic levels.

5.1 Pitfalls of elemental mass balance calculations in mesocosm enclosures and methodological improvements

Chapter 3 has shown that the closed nature of pelagic mesocosms makes them a very suitable platform for calculating elemental mass balances in water bodies hosting entire plankton communities over extended time scales. The limited exchange with the surrounding environment allowed us to follow the biologically driven cycling of elements and to assess the impact of CO₂ perturbation in the theoretical absence of any hidden sources or sinks. However, the experiences described in Chapter 3 and collected during in total seven KOSMOS mesocosm studies between 2010 to 2017 have revealed several pitfalls that can handicap calculation of elemental mass balances, even in such a largely controlled environment.

5.1.1 Mesocosm sediment trap design and sampling

The quantitative collection and removal of settling PM is not only essential for accurate vertical flux measurements inside mesocosms, but also to avoid bacterial degradation of accumulating organic matter that would otherwise consume oxygen and release unquantifiable recycled nutrients and CO₂ to the systems. Both factors are critical to allow closing of elemental mass balance calculations. The sampling method for sediment traps of KOSMOS mesocosms described in Chapter 2, was developed for daily sampling of quantitative sediment traps without any disturbance of the water column and with minimal impact on the collected PM. The main advantage of using an extraction tube to recover the samples (Fig. 2.1B in Chapter 2) over systems using replaceable collection cups or bottles (e.g. Gamble et al., 1977; Guieu et al., 2010) is that the otherwise sealed mesocosms do not need to be opened for emptying the sediment traps. Every opening of the sediment traps could cause exchange of water and PM driven by salinity differences between the internal and external water masses. When summed up over a longer period, this exchange could potentially influence element pools and mass balance calculations. Salinity differences often develop over time due to

evaporation inside the mesocosms (Taucher et al., 2017a) or exchange of the surrounding water masses, particularly in regions with freshwater inflows (Bach et al., 2016). The developed sediment trap design of KOSMOS mesocosms and sampling technique was to date applied in seven mesocosm studies and has proven highly reliable performance. Only solid objects larger than 1 cm in diameter can block the extraction tube, a problem that can be solved by opening the tube connector (Chapter 2). The downside of quantitative sediment traps is the handling of large sample volumes during times of high primary production with up to 4 L of dense particle suspension that could contain more than 450 mol of C (Boxhammer et al., 2017). The newly developed processing of such samples described in Chapter 2 has proven to successfully concentrate (C concentration efficiency >98%) and process these samples for highly accurate vertical flux measurements of elements.

5.1.2 Wall growth

Wall growth is a common artefact in enclosure experiments (Chen et al., 1997) limiting their runtime and representing a sink for carbon and nutrients that prevents closure of mass balance calculations (Czerny et al., 2013a). The closed silica mass balance in Chapter 3 has shown that wall growth of cylindrical mesocosms can be overcome by regular cleaning of the inside mesocosm walls. This allowed for calculation of element mass balances over more than 100 days of experiment (Chapter 3). However, the applied ring-shaped cleaning device (Riebesell et al., 2013) does not clean the funnel shaped sediment trap in the KOSMOS setup, which is also prone to fouling and growth of epiphytes when light penetration is sufficiently deep. In eutrophic regions with relatively low light penetration depths this was found to be negligible at mesocosm lengths between 15 to 25 m (e.g. mesocosm studies in Chapters 3 and 4). In oligotrophic regions with high light penetration depths it was found that growth and related accumulation of biomass on the sediment trap funnel (13-15 m below sea surface) can be in the same order of magnitude as the measured vertical particle flux making mass balance calculations obsolete (Stange et al., accepted). Thus, in case of high light penetration depth, the regular cleaning of the sediment trap surface is essential for successful mass balance calculation of elements. The only tested solution to date is the use of a brush that is magnetically hand-operated by a diver outside of the sediment trap and needs to be improved in terms of efficiency.

5.1.3 Correction of dissolved inorganic carbon for the air-sea gas exchange of CO₂

The discrepancy between net community production of organic C and dissolved inorganic carbon (DIC) drawdown described in Chapter 3 highlights the importance of correcting the DIC pool for CO₂ air-sea gas exchange. As shown in Fig. 3.4 (Chapter 3), cumulative sedimentation of C alone exceeded the net drawdown of DIC at the end of the study by a factor of three at ambient CO₂.

Theoretically, the air-sea flux of CO₂ can be calculated from (1) the difference in partial pressure of CO₂ across the air-sea interface ($\Delta p\text{CO}_2$), which is the thermodynamic driver of the flux, (2) the solubility constant of CO₂ at a given temperature and salinity, and (3) the exchange rate that determines the actual flux, a kinetic parameter termed as the 'gas transfer velocity'. While $\Delta p\text{CO}_2$ can be easily calculated from known atmospheric $p\text{CO}_2$ and carbonate chemistry measurements inside mesocosms, the gas transfer velocity is usually parameterized as a function of wind speed causing turbulence in the open ocean (Wanninkhof, 1992). However, since mesocosm enclosures strongly influence wind and wave driven convection, relationships between wind speed and gas transfer velocity are likely very different inside pelagic mesocosms (Czerny et al., 2013b). In Chapter 3, an attempt was made to estimate the gas transfer velocity of CO₂ from the outgassing rate of the injected tracer gas, N₂O, following (Czerny et al. (2013b). In previous KOSMOS mesocosms studies with stable hydrographical conditions this technique achieved good estimates of CO₂ gas transfer velocity and exchange rates (Czerny et al., 2013a; Spilling et al., 2016). However, in the study described in Chapter 3 the complex and highly dynamic hydrographical conditions inside the mesocosms seemed to limit the applicability of this method. As illustrated in Figure 5.1, a first phase of thermal mixing caused by heat exchange with surrounding warmer bottom water was followed by a second phase of strongly varying thermal stratification caused by increasing solar heating and exchanging surrounding water masses with different temperature signature from the Baltic and the North Sea (Bach et al., 2016).

The homogeneously mixed water column of the first phase led to continuous outgassing of N₂O and reliable estimation of gas transfer velocity rates. However, the thermal stratification during the second phase physically divided the mesocosm water columns into a surface and a bottom layer, whereby only the surface layer was in gas exchange with the atmosphere. The limiting factor for the 'N₂O tracer method' (Czerny et al., 2013b) was the high day-to-day variability of the surface layer mixing depth (i.e. depth of the thermocline) and hence the vertical distribution of N₂O, which could not be resolved with the applied sampling techniques. As a consequence, measured $p\text{N}_2\text{O}_{(\text{aq})}$ in the surface layer did not display a continuous decrease but instead fluctuated strongly, depending on irregular and pulsed inputs of N₂O from the bottom layer of the mesocosm. Ultimately, this impeded an accurate and representative exponential fit of N₂O outgassing over several sampling days and a corresponding conversion into CO₂ gas transfer velocity. This demonstrates the limita-

tions on the hydrographical conditions where the ‘N₂O tracer method’ can currently be successfully applied.

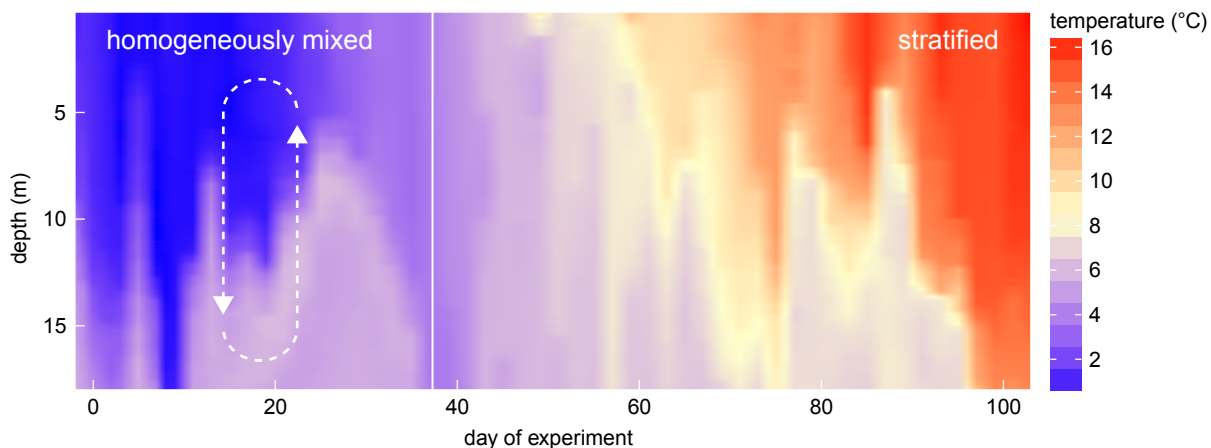


Figure 5.1. Development of the vertical temperature profile inside the mesocosms of the 2013 KOSMOS campaign in Gullmar Fjord, Sweden (Chapter 3), derived from every 2nd day CTD casts. The white dashed arrows illustrate thermal convection of the entire water column. The white solid line separates the two phases of (1) thermal convection and (2) highly variable thermal stratification of the water column.

5.1.4 Dissolved organic matter

Two mass balance approaches of KOSMOS mesocosm studies, presented in Chapter 3 as well as in Czerny et al. (2013a), have shown that DOM is highly sensitive to sample contamination. This had strong impact on elemental mass balance calculations due to DOM’s relatively large contribution to the elements net community production (see Fig. 3.4 in Chapter 3). In contrast to the open ocean, contamination is easily detected in repeatedly taken samples from enclosed water bodies. Changes in DOM concentration that are (1) not reflected in the other element pools as sources or sinks and (2) cannot be explained by biological activity in the observed order of magnitude (e.g. by rates of net primary production) are questionable for sample contamination.

In principle, measured DOM concentrations can be artificially increased during three critical steps: (1) Handling of sampling gear and samples during sampling, (2) sample processing, mainly filtration to separate DOM from POM, and (3) the analysis of the samples. While analytical accuracy can be controlled with Deep Atlantic Seawater Reference Material (DSR, D. A. Hansell, University of Miami, Miami, Florida, USA), sample collection, handling, and filtration hold greater potential for contamination. In past KOSMOS mesocosm studies, samples for DOM measurements have been taken directly from integrated water samplers (Paul et al., 2015; Schulz et al., 2017;

Zark et al., 2017; 2015) as well as pooled water samples (Czerny et al., 2013a; Schulz et al., 2013), resulting in substantial differences in data quality. In particular, DOC measurements from pooled water samples showed unexplainable day-to-day variability of up to $40 \mu\text{mol L}^{-1}$. This was likely due to insufficient cleaning of the carboys where water samples were pooled. When samples were taken directly from the water sampler, DOM data quality depended on the applied filtration protocol. Zark et al. (2015) have gravity filtered the DOM samples on board of the sampling boat. This resulted in strongly variable DOM data, which prevented closing of the mass balance calculations of C, N, and P in Chapter 3. Here, DOC concentrations between sampling days varied by up to $50 \mu\text{mol C L}^{-1}$ within 48 hours (Fig. 3.4 in Chapter 3). This was probably due to contamination during the filtration process and sample handling on board of the boat. In Paul et al. (2015), Zark et al. (2017), and Schulz et al. (2017) samples were transferred from the water sampler into acid rinsed sample bottles and filtered later on in a clean laboratory environment. This technique has led to the most reliable DOM data from KOSMOS mesocosms so far. In this case, DOC day-to-day variability was usually $< 10 \mu\text{mol C L}^{-1}$ with only very few exceptions. The latter technique obviously minimises sources of contamination for DOM samples and thus should be applied in future studies to also minimise the impact of these artefacts on mass balance calculations.

5.1.5 Relevance of the mesozooplankton pool for particulate organic matter

During the KOSMOS long-term experiment described in Chapter 3, the relative contribution of mesozooplankton to bulk particulate organic carbon in the water column fluctuated between 10 to 40% over the course of the study (Fig. 5.2). This strongly highlights the role of mesozooplankton within the POM pool (Fig. 1.2 in Chapter 1) and their importance for successful mass balance calculations that otherwise likely underestimate the pool of particulate organic matter.

While the contribution of mesozooplankton to the POM pool is clearly substantial, it is unlikely that mesozooplankton biomass is accurately accounted for by standard sampling methods for suspended POM, which collect organisms and particles on $0.7 \mu\text{m}$ pore size filters. It is known that copepods, often dominating mesozooplankton assemblages (Kiørboe, 2011), exhibit escape reactions to hydrodynamic stimuli (Fields and Yen, 1997; Waggett and Buskey, 2007), which can be triggered by predators as well as sampling gear for water samples. Thus, their behaviour prevents representative sampling of mesozooplankton biomass with water samplers, especially those that take integrating water samples. Furthermore, the typically used filtration volume of 0.5 to 2 L for POM analysis (Ehrhardt and Koeve, 2007) does not sufficiently account for the relatively low concentrations of mesozooplankton organisms and their patchy distribution. Therefore, quantification of elements in suspended POM needs to include standard filtration of water samples as well as

separate determination of elements in mesozooplankton biomass using large volume net catches. This is especially critical for elemental mass balance approaches but also when biomass in the water column is related to sedimentation fluxes measured at depth.

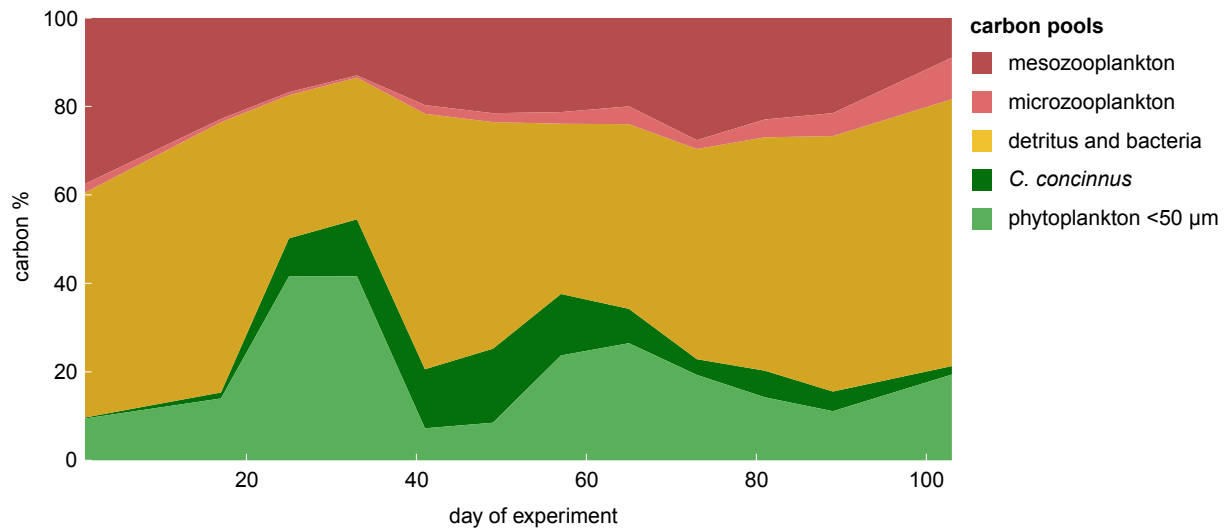


Figure 5.2. Time course of the relative contribution of individual carbon pools to total particulate carbon during the KOSMOS long-term experiment in Gullmar Fjord (Sweden) (Chapter 3). Values represent an average of the ambient CO₂ mesocosms. Phytoplankton carbon (light green) was calculated from flow cytometer counts (0.8-50 µm in diameter) based on measurements of size-fractionated samples and subsequent conversion of forward-scatter to particle diameter (Taucher et al., 2017b), *Coscinodiscus concinnus* carbon (dark green) was calculated from cell abundance (Bach et al., 2017) and a species specific conversion factor of 0.35 µg C cell⁻¹ (Wiltshire and Dürselen, 2004), microzooplankton carbon (light red) data originate from Horn et al. (2016), mesozooplankton biomass (dark red) was calculated as described in Chapter 3, detritus and bacterial biomass (ochre) reflects the bulk organic carbon collected on 0.7 µm pore size filters (GFF, Whatman) subtracting calculated phytoplankton, *C. concinnus*, and microzooplankton carbon. It should be noted that C content of *C. concinnus* was likely underestimated after day 30, as their cellular C:N ratio strongly increased after inorganic nutrients were used up (Fig. 3.5C in Chapter 3).

5.2 Ocean acidification effects on carbon and nutrient cycling

5.2.1 Impact of ocean acidification on the carbon to nitrogen ratio of particulate organic matter

Both Chapters 3 and 4 have shown that OA can affect the C:N stoichiometry of POM with different and even variable responses over time. This observation is in line with a review by Hutchins et al. (2009) that compared mainly small-scale and short-term plankton community incubations with early *in situ* mesocosm OA studies (Engel et al., 2005; Riebesell et al., 2007). These first *in situ* OA studies gave the impression that the C:N ratio of natural plankton assemblages might generally increase or remain stable under high CO₂ (Riebesell and Tortell, 2011). This was also the case during the long-term community study in Chapter 3, where the increase of C:N in bulk POM under OA was driven by only one phytoplankton species *C. concinnus* (see Fig. 3.6 in Chapter 3). In contrast, the plankton community in Chapter 4 showed a variable OA induced response of POM C:N over time (Fig. 4.3 in Chapter 4) that was associated with shifting dominance of phytoplankton groups during bloom and post-bloom phases as well as between CO₂ treatments. Comparing these results with three other OA *in situ* mesocosm studies in different oceanic regions and ecosystems between 2010 and 2014, reveals a highly diverse response of the POM C:N ratio to increasing CO₂ levels (Table 5.1). Effect sign and strength vary between oceanic regions and ecosystems (i.e. plankton assemblages), phytoplankton growth phases (pre-bloom, bloom, and post-bloom), successive phytoplankton blooms during the same study, and between suspended POM in the water column and sinking particles collected in the mesocosm sediment traps.

Two major mechanisms and their interaction likely drive the C:N responses to OA in suspended POM: (1) Physiological responses by the dominating phytoplankton species, such as the enhanced excess C fixation by *C. concinnus* in Chapter 3, (2) a shift in dominating phytoplankton groups or species with different inherent C:N ratios, or a mixture of mechanisms (1) and (2) with a simultaneous shift of dominating species that show physiologically driven changes in their cellular C:N ratios. In Chapter 4 it was concluded that the OA induced changes in the bulk POM C:N ratio was mainly caused by shifting dominance of different phytoplankton groups (mechanism 2). However, individual responses of phytoplankton groups or species (mechanism 1) cannot be totally excluded as suspended particle size classes of pico-, nano- and microplankton showed differently pronounced trends (Fig. 4.3 in Chapter 4). It should also be noted that this interpretation focuses on the photoautotrophic community and thus disregards the heterotrophic biomass (e.g. bacteria or zooplankton organisms) that also influences the bulk POM C:N ratio, especially during pre- and post-bloom phases of the phytoplankton (Fig. 5.3). In Chapter 3 any potential responses of the heterotrophic community was likely masked by the response of the photoautotrophic diatom *C. concinnus*, favoured by the fact that this diatom species was too large to be grazed on by any heterotrophs

(see Sect. 5.2.2 of this chapter). In contrast, during the '2012 Finland' study listed in Table 5.1 it seems likely that heterotrophic organisms caused a significant increase of the POM C:N ratio under high CO₂. The CO₂ effect was only observed during the second half of the study, when biomass was shifted from autotrophic to heterotrophic organisms (Paul et al., 2015). Heterotrophic organisms also play a major role in the transformation of sinking POM, capable to alter OA induced tendencies and effects on the C:N ratio during the particles descent, as visible from Table 5.1. Their influence became most obvious in the '2014 Gran Canaria' study, where the 'tendency' (i.e. an insignificant linear trend) of increasing POM C:N stoichiometry at high CO₂ in the water column was reversed into a significantly negative CO₂ effect on C:N ratios found in sinking particles during the post-bloom phase (Table 5.1). Stange et al. (accepted) explained this reversal of the C:N trend from suspended POM to sinking particles with OA induced differences in micro- and mesozooplankton abundances and thus differences in particle transformation by phytoplankton grazers. Their example suggests that depending on the food web structure, enhanced C fixation by phytoplankton under high CO₂ does not necessarily enhance C export. This should be considered when modelling C cycling under future OA.

From all five OA studies listed in Table 5.1, it is clear that the modification of POM elemental stoichiometry by the plankton community in response to OA is highly variable (in sign and strength) and depends on the investigated plankton community composition in the specific oceanic region. Furthermore, OA induced changes in C:N stoichiometry of POM in the surface ocean may not directly translate into similar changes of sinking POM, but are often transformed by the heterotrophic plankton community. Thus, for prediction of C and N cycling under future OA both stoichiometric changes in POM in the water column and further transformations in sinking particles need to be taken into account.

The high variability of the C:N responses to OA found under different plankton community settings (Table 5.1), complicates prediction for the future C:N ratio of bulk suspended POM or sinking particles. However, it is likely that under OA the C:N stoichiometry of POM will be influenced on a local scale, regionally impacting C:N dependent processes such as C sequestration, which in turn might impact global cycling of C and N.

The CO₂ effects on the POM C:N ratio listed in Table 5.1 were in most cases driven by CO₂ levels higher than 480 ppm. This CO₂ concentration is the maximum concentration predicted by the global CO₂ emissions scenario RCP2.6 that leads to global warming of in maximum 2.3°C by the year 2100 (see Fig. 1.3B in Chapter 1). Thus, our results suggest limited effects of OA on C:N stoichiometry if humankind successfully restricts CO₂ emissions to keep global warming below the 2°C goal of the 'Paris Agreement' (see Epilogue).

Table 5.1. C:N ratios of POM in the water column and collected in sediment traps during pre-bloom, bloom, and post-bloom phases of five KOSMOS mesocosm studies in different oceanic regions and ecosystems. The colour scheme and symbols indicates whether a specific phase was not investigated during the study (white, no symbol), a positive or negative (non-significant) tendency was observed (light blue \uparrow and light red \downarrow , respectively), a positive (dark blue \uparrow) or negative effect (dark red \downarrow) was found or no CO₂ effect was observed (grey $\leftarrow \rightarrow$). Details on the experiments and data analysis are described in the referenced publications.

Study	2010 Svalbard	2011 Norway	2012 Finland	2013 Sweden	2014 Gran Canaria
Ocean region	Arctic Ocean	Temperate North Atlantic Ocean	Baltic Sea	North Sea	Subtropical North Atlantic Ocean
Duration (days)	35	39	47	107	61
Average CO ₂	177 - 1134 pCO ₂	310 - 1615 fCO ₂	365 - 1231 fCO ₂	377 and 756 pCO ₂	352 - 1025 pCO ₂
Experimental design	linear regression	linear regression	linear regression	2 x 5 replicates	linear regression
water column	C:N pre bloom			$\leftarrow \rightarrow$	\downarrow
	C:N bloom	\uparrow		\uparrow	$\leftarrow \rightarrow$
	C:N post bloom		\uparrow	$\leftarrow \rightarrow$	\uparrow
	C:N pre bloom			$\leftarrow \rightarrow$	$\leftarrow \rightarrow$
	C:N bloom	\uparrow			\uparrow
	C:N post bloom			$\leftarrow \rightarrow$	\uparrow
sediment trap	C:N pre bloom			$\leftarrow \rightarrow$	$\leftarrow \rightarrow$
	C:N bloom	\uparrow		\uparrow	$\leftarrow \rightarrow$
	C:N post bloom			\uparrow	\downarrow
Publications	Schulz et al., 2013 Czerny et al., 2013	Chapter 4	Paul et al., 2015	Chapter 3	Stange et al., accepted

5.2.2 Impact of ocean acidification on transfer of photoautotrophic biomass to higher trophic levels

The results presented in Chapter 3 provide one of the first evidences that physiological OA effects on primary producers can cascade through the food web, modifying the partitioning of element pools and thus impacting biogeochemical cycling. The amplified transfer of biomass from photoautotrophs to higher trophic levels significantly impacted retention time of elements such as C, N, and P in the water column as well as their downward flux.

Generally, there are two mechanisms by which OA could influence the transfer of biomass from primary producers to higher trophic levels: (1) CO₂ induced changes in primary production and thus food availability for herbivorous predators, or (2) CO₂ related changes in trophic transfer efficiency, defined as the energy or biomass that is transferred from one trophic level to the next, which could be altered by the prey's nutritional quality or predator energy demand. In Chapter 3, the amplified transfer of biomass from phytoplankton to mesozooplankton (dominated by copepods) under high CO₂ was attributed to increased primary production of about 20 μmol C L⁻¹ summed up over the course of the study (Eberlein et al., 2017). This likely promoted the food supply for copepods, resulting in elevated copepod biomass of about 2.5 μmol C L⁻¹ under high CO₂ (Fig. 3.5 in Chapter 3). Assuming a direct transfer of C from primary producers to copepods this would correspond to a theoretical C transfer efficiency of roughly 12.5%, which agrees well with the commonly assumed trophic transfer efficiency of ~10% per trophic level. Picophytoplankton as well as *C. concinnus* abundances were temporarily increased under high CO₂ (Bach et al., 2017), but both were either too small (<2 μm) or too large (>200 μm) to be directly grazed on by the dominant copepod species *Pseudocalanus ascuspes*. This exposes a bottleneck for transfer of OA induced changes on primary producers through the food web: The size match or mismatch of predator (mesozooplankton) and prey (phytoplankton). Thus, primarily nanophytoplankton must have fuelled the amplified transfer of biomass in terms of C and nutrients to mesozooplankton under high CO₂, despite the absence of a visible CO₂ effect on the abundance of this phytoplankton group. However, it cannot be excluded that to some extent *P. ascuspes* was also feeding on microzooplankton that in turn could feed on picophytoplankton, but microzooplankton also did not show any CO₂ effect on their abundance (Horn et al., 2016). The question of the exact origin of indirect food web effects underscores the difficulty of understanding mechanistic principles behind biogeochemical changes observed in plankton community experiments.

To date, Cripps et al. (2016) is the only published study that actually measured the impact of OA on trophic transfer efficiency of C by calculating the C allocation budgets of adult copepods. At 1000 μatm pCO₂ they found a reduction in C transfer efficiency of more than 50% from three different phytoplankton species to the copepod species *Acartia tonsa*. This was attributed to OA induced changes of the biochemical stoichiometry (carbohydrate : lipid : protein ratio) of

phytoplankton prey organisms indirectly impacting the copepods. In fact, changing phytoplankton nutritional quality in terms of algal fatty acid composition and C to nutrient ratios under OA were also found in other studies (Bermúdez et al., 2016; Rossoll et al., 2012; Schoo et al., 2012), showing decreased growth, development, fatty acid composition or egg production of herbivorous copepods, but lacking measurement of the actual trophic transfer efficiency.

Unfortunately, neither direct measurements of trophic transfer efficiency nor phytoplankton nutritional quality (e.g. fatty acid or biochemical composition) were conducted during the plankton community study in Chapter 3. Likely reduced nutritional quality in terms of increased C to nutrient content under high CO₂ was only found in cells of *C. concinnus* but the size mismatch with the present grazers prevented trophic transfer of this OA effect through the food web. If nutritional quality of phytoplankton grazed by *P. ascuspes* was reduced, the potentially negative impact was outbalanced by increased primary production and thus food availability.

Thus an open question for future OA studies is if changing primary production or changing trophic transfer efficiency will dominate and determine the transfer of biomass from primary producers to higher trophic levels in a future high CO₂ ocean.

5.3 Future perspectives

5.3.1 Future methodological improvements for biogeochemical research with pelagic mesocosms

As evident from previous sections and chapters of this thesis, there is still considerable limitation in measurement accuracy of numerous biogeochemical parameters measured inside pelagic mesocosms. These require methodological improvements to increase their measurement accuracy in the future for successful closure of elemental mass balance calculations.

To assess the CO₂ air-sea gas exchange under highly variable thermal stratification inside mesocosms, N₂O sensors that are currently under development should be tested for high temporal and small-scale resolution of the vertical tracer gas concentration gradients and partial pressures. This would likely allow us to develop a box model for daily N₂O and corresponding CO₂ gas exchange rates between (1) layers in the water column that are separated by a pycnocline and (2) between the actual surface layer of the water column and the atmosphere. A comparable approach was successfully applied by Kock et al. (2012) to assess the diapycnal flux of N₂O in a field study off the coast of Mauretania.

Although the best practice for DOM sampling in pelagic mesocosms to date was pointed out in Sect. 5.1.4 of this chapter, alternative sampling methods should be tested to further minimise the contamination of DOM samples. This could be the use of ultra-clean acid rinsed samplers that are directly transported back from each mesocosm to the lab for both subsampling and filtration in a clean environment.

Furthermore, the mesozooplankton biomass in future studies should be investigated in the same temporal resolution as the other element pools to better resolve temporal dynamics in the mesozooplankton pool and to increase the temporal resolution of calculated net community production. This should ideally be done with *in-situ* camera systems to avoid an artificial top down control on mesozooplankton created by net catches. Additionally, the element content and stoichiometry of mesozooplankton individuals should be measured and not calculated in future studies to consider potential changes in elemental composition over time that might be caused by changing elemental stoichiometry of the prey organisms. All these improvements would contribute to successful mass balance calculations of elements inside mesocosms that could give us further insights into element cycling under manipulated environmental factors such as OA or varying nutrient regime.

The methodological improvements in flux assessment inside mesocosms (Chapter 2) were to date applied for bulk flux measurements of elements. However, the contribution of different 'particle classes' such as faecal pellet, mesozooplankton carcasses, vertical migrating mesozooplankton

(swimmers), and phytoplankton groups or detritus have been poorly investigated. A detailed analysis of their individual contributions to sinking PM could improve our mechanistic understanding of the role of phytoplankton and mesozooplankton for the downward flux of PM and their individual relevance for the sinking POM stoichiometry. Image based analysis using a flatbed scanner and subsamples of sediment trap samples were unsuccessful in the past due to the strong aggregation of the collected material and the associated optical particle overlay. This in turn made automated evaluation with the available software impossible. However, rapidly evolving machine learning for object detection will likely be able to also distinguish overlying objects in the future and should be tested as soon as this software is available. Until then, 'gel traps' collecting particles *in situ* in polyacrylamide gels (e.g. Durkin et al., 2016) or manual analysis of the sediment trap sample composition should be considered in future mesocosm studies.

5.3.2 Future perspectives of ocean acidification research on biogeochemical cycling of elements

One of the main tasks of future studies on the biogeochemical impact of OA will be to improve our mechanistic understanding of the highly diverse C:N stoichiometry response observed to date in plankton community experiments. This is mandatory to allow us to transfer the insights from mesocosm 'test tubes' to the open ocean and to make predictions for future element cycling not only on local and temporally limited scales. The *in situ* mesocosm studies on effects of OA conducted to date mainly opened a small window to the future of a very specific plankton community composition that was enclosed at the beginning of the experiment. The response of plankton elemental stoichiometry in these experiments is often seen as a change in elemental composition of bulk POM, which is not clearly attributable to certain plankton groups or changes in community composition. It is therefore essential to distinguish individual C:N stoichiometry responses of functional plankton groups to OA, and their contribution to bulk POM elemental composition to elucidate the community response. This could be achieved by using a cell-sorting flow cytometer and subsequent elemental analysis of the sorted samples (e.g. Graff et al., 2012; Martiny et al., 2013). Furthermore, the function of heterotrophic organisms in the transformation of OA induced changes in elemental composition of photoautotrophic biomass should be a focus of future research. Their capability to transform and even reverse OA effects on POM elemental stoichiometry illustrates their great importance in driving changes in composition of sinking POM and thus in export of C and nutrients at increasing CO₂ concentrations.

The question of who eats whom also needs deeper investigation in plankton community studies, to better understand the pathway of direct CO₂ effects on primary producers that cascade through

the food web. The potential impacts on biogeochemical cycling of elements through changes in biomass transfer between trophic levels can be significant and also antagonistic to other OA effects as seen for the vertical C flux in Chapter 3. Therefore a thorough investigation of these indirect impacts is as important as any direct CO₂ effect on the plankton community.

Epilogue

Research on the impacts of OA has been going on for well over a decade. Nonetheless, we still cannot accurately predict the impact of OA on all marine ecosystems and elemental cycling in the ocean. The 'Paris Agreement' of the United Nations Framework Convention on Climate Change from December 2015 was ratified by 170 nations (as of December 6th, 2017) and aims to mitigate CO₂ emissions to limit global warming below 2°C and minimise OA (UNFCCC). However, this goal can only be achieved within IPCC's CO₂ emission scenario RCP2.6 that predicts decreasing CO₂ emissions already by 2030 (Fig. 3B in Chapter 3) and includes geo-engineering to actively reduce atmospheric CO₂ concentration (Williamson, 2016). It is therefore the task of the scientific community to find solutions that reduce atmospheric CO₂ concentration to prevent the known and still unknown changes of marine ecosystems and their functioning under OA to become reality.

References

- Bach LT, Taucher J, Boxhammer T, Ludwig A, Achterberg EP, Algueró-Muñiz M, et al. Influence of ocean acidification on a natural winter-to-summer plankton succession: First insights from a long-term mesocosm study draw attention to periods of low nutrient concentrations. *PLoS ONE* 2016;11:e0159068EP-. doi:10.1371/journal.pone.0159068.
- Bach LT, Alvarez-Fernandez S, Hornick T, Stuhr A, Riebesell U. Simulated ocean acidification reveals winners and losers in coastal phytoplankton. *PLoS ONE* 2017;12:e0188198-22. doi:10.1371/journal.pone.0188198.
- Bermúdez JR, Riebesell U, Larsen A, Winder M. Ocean acidification reduces transfer of essential biomolecules in a natural plankton community. *Sci Rep* 2016;6:27749EP. doi:10.1038/srep27749.
- Boxhammer T, Algueró-Muñiz M, Anderson LG, Bach LT, Bellworthy J, Esposito M, et al. Dataset of the biogeochemical parameters measured during the long-term mesocosm study in Gullmar Fjord Sweden in 2013. *PANGAEA* 2017. doi:10.1594/PANGAEA.880789.
- Chen CC, Petersen JE, Kemp WM. Spatial and temporal scaling of periphyton growth on walls of estuarine mesocosms. *Mar Ecol Prog Ser* 1997;155:1-15. doi:10.3354/meps155001.
- Cripps G, Flynn KJ, Lindeque PK. Ocean acidification affects the phyto-zoo plankton trophic transfer efficiency. *PLoS ONE* 2016;11:e0151739. doi:10.1371/journal.pone.0151739.
- Czerny J, Schulz KG, Boxhammer T, Bellerby RGJ, Büdenbender J, Engel A, et al. Implications of elevated CO₂ on pelagic carbon fluxes in an Arctic mesocosm study - an elemental mass balance approach. *Biogeosciences* 2013a;10:3109-25. doi:10.5194/bg-10-3109-2013.
- Czerny J, Schulz KG, Ludwig A, Riebesell U. Technical Note: A simple method for air-sea gas exchange measurements in mesocosms and its application in carbon budgeting. *Biogeosciences* 2013b;10:1379-90. doi:10.5194/bg-10-1379-2013.
- Durkin CA, Van Mooy BAS, Dyhrman ST, Buesseler KO. Sinking phytoplankton associated with carbon flux in the Atlantic Ocean. *Limnol Oceanogr* 2016;61:1172-87. doi:10.1002/lno.10253.
- Eberlein T, Wohlrab S, Rost B, John U, Bach LT, Riebesell U, et al. Effects of ocean acidification on primary production in a coastal North Sea phytoplankton community. *PLoS ONE* 2017;12:e0172594-15. doi:10.1371/journal.pone.0172594.

- Ehrhardt M, Koeve W. Determination of particulate organic carbon and nitrogen. In: Grasshoff K, Kremling K, Ehrhardt M, editors. *Methods of Seawater Analysis*. 3rd ed., Weinheim, Germany: Wiley-VCH Verlag GmbH; 2007, pp. 437-44. doi:10.1002/9783527613984.ch17.
- Engel A, Zondervan I, Aerts K, Beaufort L, Benthien A, Chou L, et al. Testing the direct effect of CO₂ concentration on a bloom of the coccolithophorid *Emiliania huxleyi* in mesocosm experiments. *Limnol Oceanogr* 2005;50:493-507. doi:10.4319/lo.2005.50.2.0493.
- Fields DM, Yen J. The escape behavior of marine copepods in response to a quantifiable fluid mechanical disturbance. *J Plankton Res* 1997;19:1289-304. doi:10.1093/plankt/19.9.1289.
- Gamble JC, Davies JM, Steele JH. Loch Ewe bag experiment, 1974. *Bull Mar Sci* 1977;27:146-75.
- Graff JR, Milligan AJ, Behrenfeld MJ. The measurement of phytoplankton biomass using flow-cytometric sorting and elemental analysis of carbon. *Limnol Oceanogr Methods* 2012;10:910-20. doi:10.4319/lom.2012.10.910.
- Guieu C, Dulac F, Desboeufs K, Wagener T, Pulido-Villena E, Grisoni JM, et al. Large clean mesocosms and simulated dust deposition: A new methodology to investigate responses of marine oligotrophic ecosystems to atmospheric inputs. *Biogeosciences* 2010;7:2765-84. doi:10.5194/bg-7-2765-2010.
- Horn HG, Sander N, Stuhr A, Algueró-Muñiz M, Bach LT, Löder MGJ, et al. Low CO₂ sensitivity of microzooplankton communities in the Gullmar Fjord, Skagerrak: Evidence from a long-term mesocosm study. *PLoS ONE* 2016;11:e0165800. doi:10.1371/journal.pone.0165800.
- Hutchins DA, Mulholland MR, Fu F. Nutrient cycles and marine microbes in a CO₂-enriched ocean. *Oceanography* 2009;22:128-45. doi:10.5670/oceanog.2009.103.
- Kjørboe T. What makes pelagic copepods so successful? *J Plankton Res* 2011;33:677-85. doi:10.1093/plankt/fbq159.
- Kock A, Schafstall J, Dengler M, Brandt P, Bange HW. Sea-to-air and diapycnal nitrous oxide fluxes in the eastern tropical North Atlantic Ocean. *Biogeosciences* 2012;9:957-64. doi:10.5194/bg-9-957-2012.
- Martiny AC, Pham CTA, Primeau FW, Vrugt JA, Moore JK, Levin SA, et al. Strong latitudinal patterns in the elemental ratios of marine plankton and organic matter. *Nat Geosci* 2013;6:279-83. doi:10.1038/ngeo1757.

- Paul AJ, Bach LT, Schulz KG, Boxhammer T, Czerny J, Achterberg EP, et al. Effect of elevated CO₂ on organic matter pools and fluxes in a summer Baltic Sea plankton community. *Biogeosciences* 2015;12:6181-203. doi:10.5194/bg-12-6181-2015.
- Riebesell U, Schulz KG, Bellerby RGJ, Botros M, Fritsche P, Meyerhöfer M, et al. Enhanced biological carbon consumption in a high CO₂ ocean. *Nature* 2007;450:545-8. doi:10.1038/nature06267.
- Riebesell U, Tortell D. Effects of ocean acidification on pelagic organisms and ecosystems. In: Gattuso J-P, Hansson L, editors. *Ocean acidification*, New York: Oxford University Press Inc; 2011, pp. 99-121.
- Riebesell U, Czerny J, Bröckel von K, Boxhammer T, Büdenbender J, Deckelnick M, et al. Technical Note: A mobile sea-going mesocosm system - new opportunities for ocean change research. *Biogeosciences* 2013;10:1835-47. doi:10.5194/bg-10-1835-2013.
- Rossoll D, Bermúdez Monsalve JR, Hauss H, Schulz KG, Riebesell U, Sommer U, et al. Ocean acidification-induced food quality deterioration constrains trophic transfer. *PLoS ONE* 2012;7:e34737-6. doi:10.1371/journal.pone.0034737.
- Schoo KL, Malzahn AM, Krause E, Boersma M. Increased carbon dioxide availability alters phytoplankton stoichiometry and affects carbon cycling and growth of a marine planktonic herbivore. *Mar Biol* 2012;160:2145-55. doi:10.1007/s00227-012-2121-4.
- Schulz KG, Bellerby RGJ, Brussaard CPD, Büdenbender J, Czerny J, Engel A, et al. Temporal biomass dynamics of an Arctic plankton bloom in response to increasing levels of atmospheric carbon dioxide. *Biogeosciences* 2013;10:161-80. doi:10.5194/bg-10-161-2013.
- Schulz KG, Bach LT, Bellerby RGJ, Bermúdez Monsalve JR, Büdenbender J, Boxhammer T, et al. Phytoplankton blooms at increasing levels of atmospheric carbon dioxide: Experimental evidence for negative effects on prymnesiophytes and positive on small picoeukaryotes. *Front Mar Sci* 2017;4:1-18. doi:10.3389/fmars.2017.00064.
- Spilling K, Schulz KG, Paul AJ, Boxhammer T, Achterberg EP, Hornick T, et al. Effects of ocean acidification on pelagic carbon fluxes in a mesocosm experiment. *Biogeosciences* 2016;13:6081-93. doi:10.5194/bg-13-6081-2016.
- Stange P, Taucher J, Bach LT, Boxhammer T, Algueró-Muñiz M, Horn HG, et al. Ocean acidification-induced restructuring of the plankton food-web can influence the degradation of sinking particles. *Front Mar Sci* accepted.

- Taucher J, Bach LT, Boxhammer T, Nauendorf A, Achterberg EP, Algueró-Muñiz M, et al. Influence of ocean acidification and deep water upwelling on oligotrophic plankton communities in the subtropical North Atlantic: Insights from an *in situ* mesocosm study. *Front Mar Sci* 2017a;4:1-18. doi:10.3389/fmars.2017.00085.
- Taucher J, Haunost M, Boxhammer T, Bach LT, Alguer Mu iz MA, Riebesell U. Influence of ocean acidification on plankton community structure during a winter-to-summer succession: An imaging approach indicates that copepods can benefit from elevated CO₂ via indirect food web effects. *PLoS ONE* 2017b;12:e0169737-23. doi:10.1371/journal.pone.0169737.
- UNFCCC - United Nations Framework Convention on Climate Change. Paris Agreement - Status of Ratification [Internet]. 2017 [cited 06 December 2017]. Available from: http://unfccc.int/paris_agreement/items/9444.php.
- Waggett RJ, Buskey EJ. Calanoid copepod escape behavior in response to a visual predator. *Mar Biol* 2007;150:599-607. doi:10.1007/s00227-006-0384-3.
- Wanninkhof R. Relationship between wind speed and gas exchange over the ocean. *J Geophys Res* 1992;97:7373-82. doi:10.1029/92JC00188.
- Williamson P. Emissions reduction: Scrutinize CO₂ removal methods. *Nature* 2016;530:153-5. doi:10.1038/530153a.
- Wiltshire KH, Dürselen C-D. Revision and quality analyses of the Helgoland Reede long-term phytoplankton data archive. *Helgol Mar Res* 2004;58:252-68. doi:10.1007/s10152-004-0192-4.
- Zark M, Riebesell U, Dittmar T. Effects of ocean acidification on marine dissolved organic matter are not detectable over the succession of phytoplankton blooms. *Science Advances* 2015;1:e1500531-1. doi:10.1126/sciadv.1500531.
- Zark M, Broda NK, Hornick T, Grossart H-P, Riebesell U, Dittmar T. Ocean Acidification Experiments in Large-Scale Mesocosms Reveal Similar Dynamics of Dissolved Organic Matter Production and Biotransformation. *Front Mar Sci* 2017;4:271-11. doi:10.3389/fmars.2017.00271.

Curriculum Vitae

Tim Sven Boxhammer

Personal information

Nationality:	German
Date of birth:	24.04.1983
Place of birth:	Hamburg, Germany

Education and academic career

09. 2012 - 01. 2018 **PhD Candidate**
Christian-Albrechts-Universität Kiel, Germany
Dissertation: 'Influence of ocean acidification on elemental mass balances and particulate organic matter stoichiometry in natural plankton communities'
01. 2012 - 12. 2017 **Research Assistant in Biological Oceanography**
Research Division of Marine Biogeochemistry
GEOMAR Helmholtz Centre for Ocean Research Kiel, Germany
10. 2005 - 10. 2011 **Undergraduate and graduate studies in Biological Oceanography, Marine Chemistry, Zoology, and Toxicology**
Christian-Albrechts-Universität Kiel, Germany
Diploma Thesis: 'Impact of ocean acidification on export and composition of sedimenting material in an Arctic off-shore mesocosm study'
10. 2003 - 09. 2005 **Pharmacy studies**
Christian-Albrechts-Universität Kiel, Germany

Professional Membership

- Since 2009 **German Society of Polar Research**
(Deutsche Gesellschaft für Polarforschung e.V.)

Research experience

- 2017 (2.5 Months) KOSMOS¹ Mesocosm Campaign, Lima, Peru
- 2015 (0.5 Months) KOSMOS¹ Mesocosm Campaign, Espegrend, Norway
- 2014 (1.5 Months) KOSMOS¹ Mesocosm Campaigns, Gran Canaria, Spain
- 2013 (0.5 Months) Summer School 'From Bloom to Gloom', Hólar, Island
- 2013 (5.0 Months) KOSMOS¹ Mesocosm Campaign, Kristineberg, Sweden
- 2012 (2.0 Months) KOSMOS¹ Mesocosm Campaign, Tvärminne, Finland
- 2012 (2.0 Months) KOSMOS¹ Mesocosm Campaign, Espegrend, Norway
- 2010 (2.0 Months) KOSMOS¹ Mesocosm Campaign, Ny-Ålesund, Svalbard
- 2009 (1.5 Months) Student research assistant, Ny-Ålesund, Svalbard
- 2009 (1.5 Months) KOSMOS¹ Mesocosm Campaign, Booknis Eck, Germany

¹KOSMOS = Kiel Off-Shore Mesocosms for Ocean Simulations

Publication record

a. Published manuscripts (peer reviewed)

1. Taucher J, Bach LT, **Boxhammer T**, Nauendorf A, The Gran Canaria KOSMOS Consortium, Achterberg EP, Algueró-Muñiz M, Aristegui J, Czerny J, et al. Influence of ocean acidification and deep water upwelling on oligotrophic plankton communities in the subtropical North Atlantic: Insights from an *in situ* mesocosm study. *Front Mar Sci*. 2017;4: 85-18. doi:10.3389/fmars.2017.00085
2. Schulz KG, Bach LT, Bellerby RGJ, Bermúdez Monsalve JR, Büdenbender J, **Boxhammer T**, Czerny J, Engel A, Ludwig A, et al. Phytoplankton blooms at increasing levels of atmospheric carbon dioxide: Experimental evidence for negative effects on prymnesiophytes and positive on small picoeukaryotes. *Front Mar Sci*. 2017;4: 7193-18. doi:10.3389/fmars.2017.00064
3. Taucher J, Haunost M, **Boxhammer T**, Bach LT, Algueró-Muñiz MA, Riebesell U. Influence of ocean acidification on plankton community structure during a winter-to-summer succession: An imaging approach indicates that copepods can benefit from elevated CO₂ via indirect food web effects. *PLoS ONE*. 2017;12: e0169737-23. doi:10.1371/journal.pone.0169737
4. Stange P, Bach LT, Le Moigne FAC, Taucher J, **Boxhammer T**, Riebesell U. Quantifying the time lag between organic matter production and export in the surface ocean: Implications for estimates of export efficiency. *Geophys Res Lett*. 2017;44: 268-276. doi:10.1002/(ISSN)1944-8007
5. Riebesell U, Bach LT, Bellerby RGJ, Bermúdez Monsalve JR, **Boxhammer T**, Czerny J, Larsen A, Ludwig A, Schulz KG. Competitive fitness of a predominant pelagic calcifier impaired by ocean acidification. *Nature Geosci*. 2017;10: 19-23.
6. Spilling K, Schulz KG, Paul AJ, **Boxhammer T**, Achterberg EP, Hornick T, Lischka S, Stühr A, Bermúdez Monsalve JR, et al. Effects of ocean acidification on pelagic carbon fluxes in a mesocosm experiment. *Biogeosciences*. 2016;13: 6081-6093. doi:10.5194/bg-13-6081-2016
7. Bach LT, Taucher J, **Boxhammer T**, Ludwig A, The Kristineberg KOSMOS Consortium, Achterberg EP, Algueró-Muñiz M, Anderson LG, Bellworthy J, et al. Influence of ocean acidification on a natural winter-to-summer plankton succession: First insights from a long-term mesocosm study draw attention to periods of low nutrient concentrations. *PLoS ONE*. 2016;11: e0159068 EP -. doi:10.1371/journal.pone.0159068

8. Bach LT, **Boxhammer T**, Larsen A, Hildebrandt N, Schulz KG, Riebesell U. Influence of plankton community structure on the sinking velocity of marine aggregates. *Global Biogeochem Cycles*. 2016;30: 1145-1165. doi:10.1002/(ISSN)1944-9224
9. **Boxhammer T**, Bach LT, Czerny J, Riebesell U. Technical note: Sampling and processing of mesocosm sediment trap material for quantitative biogeochemical analysis. *Biogeosciences*. 2016;13: 2849-2858. doi:10.5194/bg-13-2849-2016
10. Spilling K, Paul AJ, Virkkala N, Hastings T, Lischka S, Stuhr A, Bermúdez Monsalve JR, Czerny J, **Boxhammer T**, et al. Ocean acidification decreases plankton respiration: Evidence from a mesocosm experiment. *Biogeosciences*. 2016;13: 4707-4719. doi:10.5194/bg-13-4707-2016
11. Jansson A, Lischka S, **Boxhammer T**, Schulz KG, Norkko J. Survival and settling of larval *Macoma balthica* in a large-scale mesocosm experiment at different $f\text{CO}_2$ levels. *Biogeosciences*. 2016;13: 3377-3385. doi:10.5194/bg-13-3377-2016
12. Paul AJ, Achterberg EP, Bach LT, **Boxhammer T**, Czerny J, Haunost M, Schulz KG, Stuhr A, Riebesell U. No observed effect of ocean acidification on nitrogen biogeochemistry in a summer Baltic Sea plankton community. *Biogeosciences*. 2016;13: 3901-3913. doi:10.5194/bg-13-3901-2016
13. Paul AJ, Bach LT, Schulz KG, **Boxhammer T**, Czerny J, Achterberg EP, Hellemann D, Trense Y, Nausch M, et al. Effect of elevated CO_2 on organic matter pools and fluxes in a summer Baltic Sea plankton community. *Biogeosciences*. 2015;12: 6181-6203. doi:10.5194/bg-12-6181-2015
14. de Kluijver A, Soetaert K, Czerny J, Schulz KG, **Boxhammer T**, Riebesell U, Middelburg JJ. A ^{13}C labelling study on carbon fluxes in Arctic plankton communities under elevated CO_2 levels. *Biogeosciences*. 2013;10: 1425-1440. doi:10.5194/bg-10-1425-2013
15. Niehoff B, Schmithüsen T, Knüppel N, Daase M, Czerny J, **Boxhammer T**. Mesozooplankton community development at elevated CO_2 concentrations: results from a mesocosm experiment in an Arctic fjord. *Biogeosciences*. 2013;10: 1391-1406. doi:10.5194/bg-10-1391-2013
16. Riebesell U, Czerny J, Bröckel von K, **Boxhammer T**, Büdenbender J, Deckelnick M, Fischer M, Hoffmann D, Krug SA, et al. Technical Note: A mobile sea-going mesocosm system - new opportunities for ocean change research. *Biogeosciences*. 2013;10: 1835-1847. doi:10.5194/bg-10-1835-2013

17. Czerny J, Schulz KG, **Boxhammer T**, Bellerby RGJ, Büdenbender J, Engel A, Krug SA, Ludwig A, Nachtigall K, et al. Implications of elevated CO₂ on pelagic carbon fluxes in an Arctic mesocosm study - an elemental mass balance approach. *Biogeosciences*. 2013;10: 3109-3125. doi:10.5194/bg-10-3109-2013
18. Lischka S, Büdenbender J, **Boxhammer T**, Riebesell U. Impact of ocean acidification and elevated temperatures on early juveniles of the polar shelled pteropod *Limacina helicina*: Mortality, shell degradation, and shell growth. *Biogeosciences*. 2011;8: 919-932. doi:10.5194/bg-8-919-2011

b. Manuscripts under review

1. **Boxhammer T**, Taucher J, Achterberg EP, Algueró-Muñiz M, Bellworthy J, Czerny J, Esposito M, Haunost M, Hellemann D, et al. Enhanced transfer of organic matter to higher trophic levels caused by ocean acidification and its implications for export production: A mass balance approach. Under revision in PLoS ONE
2. Stange P, Taucher J, Bach LT, **Boxhammer T**, Algueró-Muñiz M, Horn HG, Krebs L, Nauendorf AK, and Riebesell U. Ocean acidification-induced restructuring of the plankton food web can influence the degradation of sinking particles. Accepted in *Frontiers in Marine Science*

c. Manuscripts in preparation

1. **Boxhammer T**, Bach LT, Taucher J, Bellerby RGJ, Bermúdez Monsalve JR, Schulz KG, Schultz H, Swat M, Riebesell U. Plankton community structure controls particulate organic matter stoichiometry in a high CO₂ ocean. In preparation

d. Video publications (non-peer reviewed)

1. **Boxhammer T**, Sswat M, Kohnert P, Schrödl M, Riebesell U. Mating *Clione limacina* (Philipps, 1774). OceanRep, doi:10.3289/MATING_CLIONE_LIMACINA_2010, 2017.
2. Sswat M, **Boxhammer T**, Jutfelt F, Clemmesen C, Riebesell U. Performance of herring larvae in a simulated future ocean food web, using the 'Kiel Off-Shore Mesocosms for future Ocean Simulations' (KOSMOS). OceanRep, doi:10.3289/KOSMOS_HERRING_SWEDEN_2013, 2016.
3. Sswat M, **Boxhammer T**, Jutfelt F, Bach LT, Nicolai M, Riebesell U. Video of a plankton community enclosed in a 'Kiel Off-Shore Mesocosm for future Ocean Simulations' (KOSMOS) during the long-term study in Gullmar Fjord (Sweden) 2013. OceanRep, doi:10.3289/KOSMOS_PLANKTON_SWEDEN_2013, 2015.
4. **Boxhammer T**, Sswat M, Paul A, Nicolai M, Riebesell U. Video of a plankton community enclosed in a 'Kiel Off-Shore Mesocosm for future Ocean Simulations' (KOSMOS) during a study in Tvärminne Storfjärden (Finland) 2012. OceanRep, doi:10.3289/KOSMOS_PLANKTON_FINLAND_2012, 2015.
5. **Boxhammer T**, Bach LT, Nicolai M, Riebesell U. Video of a plankton community enclosed in a 'Kiel Off-Shore Mesocosm for future Ocean Simulations' (KOSMOS) during the SOPRAN study in Raunefjord (Norway) 2011. OceanRep, doi:10.3289/KOSMOS_PLANKTON_NORWAY_2011, 2015.
6. **Boxhammer T**, Bach LT, Czerny J, Nicolai M, Posman K, Sswat M, Riebesell U. Video of the sampling strategy to empty sediment traps of the 'Kiel Off-Shore Mesocosms for future Ocean Simulations' (KOSMOS). OceanRep, doi:10.3289/KOSMOS_SEDIMENT_TRAP_SAMPLING, 2015.

Danksagung

Mein Dank gilt allen, die mich in den letzten fünf Jahren auf dem Weg zur Fertigstellung dieser Dissertation begleitet haben. Zuallererst möchte ich mich jedoch bei meinen wissenschaftlichen Betreuern Ulf Riebesell, Leif Anderson, Lennart Bach und Jan Taucher bedanken.

Danke Ulf, für dein seit 2009 in mich gesetztes Vertrauen und die Möglichkeit, meine Promotion im Rahmen der KOSMOS Experimente zu realisieren. Während wir in den vergangenen acht Jahren mit den Mesokosmen um die Welt gereist sind, hast du mir immer wieder die Möglichkeit gegeben neue Aufgaben und Verantwortungen wahrzunehmen. Am Ende waren es nicht weniger als neun KOSMOS Studien - von der Arktis bis nach Südamerika. Unsere inspirierenden Gespräche, die sich neben wissenschaftlichen Fragestellungen und Experimentplanungen auch gerne um Themen wie selbstfahrende Fahrzeuge oder Geräte aus dem Hause Apple drehten, werde ich immer in guter Erinnerung behalten. Ich danke dir, dass du meinen wissenschaftlichen Horizont um Welten erweitert und mich persönlich unterstützt hast, wo immer möglich.

Leif möchte ich danken für die sehr fruchtbare Zusammenarbeit in Göteborg bei der Analyse von fast 22.000 Datenpunkten des biogeochemischen Datensatzes aus Schweden (KOSMOS 2013). Danke ebenfalls, dass du dir die Zeit nimmst, für meine Disputation nach Kiel zu reisen. Tack så mycket!

Lennart, auch ohne dich wäre diese Arbeit wohl nie zustanden gekommen. Ich danke dir für deine Freundschaft und die wahrlich prägende und inspirierende Zusammenarbeit - zwischen Kühlraum und Textsalat - in über fünf Jahren. Auf deine Unterstützung konnte ich immer zählen.

Ich danke auch dir Jan, für deine Freundschaft und Unterstützung in den letzten Jahren meiner Promotion. Unsere Diskussionen über Wissenschaft und Kryptowährung während der gemeinsamen Spätschichten im Büro werde ich in guter Erinnerung behalten.

Warum ich nach der Diplomarbeit im KOSMOS-Team bleiben wollte? Diese Frage ist leicht beantwortet. Der ‚Team-Spirit‘ in unserer Arbeitsgruppe ist einzigartig und hat mich schon zu Studienzeiten in Booknis Eck (2009) in seinen Bann gezogen. Für diese Erfahrung und die besondere Zusammenarbeit im Ausland aber auch in der Heimat Kiel möchte ich mich bei allen Freunden und Kollegen aus der Arbeitsgruppe bedanken. In über eineinhalb Jahren auf Expedition sind viele Freundschaften entstanden. Besonders bedanken möchte ich mich an dieser Stelle bei Alice, Aljosa, Allanah, Andrea, Annegret, Carsten, Christian, Claudia, Dana, Fabrizio, Hendrik, Jana, Janina, Jan B., Jan C., Jan H., Jan T., Judith, Kai S., Kerstin, Lennart, Linn, Magda, Mathias H., Matias S., Matthias F., Michael K., Michael M., Michael S., Rafael, Sarah, Saskia, Paul, Peter, Sebastian, Signe, Silke, Silvana, Ulf, Veit und Verena. Eine besondere Rolle nehmen dabei meine langjährigen Bürokollegen Michael Sswat und Judith ein, mit denen ich so manch hochkonzentrierte Stunde zu dritt im Büro verbracht habe. Die häufig auch sehr lustigen Stunden mit euch und die nötige Portion Wind im Kopf möchte ich nicht missen. Danke Michael für deine langjährige Freundschaft und die unvergesslichen Roadtrips mit deinem Bulli. Allanah, auch dir danke ich speziell für deine Freund-

schaft, unermüdliche Unterstützung und deine Geduld, meinen sprachlichen Horizont um ‚R‘ zu erweitern. Kai Schulz hat ins besondere im ersten Jahr meiner Promotion eine sehr inspirierende Rolle eingenommen, wenn es mal wieder so weit war, Daten zu besprechen oder in Finnland über Wissenschaft und das Leben zu philosophieren. Ich danke euch allen für die gute Zeit.

Bedanken möchte ich mich auch bei allen nicht namentlich genannten Kolleginnen und Kollegen am GEOMAR, jedoch ausdrücklich bei Catriona, Corinna, Kai L., Luisa, Sonja, Till und Zeynep für eure Freundschaft und Unterstützung. Kai Lohbeck fällt dabei eine besondere Rolle zu, da ich ohne ihn wohl Arzt und kein Meeresbiologe geworden wäre.

Mein ganz besonderer Dank gilt meiner Familie für den Rückhalt den sie mir in jeder Lebenslage gibt. Meine Eltern haben in mir die Liebe zur Natur und den Naturwissenschaften geweckt und damit den Grundstein für meinen Lebenslauf gelegt. Mein ganz spezieller Dank gilt meiner in diesem Jahr verstorbenen Oma Irene Quednau, der ich diese Arbeit gewidmet habe. Sie war ein ganz besonderer Mensch in meinem Leben und hat immer voller Stolz und Vertrauen auf meine Arbeit geblickt.

Zuletzt möchte ich der wohl wichtigsten Person in meinem Leben danken, meiner Freundin Kristina. Danke, dass du seit bald neun Jahren an meiner Seite bist und tapfer ertragen hast, dass ich fast jedes Jahr für bis zu fünf Monate im Ausland war. Ich danke dir, dass du mich auf dem Weg zu dieser Arbeit begleitet und mich mit deiner Liebe und Expertise unterstützt hast!

Eidesstattliche Erklärung

Hiermit erkläre ich, dass die vorliegende Dissertation mit dem Titel

Influence of ocean acidification on elemental mass balances and particulate organic matter stoichiometry in natural plankton communities

von mir selbstständig verfasst worden ist und keine weiteren Quellen und Hilfsmittel als die angegebenen verwendet wurden. Die vorliegende Arbeit ist unter Einhaltung der Regeln guter wissenschaftlicher Praxis der Deutschen Forschungsgemeinschaft entstanden und wurde weder ganz noch in Teilen an anderer Stelle im Rahmen eines Prüfungsverfahrens vorgelegt oder veröffentlicht. Veröffentlichte oder zur Veröffentlichung eingereichte Manuskripte wurden kenntlich gemacht.

Ich erkläre mich einverstanden, dass diese Dissertation an die Bibliothek des GEOMAR Helmholtz-Zentrum für Ozeanforschung Kiel und die Universitätsbibliothek der Christian-Albrechts-Universität zu Kiel weitergeleitet wird.